Operator Product Expansion in 2 dimensional Quantum Gravity

Sune Rastad Bahn

October 8, 1996

Contents

List of Figures

Introduction

The problem of finding a quantum theory for gravity has resisted solution for many decades. A lot of difficulties of various kinds are present in this field. Some of these are seemingly of a quite technical nature, such as the lack of renormalizability, the unboundedness of the Euclidean action etc. Other problems, however, are fundamental to our understanding of such important physical concepts as distance and time.

In the last ten years a framework has been built up which makes it possible, at the cost of a few dimensions, to discuss some of the conceptual problems, avoiding the more technical issues. This model of *two dimensional gravity* is the topic of this thesis.

I start with a general introduction to the subject of quantum gravity in chapter 1. The next chapter is then devoted to the identification of the two dimensional theory, and the introduction of a lot of concept which will be used throughout the thesis. In chapter 3 I formulate the all important discrete approach known as *Dynamical Triangulation*, and the model is solved in the disguise of a matrix model. Chapter 4 describes the continuum limit of the theory giving quantitatively meaning to the very formal entities of chapter 2. I also introduce a set of operators which will be become important later. Chapter 5 and 6 contains results and applications of the theory. The first of these parts is more or less an overview of some of the remarkable results obtained in this framework, whereas the last chapter contains a more detailed discussion of one specific aspect of the theory, namely the *Operator Product Expansion* among the operators introduced earlier. I have tried to keep the text self-contained throughout and at a level such that no prior knowledge of the specific model should be necessary for the understanding.

Having briefly described the content of the next few pages, it is in place to mention some of the important themes which I (consciously) have left out. First and foremost I almost completely ignore the relation to string theory. This is done in realization that I could not treat the subject in any way it deserves, due to the combination of lack of space, time and insight. The omission of a detailed discussion of the *loop equation* is perhaps harder to justify, as it lies in the heart of many expositions of the subject. I do derive the equation from ordinary combinatorial considerations, but only after having obtained the solution. One could also have chosen to use the loop equation to solve the model directly, and leave out the treatment of matrix models. It is of course more or less a matter of taste which way the solution is obtained. Since the matrix model is used several places in the text, for instance when interpreting the operators, it is, however, my firm believe that its introduction is not superfluous.

Finally I apologize for any important things I might have left out unconsciously.

Acknowledgements

The present work was done in the period January-October 1996. It is a pleasure to thank my supervisor Jan Ambjørn for lively discussions and good advice, Solveig Skadhauge and Jakob L. Nielsen for carefully reading the manuscript and suggesting many improvement, and Ove Scavenius for inspiring the necessary work morale.

Sune R. Bahn,
Copenhagen October 1996

Chapter 1

Theories of Gravity

Newton was the first to give a scientific explanation of the fact that things tend to fall downward, and the first to realize that the scope of the force of gravity was not bounded to the neighbourhood of the earth but rather encompassed all the celestial bodies. Ever since this discovery gravity has been a cornerstone in the foundation of physics. Newtons theory was so successful that more than two centuries should pass before a new theory was proposed and was taken seriously. This theory, the general theory of relativity, had an even wider scope than Newtons. Not only was it tremendously successful in explaining the phenomenon of present day universe, it also opened for the possibility of discussing the History of the universe.

1.1 Einsteins theory of gravity

Gravity was the first force to be described in a purely geometric language. The differential equations of general relativity are most beautifully written in the language of differential geometry, a fact which has lead some people to coin the term geometrodynamics[58]. GR describes the motion of any object not as a result of forces in the Newtonian sense, but rather as "free" motion (motion along geodesics) on a curved surface, a curvature which on its side is determined by the distribution and motion of matter through the famous Einstein equation:

$$G_{\mu\nu} = 8\pi G(T_{\mu\nu} + \frac{1}{4}\Lambda g_{\mu\nu})$$

where $G_{\mu\nu}$ is the Einstein tensor[1], G is Newtons gravitational constant, $T_{\mu\nu}$ is the energy-momentum tensor (in units where the speed of light is equal one) and Λ is the cosmological constant. A few comments regarding Λ are in place at this point. It has a very long and exciting story (to long to be told here), and plays different roles in the various disciplines, which uses GR. In astrophysics it is usually assumed to be identically zero, in accordance with observations. In cosmology it is often used to fix theories which otherwise would give outrageous results when compared with reality. Within particle physics an increasing amount of time and effort is spend in attempts to explain why the observational value is so much smaller than the Planck mass scale. In quantum gravity Λ plays an important

[1] the Einstein tensor is related to the Riemann tensor through $G_{\mu\nu} = R_{\mu\nu} - 1/2 g_{\mu\nu} R$

rôle as the conjugate of the volume, as will become clear when we turn towards the more detailed exposition of two dimensional quantum gravity. For this last reason we intend to keep the cosmological constant term, even if Einstein advocated one should discard it.

To further elucidate the geometrical nature of the theory we can rewrite the Einstein equation in a form which is also more convenient for our approach, namely as the Euler-Lagrange equations for the *Hilbert Action*:

$$S_{Hilbert} = \int (\frac{1}{4\pi G} R + \Lambda) \sqrt{-g}\, d^4x \tag{1.1}$$

where R is the scalar curvature and g the determinant of the metric. In order to include matter we have to add to this pure gravity action a covariant action for the matter:

$$S_{matter} = \int \mathcal{L}_{matter} \sqrt{-g}\, d^4x$$

where $\mathcal{L}_{matter}$ is the Lagrangian density of the matter part. We might note that the appearance of the factor $\sqrt{-g}$ is in order to achieve covariance, since the invariant four-volume element is given exactly by $\sqrt{-g}\, d^4x$ not just d^4x.

1.2 Why quantum gravity?

There are several reasons why Einsteins theory cannot be the final theory for the structure of space-time. The theory holds in itself the seed for its own breakdown in the sense that it predict the formation of singularities, such as black holes, but does not say anything about what happens in these singularities. Another problem is that it is inherently a classic theory, its most basic equations involves such classical concepts as the energy momentum tensor. These equations can at most be considered to hold between expectation values in a full quantum theory.

1.3 Gravity as a quantum field theory

Since gravity in many respect looks like any other field theory it is tempting to quantize it in a complete analogous way. One of the common procedures to get from the classical theory to a quantum version is by means of Feynmans Path-Integral. One simply integrate over all the possible configurations (not just the ones obeying the equation of motion), and weight them by the exponential of the action:

$$Z[\Lambda, G] = \int e^{iS[g_{\mu\nu}, \Lambda, G]}\, \mathcal{D}g \tag{1.2}$$

From this *partition function* we can now obtain, in a formal way, the n-point functions adding a source term $J^{\mu\nu} g_{\mu\nu}$ to the action and perform functional derivatives:

$$\langle g_{\alpha\beta}(x_1) \dots g_{\rho\sigma}(x_n) \rangle = \left. \frac{\partial^n Z[\Lambda, G, J^{\mu\nu}]}{\partial J^{\alpha\beta}(x_1) \partial J^{\rho\sigma}(x_n)} \right|_{J^{\mu\nu}=0} \tag{1.3}$$

This approach has severe problems however due to the nonrenormalizability of gravity. The divergences which appears in the loop diagrams cannot be absorbed in a redefinition of the terms already appearing in the Lagrangian. A more physical description of the problem is the following. It is not possible, by the usual means, to get from the results on the low, everyday scale to the behaviour of gravity on a high energy scale. This makes any predictions of the quantum nature of singularities impossible. The problem has caused a veritable zoo of attempts to circumvent the problems. It seems however that we are still far from a solution, and that none of the attempts has been completely successful.

1.4 Two dimensional quantum gravity

One of the approaches to solving the riddles of quantum gravity is to simplify the problem by looking at two dimensions instead of the physical four dimensions. The hope is then that some of the intuition obtained in the lower dimensional toy model, will be useful when formulating the full four dimensional theory. The reduction in dimensions has rather drastic implications for the model. Among the positive ones are

- The theory is renormalizable.
- There is a solvable continuum approach (Liouville Theory).
- There is a discretized version (Dynamical Triangulation).

The approach also have some severe drawbacks due to its simplicity, mainly the fact that it contains no dynamical degrees of freedom, only topological. This makes it very much a toy model, unable to describe a lot of the interesting physics in the four dimensional theory, e.g. gravitational waves.

1.5 2d gravity as strings.

There is a independent reason for studying two dimensional gravity even if it turns out that the theory is too far from reality to provide any help in constructing the four dimensional theory. It turns out that the theory coincide with that of string theory, since a string propagating in time spans out a two dimensional manifold, which is exactly the subject of investigation for two dimensional quantum gravity. To be more precise consider the simplest action for a string in d dimensional space time[50]

$$S[X^a, g_{\mu\nu}] = \int \partial^\mu X^a(y)\partial^\nu X_a(y) g_{\mu\nu}(y)\sqrt{-g(y)}d^2y \tag{1.4}$$

where $y = (y_1, y_2)$ are coordinates on the string, X^a are the space time coordinates $a = 1, 2, \ldots, d$ and $g_{\mu\nu}$ is the worldsheet metric. This action can also be interpreted as d boson fields coupled to 2-dimensional gravity, establishing the connection between the two subjects. In what follows we will, due to lack of space-time, restrain from discussing the string theoretical impact of the theory. Instead the focus will be on the discrete model known as Dynamical Triangulation. Before introducing this model, however, it will be of some value to take a look at the continuum formulation, in order to get a feeling for the kind of objects we want to consider.

Chapter 2

Continuum Formalism

In this chapter I describe the continuum notations. The intention is to make the physical results, we will calculate in the discrete theory, more apparent, by comparing with continuum results. Before going into details it is worthwhile to identify more precisely the notion of two dimensional gravity. In order to do so we will generalize the ordinary four dimensional theory in a natural way to a very broad class of theories. Of all these theories we will then identify a proper candidate for the name 2D quantum gravity, and restrict ourselves to the study of this.

2.1 The functional measure

We want to generalize Eq. (1.2) slightly, to identify what we will mean by two dimensional quantum gravity. For any d-dimensional manifold M with metric $g_{\mu\nu}$, and the invariant measure $dM = \sqrt{\det g_{\mu\nu}} d^d x$ we can form, in direct analogy to the Einstein Hilbert action, the pure gravity action

$$S[(M, g_{\mu\nu}), \Lambda, G] = \int_M (\frac{R}{4\pi G} + \Lambda)\ dM \tag{2.1}$$

Note that the measure dM becomes complex for Lorentzian signature. For this reason one usually introduces a minus sign in the definition, as was also done in the former chapter, i.e $dM = \sqrt{-\det g_{\mu\nu}} d^d x$. We will *not* adopt this convention, but stick to the action Eq. (2.1) even if it becomes complex when considering Minkowski-like spacetimes. Let us give a few arguments why this unorthodox choice is valid. On the classical level the theory is unchanged, since the stationary points are the same regardless of multiplication of the action with some constant.

In the quantum theory the fact that we have a complex action when considering Lorentzian signature metrics has as a consequence that the auxiliary prescription of an i in front of the action (as in Eq. (1.2)) is not needed.

Furthermore this have the advantage of making it possible to treat metric with any signature using the same form of the action and the same general partition function,

$$Z[\Lambda, G] = \int_{\mathcal{G}} e^{-S[g_{\mu\nu}, \Lambda, G]}\ \mathcal{D}\mathcal{G} \tag{2.2}$$

where $\mathcal{G}$ is a set of geometries, i.e. pairs of the form $(M, g_{\mu\nu})$, M being a manifold equipped with a metric $g_{\mu\nu}$. $\mathcal{DG}$ is some measure on $\mathcal{G}$, usually induced by the metric via for instance the distance element in super-space[29]:

$$\| \delta g \|^2 = \int_M \delta g_{\mu\nu} [\alpha g^{\mu\rho} g^{\nu\sigma} + \beta g^{\mu\nu} g^{\rho\sigma}] \delta g_{\rho\sigma} dM \tag{2.3}$$

where, as before, dM is the measure on $(M, g_{\mu\nu})$. The constants α and β can partly be determined by the normalisation of the measure, but this still leaves one constant undetermined, which has to be fixed by other requirements. If M is not the same for all the geometries in $\mathcal{G}$ the integration over $\mathcal{G}$ splits up in a sum over manifolds and integration over the metric $g_{\mu\nu}$. Common choices for the set $\mathcal{G}$ are:

- $\mathcal{G}$ is the set of four-dimensional Riemannian manifolds. The measure is the one induced by δg. The result is (presumably) 4-dimensional Euclidean quantum gravity.
- $\mathcal{G}$ is the set of four-dimensional pseudo-Riemannian[1] manifolds. The result is (presumably) 4-dimensional quantum gravity.
- $\mathcal{G}$ is the set of compact, orientable 2-dimensional Riemannian manifolds. We can furthermore choose to fix the topology to be for instance spherical. The result is 2 dimensional Euclidean quantum gravity.

More exotic choices could be made. One could for instance include both Riemannian and pseudo-Riemannian manifolds in order to find a possible dynamical origin of the Lorentz signature we observe in Nature[45], or one could even attempt to include manifolds of arbitrary dimension.

It should be mentioned that the above are to be seen as definitions for what we will call d-dimensional (Euclidean) quantum gravity. In particular the Euclidean versions are *not* to be interpreted just as Wick rotated versions of the Lorentz-signature model. On the other hand, in the case of flat space the action of the Euclidean model is identical to the Wick rotated version of the conventional non-complex action, even when various matter is included (see App. (A)).

Taking the above as definitions still leaves us with the question of how to make sense of the integral over $\mathcal{G}$. In four dimensions it is far from settled how to perform the integration, and even quite disputable to what extent it is possible to do at all.

In the case of 2 dimensional compact surfaces one can perform the integration, and we will therefore restrict ourselves to that case for the remainder of this thesis.

2.2 The partition function

With this choice of manifolds we can parameterize the set $\mathcal{G}$ by the metric g and the topology τ reducing the measure to

$$\int_{\mathcal{G}} \mathcal{DG} = \sum_{\tau} \int \frac{1}{\text{VolDiff}} \mathcal{D}g \tag{2.4}$$

[1] i.e. with Lorentz or more general non positive definite signature

where we have divided by the volume of the auto-diffeomorphism group[2]. Using Gauss-Bonnet theorem $\int \frac{R}{4\pi}\sqrt{g}d^2x = \chi$, where χ is the Euler character[3], we can write the partition function

$$Z[\Lambda, G] = \sum_{\chi=2,0,-2,\ldots} e^{-\frac{\chi}{G}} \int e^{-\int \Lambda\sqrt{g}d^2x} \frac{1}{\text{VolDiff}}\mathcal{D}g \tag{2.5}$$

This sum is quite divergent due to the sum over topologies. There have been a fair lot of attempts to make sense out of it anyway, most notably the so called *double scaling limit*, which will be discussed later (see Sec. (5.4)). For the time being (and the following chapters) we will stick to spherical topology. In this case we can drop the sum, and the pre-factor of $e^{-\frac{2}{G}}$ with the result

$$Z[\Lambda] = \int_{S^2} e^{-\int \Lambda\sqrt{g}d^2x} \frac{1}{\text{VolDiff}}\mathcal{D}g \tag{2.6}$$

where S^2 is the set of metrics on the sphere. This form of the partition function is our starting point for the continuum formalism described in this chapter.

2.3 Geometrical invariants

The physical observables in the theory are the geometrical invariant quantities, meaning quantities which are invariant under change of coordinates. Examples includes the volume, the distance between point, and many more. Let us first look at the volume. The number of surfaces with a fixed volume V is given by

$$Z[V] = \int_{S^2} \delta(\int \sqrt{g}d^2x - V)\mathcal{D}\mathcal{G} \tag{2.7}$$

note that (with $V(g) = \int \sqrt{g}d^2x$)

$$Z[\Lambda] = \int_{S^2} e^{-\Lambda V(g)}\mathcal{D}\mathcal{G} = \int_0^\infty e^{-\Lambda V} Z[V]dV \tag{2.8}$$

which shows that $Z[\Lambda]$ is the Laplace transform of $Z[V]$. We will see other examples of the usefulness of Laplace transformation later.

The average volume in the ensemble can be found as

$$\langle V(\Lambda)\rangle = \frac{\int_{S^2} V(g)e^{-\Lambda V(g)}\mathcal{D}\mathcal{G}}{Z[\Lambda]} = -\frac{1}{Z[\Lambda]}\frac{\partial Z}{\partial \Lambda} \tag{2.9}$$

We can form other invariants by integrating powers of the curvature R (the above corresponding to R^0). For R^1 this is trivial since, in our case of fixed topology, $R(g) = \int R\sqrt{g}d^2x = 4\pi\chi$ is constant.

[2] an auto-diffeomorphism is a bijective differentiable function $f : M \to M$ such that the inverse is also differentiable, i.e. a change of coordinates on M.

[3] in terms of the genus h of the surface $\chi = 2 - 2h$ i.e. 2 for a sphere, 0 for a torus etc.

2.4 Universe with a boundary

Let us now introduce loops on the surface. We do this by choosing a different set of manifolds, namely spheres where we cut out some boundaries in the form of a loop. For

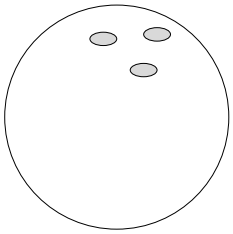

Figure 2.1: A sphere with 3 boundaries.

instance the partition function for n loops of length $L_1, \ldots, L_n$ will be

$$F[\Lambda, L_1, \ldots, L_n] = \int_{S^2 \setminus l_1 \cup \cdots \cup l_n} e^{-\int \Lambda \sqrt{g} d^2 x} \mathcal{D}\mathcal{G} \tag{2.10}$$

where $S^2 \setminus l_1 \cup \cdots \cup l_n$ is the set of metrics on the sphere with n loops such that these have length $L_1, \ldots, L_n$. In the same way as before we can form the Laplace transformed

$$F[\Lambda, X_1, \ldots, X_n] = \int_0^\infty e^{-\Lambda V} e^{-X_i L_i} F[V, L_1, \ldots, L_n] dV dL_1 \cdots dL_n \tag{2.11}$$

Where now X_i is the "cosmological constants" of the boundary.

In the case of just one loop we are dealing with Hartle-Hawking wave functionals, which can be interpreted as the amplitude for creating a universe of length L out of nothing. These play a major role in quantum cosmology, but we will not pursue this specific aspect of $F[\Lambda, X_1]$ further.

2.5 Distance

The concept of distance is rather easily introduced in the formalism. We simply define the distance between loops as

$$d(l_1, l_2) = \min_{x_1 \in l_1, x_2 \in l_2} d(x_1, x_2) \tag{2.12}$$

where $d(x_1, x_2)$ is the geodesic distance with respect to the metric g defined as

$$d(x_1, x_2) = \min_{x(t) \in L} \int \sqrt{g^{ij} \frac{dx_i}{dt} \frac{dx_j}{dt}} dt \tag{2.13}$$

with L the set of curves from x_1 to x_2. With this definition we can introduce the two-loop-with-fixed-distance correlation function as

$$G[L_1, L_2, D] = \int_{S^2 \setminus l_1 \cup l_2} e^{-\int \Lambda \sqrt{g} d^2 x} \delta(d(l_1, l_2) - D) \mathcal{D}\mathcal{G} \tag{2.14}$$

or we can fix the distance further by requiring each point on the first loop to have distance D from the second loop

$$N[L_1, L_2, D] = \int_{S^2 \setminus l_1 \cup l_2} e^{-\int \Lambda \sqrt{g} d^2x} \Pi_{x_1 \in l_1} \delta(d(x_1, l_2) - D) \mathcal{DG} \tag{2.15}$$

where $d(x_1, l_2) = \min_{x_2 \in l_2} d(x_1, x_2)$.

We can also introduce a new set of geometrical invariants. The average distance between points can be defined as

$$\langle D(\Lambda) \rangle = \frac{1}{Z[\Lambda]} \int_{S^2} e^{-\Lambda V(g)} \frac{1}{V(g)^2} \int \int d(x,y) \sqrt{g(x)} d^2x \sqrt{g(y)} d^2y \mathcal{DG} \tag{2.16}$$

or perhaps more important, we can fix the volume and consider

$$\langle D(V) \rangle = \frac{1}{Z[V]} \frac{1}{V^2} \int_{S^2} \int \int d(x,y) \sqrt{g(x)} d^2x \sqrt{g(y)} d^2y \delta(\int \sqrt{g} d^2x - V) \mathcal{DG} \tag{2.17}$$

Finally we can introduce

$$\langle V'(D, V) \rangle = \frac{1}{Z[V]} \frac{1}{V} \int_{S^2} \int \int \delta(d(x,y) - D) \sqrt{g(x)} d^2x \sqrt{g(y)} d^2y \delta(\int \sqrt{g} d^2x - V) \mathcal{DG} \tag{2.18}$$

the interpretation of which is the average of the measure of points at a distance D from some fixed point. In this sense it can be seen as the derivative (with respect to D) of the volume of the sphere with radius D. Hence the notation V'.

We recall that a set with Hausdorff dimension d_h will have $V' \propto D^{d_h - 1}$ for small distances, so the last quantity will give us a handle on how crumbled the effective surface[4] is.

2.6 Including matter

It is quite easy, on the formal level, to include matter. One simply add to the action a term of the form

$$S_{matter} = \int \mathcal{L}_{matter} \sqrt{g} d^2x \tag{2.19}$$

where $\mathcal{L}_{matter}$ is the Lagrangian density. Any differential operators in $\mathcal{L}$ should be in covariant form. Interaction with gravity is a result both of the derivatives being covariant, and the integration being invariant, i.e. include a factor $\sqrt{g}$.

For example, to describe a free, massless scalar field[5] X, we simply add

$$S_{matter}[g_{\mu\nu}, X] = \int (\partial_\mu X \partial^\mu X) \sqrt{g} d^2x \tag{2.20}$$

To get the partition function we must also integrate over matter configurations so the final result is

$$Z[\Lambda] = \int_{\mathcal{G}} e^{-S[g_{\mu\nu}, \Lambda] - S_{matter}[g_{\mu\nu}, X]} \mathcal{D}X \mathcal{DG} \tag{2.21}$$

In the following we will emphasize heavily on pure gravity, only sporadic mentioning matter.

[4] The notion of effective surface will be explained in Chap. (5).

[5] The field are called X in analogy with string theory where we interpret the value of X as coordinate in physical space

2.7 Liouville theory

We will now sketch how it is possible to do the integration of Eq. (2.5).

It is well known that any compact orientable 2 dimensional Riemannian surface, locally can, by means of a diffeomorphism, be brought into the form[59]:

$$g_{ij}(x) = f(x)\delta_{ij} \tag{2.22}$$

This is also true globally if the surface have spherical topology. This means that the space M_0 of genus 0 surfaces modulus diffeomorphisms and conformal transformations[6], is trivial. For higher genera surfaces the modular space

$$M_h = \text{genus } h \text{ surface mod diff. conf.} \tag{2.23}$$

is no longer 0-dimensional. For the torus it is 2-dimensional and for higher genus $6h-6$ dimensional[50]. The metric can now be brought into the form

$$g_{ij}(x) = f(x)\hat{g}_{ij}(\tau, x) \tag{2.24}$$

where we have chosen a representative $\hat{g}(\tau, \cdot)$ for each $\tau \in M_h$.

Since f is positive we can write $f(x) = e^{\phi(x)}$ where ϕ is known as the Liouville field. This whole procedure of bringing the metric into conformal form corresponds to gauge fixing in ordinary field theory. The chosen gauge is also known as conformal gauge.

As usually a gauge choice introduces a Faddeev-Popov determinant[23]

$$\int \mathcal{D}M \to \sum_{h=0}^{\infty} \int_{M_h} \int \Delta_{FP}(e^{\phi(x)}\hat{g}(\tau))\mathcal{D}\phi d\tau \tag{2.25}$$

We can factor out the conformal mode ϕ:

$$\Delta_{FP}(e^{\phi(x)}\hat{g}(\tau)) = \Delta_{FP}(\hat{g}(\tau))e^{\frac{-25}{48\pi}S_L[\phi,\hat{g}]} \tag{2.26}$$

where

$$S_L[\phi, \hat{g}] = \int (\frac{1}{2}\hat{g}_{ij}(\tau)\partial^i\phi\partial^j\phi + \hat{R}\phi)\sqrt{\hat{g}}d^2x \tag{2.27}$$

is the Liouville action. In the case of matter being present the factor in front of the Liouville action changes to $\frac{c-25}{48\pi}$ where c is *the central charge* of the matter sector[7].

It is possible to do explicit calculation, and find many interesting properties of this model. In the case of fixed spherical topology, the formula simplifies a lot. The integration over modular space drops out. Since $\hat{g}_{ij} = \delta_{ij}$ the curvature $\hat{R}$ is zero and the action is simply:

$$S_L[\phi] = \frac{1}{2}\int [(\partial_1\phi)^2 + (\partial_2\phi)^2]d^2x \tag{2.28}$$

The only nontrivial part in the spherical case is $\Delta_{FP}(\hat{g}(\tau))$. A careful treatment of this involving a reasonable assumption for the renormalization of the cosmological constant term reveal the following behavior of the partition function[27]

$$Z[V] \propto Z^{\gamma-3} \tag{2.29}$$

where $\gamma = \frac{c-1-\sqrt{(c-1)(c-25)}}{12}$ is called the string susceptibility. In the pure gravity case $c = 0$ we have $\gamma = -1/2$.

[6] transformations of the form $g_{ij} \to f(x)g_{ij}$, where f is positive.

[7] each scalar field adds one to the central charge.

2.8 Why a discrete model?

We will now turn towards the formulation of a discrete version of the concept introduced in this chapter. But before embarking on this project it is appropriate to discuss the reason for this step. In order words, if it is possible to do the calculations in the continuum formalism, why should we care to build up a discrete, lattice-like formulation? The common reason for studying lattice theories is to make computer simulations where no exact results are obtainable. This is not the main reason in this case, although simulations are used when coupling to matter and are very important when generalizing to higher dimensions. For two dimensional pure gravity, the interesting point is that the discrete version is actually easier and more intuitive to work with than the continuum theory. A lot of concepts, especially geodesic distance, are far more easily coped with in that framework, and a lot of exact result can be obtained, which so far have avoided calculation in Liouville theory. This is somewhat surprising compared with normal lattice theory, which often is harder to work with from a theoretical point of view than the original theory.

Chapter 3

Dynamical Triangulation

In this chapter I go through the basics of dynamical triangulation, including the relation to matrix models, calculation of cap and cylinder amplitudes. The goal is to reformulate the concepts introduced in the former chapter, this time on a discrete level, in terms of finite triangulations.

3.1 From surface to polygon net

We want to discretize the concept of an arbitrary 2-dimensional manifold. One way suggested by Regge[63], is to build up the surface from triangles, and then let the length of the sides be the dynamical variable. This approach is very convenient if we want to see the time evolution of a surface. Given the initial conditions we can specify the link length at some time, and then calculate the evolution by means of some suitable (discrete) variational principle. The result is a numerical solution to the classical field equations (see [58] for more on this).

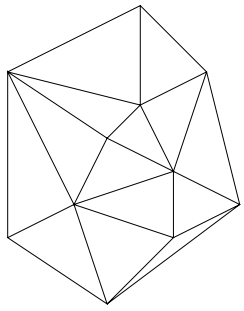

Figure 3.1: Regge triangulation

We will use a slightly different approach known as *Dynamical Triangulation*. The idea is that instead of first building up some fixed triangulation, and then vary the link length, we want to consider all possible build ups, with fixed equilateral triangles. This reduces the calculation of the surface area to a mere counting of triangles. The path integral is also reduced to the combinatorial problem of gluing together triangles, a problem which can be

solved quite elegantly by means of matrix-methods. In short the partition function (2.6) takes the form

$$Z[\Lambda] = \int e^{\int_\Lambda \sqrt{g}\ d^2x}\ \mathcal{D}g \sim \mathsf{Z}[\mu] = \sum_{\tau\in\mathcal{T}} e^{-\mu\sum_{v\in\tau}} = \sum_{n=0}^{\infty} e^{-\mu n}\mathsf{z}_n \tag{3.1}$$

Where $\mathcal{T}$ is the set of triangulations, v the set of triangles in a triangulation τ, μ the discrete cosmological constant and z_n the number of triangulations with n triangles.

The reasons for choosing Dynamical Triangulation instead of Regge calculus are numerous. In DT we are directly counting different geometries. This can be deduced from the fact that different triangulations will have different distribution of curvature, and hence not be diffeomorphic. Each triangulation therefore represents a point in our collection of geometries $\mathcal{M}$. Strictly speaking since they are not smooth, they represents some sort of limit points, and we will have to smooth out the curvature a bit to get a proper geometry, but we will not worry too much about this. In Regge calculus different set of side length might conspire to give the same geometry, as can easily be seen from the infinite many ways of triangulating the plane, using a fixed set of triangles with varying side length. This means that if we want to count the number of geometries, not just the number of ways we can assign side length, we have to be very careful. Another problem is that fixing the triangulation seems to favour some geometries. If for instance the triangulation consist of n triangles, it will be quite hard to find a set of side length that mimic a surface with much more than n blobs. In order to avoid this problem, we must increase or vary the number of triangles, but this would make the problem of double counting of geometries even harder to handle[1]. The only way out seems to be, that we drop the variation of side length. This exit leads us directly to Dynamical Triangulation.

Of course it is not trivial whether the set of geometries obtained in this way, is in any sense dense in $\mathcal{M}$. We have however indirect support for this assumption, from the fact that the critical exponents are the same in dynamical triangulation, as in Liouville theory. More on this later.

A final brick to support the choice of Dynamical Triangulation in favour of Regge, is recent simulations[35] which seems to indicate the failure of the latter to describe gravitational effect when coupled to matter (see however[13]).

3.2 Matrix model

Consider an action for some imagined[2] quantum theory given by

$$S[M] = N(\frac{1}{2}\mathrm{tr}M^2 - \frac{g}{3}\mathrm{tr}M^3) \tag{3.2}$$

where M is a hermitian $N \times N$ matrix. The Feynman diagram expansion, see App. (B), consist of a propagator represented by a double line with two arrows , and a vertex[3] drawn in a similar way (Fig. (3.2)).

[1] for some early attempts in this direction see [46, 47]

[2] The "physical" interpretation could be that of an 0 dimensional $SU(N)$ theory

[3] The absence of the factor $\frac{1}{3}$ in front of the vertex is due to symmetry as explained in App. (B)

Figure 3.2: Matrix model propagator and vertex

Now the important point is that each distinct diagram corresponds to a gluing of triangles in the following way. Each vertex corresponds to a face of a triangle, and each propagator to a gluing of sides.

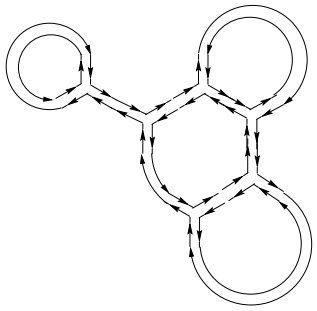

Figure 3.3: A matrix model Feynman diagram

We see that a $n-$th order diagram corresponds to a surface build up from n triangles. The advantage of drawing the diagram instead of the triangulation itself, is obvious if one tries to draw a picture of the above triangulation.

We could have introduced the diagram as dual graphs without making the connection to the matrix model, and just use them as a help in drawing the triangulations. There are, however, independent reasons for introducing the matrix-model. One is that the model can be solved nonperturbatively (in a sense we shall see soon in Sec. (3.3)), and we can then extract the perturbation series. This gives us an "automatic" counting of the possible diagrams. Another reason is that the matrix approach gives a framework which can easily be generalized to include matter fields on the triangles. These so called multi matrix models will be described in Chap. (5).

Even with all these advantages of the matrix point of view, we will sometimes switch to the triangle representation, giving a more immediate intuition for the geometry of the surface in question. This switching of languages should hopefully not cause any misunderstandings. In order to get acquainted with the interpretation of dual graphs the reader is encouraged to consult the "dictionary", App. (C).

We are only interested in counting connected surfaces. This corresponds to connected diagrams, so we consider the partition function W given by

$$e^W = \int e^{N(-\frac{1}{2}\mathrm{tr}M^2+\frac{g}{3}\mathrm{tr}M^3)}dM \tag{3.3}$$

The weight given to any diagram is specified by the Feynman rules (see App. (B)), i.e. a factor of N^{-1} for each propagator,a factor gN for each vertex, and a N for each closed

loop. The overall factor of N is therefore given by:

$$N^{V-E+F} = N^{\chi} \tag{3.4}$$

where V is the number of vertices in the diagram (or equivalently the number of triangles in the surface), E is the number of propagators (edges), F is the number of loops (spikes) and χ is the Euler character of the surface. This relation between geometry and the $\frac{1}{N}$ expansion was first noted by 't Hooft and have had far reaching application in such diverse fields as spin systems, QCD and, as we shall see, quantum gravity. For an anthology see [49].

We are only interested in triangulation of the sphere $\chi = 2$. This can be obtained by taking the $N \to \infty$ since this will suppress diagrams with another topology with a factor of N^{2g} where g is the genus. We will now proceed to solve the model in this limit.

3.3 The large N-limit

The problem of finding the large N limit was first solved by Brézin et al. in a now classic paper[48]. There exist other ways of obtaining the same result, see e.g. [51] but we will follow their approach rather strict. First we will rewrite the integral of Eq. (3.3) in a way similar to the Faddeev-Popov trick known from gauge theories[50].

Let $\Lambda(\lambda_i)$ denote the diagonal matrix $d(\lambda_1, \ldots, \lambda_N)$ and define *the Vandermonde determinant*

$$\Delta(\Lambda) = \prod_{k<l}(\lambda_k - \lambda_l) \tag{3.5}$$

Let M be some Hermitian matrix and consider the integral

$$I(M) = \int dU \int_{-\infty}^{\infty}\int_{\lambda_1}^{\infty}\cdots\int_{\lambda_{N-1}}^{\infty}\prod_{i=1}^{N} d\lambda_i \Delta^2(\Lambda)\delta^{N^2}(UMU^{\dagger} - \Lambda(\lambda_i)) \tag{3.6}$$

We only get a contribution to $I(M)$ from the vicinity of $U = U_0$ where U_0 is the unitary matrix that diagonalizes M with increasing diagonal, i.e. $U_0 M U_0^{\dagger} = \Lambda_0$,where Λ_0 is a diagonal matrix with eigenvalues $\lambda_1' \leq \lambda_i' \leq \lambda_N'$. In the case where M has two identical eigenvalues there are more than one U_0 which do the job, but here the Vandermonde determinant makes the contribution vanish anyway so in this case we have $I(M) = 0$. Assuming now M has distinct eigenvalues we can evaluate the integral by noticing that in the infinitesimal neighborhood of U_0 we have $U = (1+T)U_0$ where T is a hermitian matrix and hence

$$\begin{aligned} I(M) &= \int dT \int_{-\infty}^{\infty}\int_{\lambda_1}^{\infty}\cdots\int_{\lambda_{N-1}}^{\infty}\prod_{i=1}^{N} d\lambda_i \Delta^2(\Lambda)\delta^{N^2}((1+T)U_0 M U_0^{\dagger}(1-T) - \Lambda(\lambda_i)) \\ &= \int dT \int_{-\infty}^{\infty}\int_{\lambda_1}^{\infty}\cdots\int_{\lambda_{N-1}}^{\infty}\prod_{i=1}^{N} d\lambda_i \Delta^2(\Lambda)\delta^{N^2}(\Lambda_0 - [T,\Lambda_0] - \Lambda(\lambda_i)) \\ &= \int dT \int_{-\infty}^{\infty}\int_{\lambda_1}^{\infty}\cdots\int_{\lambda_{N-1}}^{\infty}\prod_{i=1}^{N} d\lambda_i \Delta^2(\Lambda)\delta^{N}(\Lambda_0 - \Lambda(\lambda_i))\delta^{N(N-1)}([T,\Lambda_0]) \end{aligned} \tag{3.7}$$

Now the i,j-th entry of $[T,\Lambda_0]$ is $T_{ij}(\lambda'_j-\lambda'_i)$ giving

$$\begin{aligned} I(M) &= \int dT \prod_{i=1}^{N} d\lambda_i \Delta^2(\Lambda)\delta^N(\Lambda_0-\Lambda)\delta^{N(N-1)}([T,\Lambda_0]) \\ &= \int \prod_{i=1}^{N} d\lambda_i \Delta^2(\Lambda)\delta^N(\Lambda_0-\Lambda)\prod_{k\neq l}|\lambda'_k-\lambda'_l|^{-1}=1 \end{aligned} \tag{3.8}$$

where we have used $\int\delta(ax)=|a|^{-1}$ and dropped the limits on the integral for simplicity. Inserting this advanced way of writing 1 for almost any M into (3.3) gives:

$$\begin{aligned} e^W &= \int I(M)e^{N(-\frac{1}{2}\mathrm{tr}M^2+\frac{g}{3}\mathrm{tr}M^3)}dM \\ &= \int\int dU\prod_{i=1}^{N} d\lambda_i\Delta^2(\Lambda)\delta^{N^2}(UMU^\dagger-\Lambda)e^{N(-\frac{1}{2}\mathrm{tr}M^2+\frac{g}{3}\mathrm{tr}M^3)}dM \\ &= \int\prod_{i=1}^{N} d\lambda_i\Delta^2(\Lambda)e^{N(-\frac{1}{2}\mathrm{tr}\Lambda^2+\frac{g}{3}\mathrm{tr}\Lambda^3)}\int dU \\ &= \int_{-\infty}^{\infty}\int_{\lambda_1}^{\infty}\cdots\int_{\lambda_{N-1}}^{\infty}\prod_{i=1}^{N} d\lambda_i e^{N\sum_{j=1}^{N}(-\frac{1}{2}\lambda_j^2+\frac{g}{3}\lambda_j^3+\frac{1}{N}\sum_{k\neq j}\ln|\lambda_j-\lambda_k|)} \end{aligned} \tag{3.9}$$

where we have used that $\mathrm{tr}M=\mathrm{tr}UMU^\dagger$, and the normalisation $\int dU=1$.

The expression Eq. (3.9) is strictly speaking not well-defined for real g since the action is not bounded. For imaginary g, however, the second term will be purely oscillatory, and the first term will cause an exponential damping. The integral will therefore be well defined. It turns out that the final result, after taking $N\to\infty$, is analytical in g, with a positive radius of convergence, and since we are only interested in the power series expansion we can do the calculations with imaginary g and go back to real g after the calculation.

The whole expression can now be estimated in the $N\to\infty$ limit using the method of steepest descent(see e.g [60]), as

$$W=N\sum_{j=1}^{N}(-\frac{1}{2}\lambda_j^2+\frac{g}{3}\lambda_j^3+\frac{1}{N}\sum_{k\neq j}\ln|\lambda_j-\lambda_k|) \tag{3.10}$$

The λ_j are required to fulfill the stationarity condition:

$$\begin{aligned} \frac{\partial}{\partial\lambda_i}\left[\sum_{j=1}^{N}(-\frac{1}{2}\lambda_j^2+\frac{g}{3}\lambda_j^3+\frac{1}{N}\sum_{k\neq j}\ln|\lambda_j-\lambda_k|\right] &= -\lambda_i+g\lambda_i^2+\frac{1}{N}\sum_{k\neq i}\frac{1}{\lambda_i-\lambda_k}+\sum_{j\neq i}\frac{1}{N}\frac{-1}{\lambda_j-\lambda_i} \\ = -\lambda_i+g\lambda_i^2+\frac{2}{N}\sum_{k\neq i}\frac{1}{\lambda_i-\lambda_k} &= 0 \end{aligned} \tag{3.11}$$

in the limit λ becomes a continuous, monotonous increasing function $\lambda(x)$ such that $\lambda_j=\lambda(j/N)$ and $\frac{1}{N}\sum\to\int dx$. Inserting this we obtain

$$N^{-2}W=\int_0^1 -\frac{1}{2}\lambda(x)^2+\frac{g}{3}\lambda(x)^3dx+\int_0^1 dx\int_0^1 dy\ln|\lambda(x)-\lambda(y)| \tag{3.12}$$

The condition on the eigenvalues become

$$\lambda(x) - g\lambda(x)^2 = 2\mathrm{P}(\int_0^1 dy \frac{1}{\lambda(x) - \lambda(y)}) \tag{3.13}$$

where P indicates that we take the principal part of the integral, the natural generalization of leaving out $k = i$ in the sum Eq. (3.11).

We now introduce the *eigenvalue density*

$$v(\lambda) = \langle \frac{1}{N} \sum_{i=1}^{N} \delta_{\lambda_i \lambda} \rangle \sim \langle \int_0^1 \delta(\lambda - \lambda(x)) dx \rangle = \langle \sum_{x \in \lambda^{-1}(\lambda)} \frac{1}{|\lambda'(x)|} \rangle = \langle \frac{dx}{d\lambda}|_\lambda \rangle \tag{3.14}$$

where the brackets indicate expectation values, i.e. that the eigenvalues are subject to the condition (3.13). The density is normalized, since it satisfies

$$\int_a^b v(\mu) d\mu = \int_0^1 dx = 1 \tag{3.15}$$

for $[a; b]$ being the support of v. To see why v must have compact support, we note that since $\lambda(x)$ is continuous, monotonous increasing, we will have compact support unless $\lambda(x) \to \infty$ for $x \to 1$ or $\lambda(x) \to -\infty$ for $x \to 0$. Both these cases would however be in contradiction with Eq. (3.13).

If we substitute $\lambda(y) = \mu$ and $dy = v(\mu)d\mu$ into Eq. (3.13), we obtain

$$\lambda(x) - g\lambda(x)^2 = 2\mathrm{P}(\int_a^b \frac{v(\mu)}{\lambda - \mu} d\mu) \tag{3.16}$$

This equation can be solved in the following way. Let

$$\text{𝓕}(\lambda) = 2 \int_a^b \frac{v(\mu)}{\lambda - \mu} d\mu \tag{3.17}$$

this function has the following properties:

- 𝓕 is analytic outside $\lambda \in [a; b]$ by construction[4].
- 𝓕 $\sim \frac{2}{\lambda}$ for $|\lambda| \to \infty$ due to (3.15).
- $\lim_{\epsilon \to 0}$ 𝓕$(\lambda \pm i\epsilon) = \mathrm{P}(\int_a^b \frac{v(\mu)}{\lambda - \mu} d\mu) \mp 2i\pi v(\lambda) = \lambda(x) - g\lambda(x)^2 \mp 2i\pi v(\lambda)$

To obtain a function with these qualities we let

$$\text{𝓕}(\lambda) = \lambda - g\lambda^2 + f(\lambda)\sqrt{(a - \lambda)(b - \lambda)} \tag{3.18}$$

where f is a polynomial. We must now require that the terms with λ and λ^2 vanish at infinity, i.e:

$$f(\lambda)\sqrt{\lambda^2 - (a + b)\lambda + ab} \simeq f(\lambda)(\lambda - \frac{a + b}{2}) \sim -(\lambda - g\lambda^2) \tag{3.19}$$

[4]Since v is integrable, we can interchange integration and differentiation, and thus show that Cauchy-Riemann differential equations hold, from the fact that they hold for $\frac{1}{\lambda - \mu}$

which means that $f(\lambda) = g\lambda - 1 + g\frac{a+b}{2}$. The final result is

$$\rho(\lambda) = \lambda - g\lambda^2 - (1 - g\frac{a+b}{2} - g\lambda)\sqrt{(a-\lambda)(b-\lambda)} \tag{3.20}$$

from this (and property 3° of ρ)

$$v(\lambda) = \frac{1}{2\pi}(1 - g\frac{a+b}{2} - g\lambda)\sqrt{(a-\lambda)(\lambda-b)} \tag{3.21}$$

We still need to find a and b. We note that for $\lambda \to \infty$ we have by expansion in $\frac{1}{\lambda}$:

$$\begin{aligned}\rho(\lambda) &= \lambda - g\lambda^2 - (1 - g\frac{a+b}{2} - g\lambda)(\lambda - \frac{a+b}{2} + (\frac{ab}{2} - \frac{(a+b)^2}{8})\frac{1}{\lambda} + (\frac{(a+b)ab}{4} - \frac{(a+b)^3}{16})\frac{1}{\lambda^2}) \\ &= g\frac{4ab - 3(a+b)^2}{8} + \frac{a+b}{2} + [\frac{(a-b)^2}{8} - g\frac{(a+b)(a-b)^2}{8}]\frac{1}{\lambda}\end{aligned} \tag{3.22}$$

from this (and using property 2° of ρ) we see that

$$\frac{3g}{4}(a+b)^2 - gab = a + b \tag{3.23}$$

since the constant term must vanish and,

$$(a-b)^2\frac{1 - g(a+b)}{8} = 2 \tag{3.24}$$

since the coefficient in front of $\frac{1}{\lambda}$ must be 2. Let us reformulate Eq. (3.23) by introducing the variable $c = g(a+b)$ and using $ab = \frac{1}{4}((a+b)^2 - (a-b)^2)$

$$3c^2 - (c^2 - g^2(a-b)^2) = 4c \tag{3.25}$$

using Eq. (3.24) in the form

$$(a-b)^2 = \frac{16}{1-c} \tag{3.26}$$

we arrive at

$$2c^2 + \frac{16g^2}{1-c} = 4c \tag{3.27}$$

or

$$c^3 - 3c^2 + 2c - 8g^2 = 0 \tag{3.28}$$

which determines $c = g(a+b)$ in terms of g. Together with (3.26) this give a complete determination of $a(g)$ and $b(g)$.

Let us look at the special case of $g = 0$. Here Eq. (3.23) implies $a = -b$ and from Eq. (3.26) we get $a - b = 4$. For v we therefore obtain:

$$v(\lambda) = \frac{1}{2\pi}\sqrt{4 - \lambda^2} \tag{3.29}$$

which we recognize as the *Wigner-semicircle distribution*. In the more general case $g \neq 0$

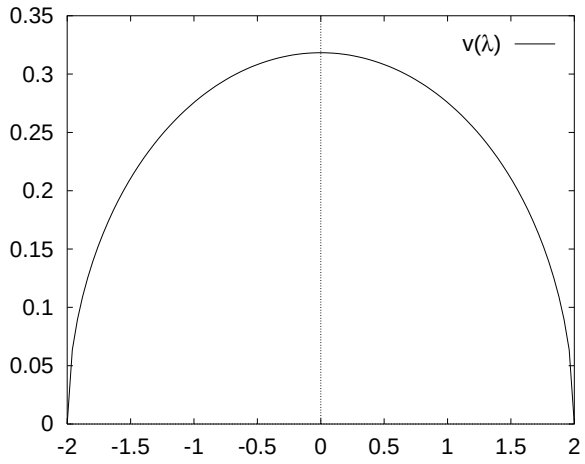

Figure 3.4: The Wigner distribution

we have to decide which of the roots we should use. In the limit $g \to 0$ we have $c \to 0$ which corresponds to the root

$$c(g) = 1 - \frac{1}{2}(S + T - i\sqrt{3}(S - T)) = 4g^2 + O(g^3) \tag{3.30}$$

where (using the principal branch of the cubic root)

$$S = \sqrt[3]{4g^2 + \sqrt{16g^4 - \frac{1}{3^3}}} \qquad T = \sqrt[3]{4g^2 - \sqrt{16g^4 - \frac{1}{3^3}}} \tag{3.31}$$

This shows that $c(g)$ has singularities (or rather branch points) at $g^4 = \frac{1}{3^3 2^4}$ but is analytic inside the circle in the complex plane of radius $g_{crit} = \frac{1}{2}3^{-\frac{3}{4}}$. Using Eq. (3.23) we can write the solution to Eq. (3.17) as

$$\begin{aligned} \rho(\lambda) &= \lambda - g\lambda^2 - (1 - g\frac{a+b}{2} - g\lambda)\sqrt{(\lambda - a)(\lambda - b)} \\ &= \lambda - g\lambda^2 - (1 - \frac{c}{2} - g\lambda)\sqrt{\lambda^2 - \frac{c\lambda}{g} + (\frac{3}{4}c^2 - c)\frac{1}{g^2}} \end{aligned} \tag{3.32}$$

This solution is also seen to be analytic in the same domain as c, since the singularity at $g = 0$ is finite by the choice of root for $c(g)$. We can now go back to real $g < g_{crit}$ as anticipated above.

Having obtained the solution[5] to (3.17) we could rewrite Eq. (3.12) in terms of $v(\lambda)$ and calculate the partition function. This would satisfy:

$$N^{-2}W[g] = \sum_{d \in D} \omega(d) g^{V(d)} \tag{3.33}$$

[5]The solution is not unique. We have imposed the condition that the support consist of one interval only. If we loosen this we can obtain multi-cut solutions[15]

where D the set of diagrams with spherical topology, $\omega(d)$ is the statistical weight (see App. (B)) and $V(d)$ is the number of vertices in the diagram d.

By power series expansion in g

$$N^{-2}W[g] = \sum_n w_n g^n \tag{3.34}$$

we could get (apart from statistical weight) the number of diagrams with n vertices as the coefficient w_n, or by letting $g = e^{-\mu}$ the partition function for triangulations

$$N^{-2}W[e^{-\mu}] = \sum_n w_n e^{-\mu n} \sim \sum_n e^{-\mu n}\mathsf{z}_n = \mathsf{Z}(\mu) \tag{3.35}$$

where μ is the discrete cosmological constant.

An explicit calculation of W would involve a lot of tedious calculus, and since the quantities we will use later on will be the Greens functions, we will concentrate on calculating these instead.

3.4 1-loop function

Until now we have been counting vacuum diagrams or closed surfaces[6]. We now want to consider surfaces with a boundary.

To obtain a boundary we leave some of the sides of the triangles free. In the matrix language this means we have some external legs. A triangulation with l sides left unglued is represented by a diagram with l external legs. We can therefore count the number of diagrams, using the Feynman rules for the Greens functions.

If we want a connected boundary, a loop, we must require that each boundary link can be reached from any other by moving along the boundary. This can be obtained by gluing triangles onto an l-gon (an l sided polygon). In matrix language an l-gon corresponds to a "vertex" or l-ped (an l legged multi-ped) as shown in Fig. (3.5). We draw the multi-ped with a dashed line, to emphasize its role as an l-link boundary, not an l-plaquette. Note that contracting two legs of the l-ped will give rise to a so called double link.

We can now count the possible triangulations with a boundary loop of l links in the following way. The introduction of an l-ped in the diagram can be obtained by considering the expectation value $\langle N\mathrm{tr}M^l\rangle = \int N\mathrm{tr}M^l e^{-S[M]}dM$ (in complete analogy with the insertion of a vertex, App. (B)). Since we are in the large N limit only diagrams with a value of N^2 will survive giving

$$\langle N\mathrm{tr}M^l\rangle = \sum_{d\in D_l} \omega_d N^2 g^{V(d)} \tag{3.36}$$

where D_l is the set of different diagrams, with the legs on the l-ped distinguished. Distinguishing between the legs on the l-ped amounts to marking one of them, so what we are counting is triangulations with a marked boundary.

Alternatively we could count the number of triangulations with a boundary with no marking by multiplying with a factor of l since the marking can be done l different ways

[6] all sides on every triangle is glued to some other triangle

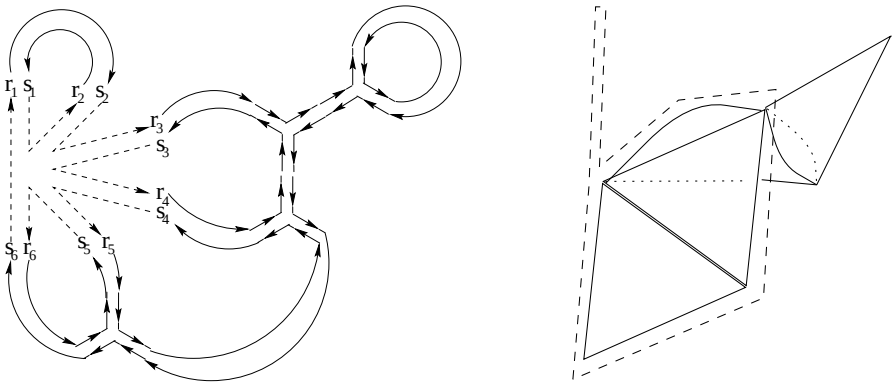

Figure 3.5: A loop represented by a gluing onto an l-ped and the corresponding triangulation.

(except if the diagram has some sort of symmetry). This corresponds to the fact that cyclic permuting the indices of the l-ped will give us different contractions of indices (except if the diagram has some sort of symmetry) without changing the triangulation. This is completely analogous to the factor which cancelled the $\frac{1}{3}$ in front of the vertex in the Feynman rules (see App. (B)). Notice, however, that by counting diagrams with a marked external leg, we ensure that the statistical weight will be $\omega_d = 1$, since the marking together with the orientability will ruin any symmetry. To be more precise, consider a general diagram as for instance the one shown in Fig.3.5. It is clear that if we do not change the indices on the l-ped, interchanging the indices on any of the vertices directly connected to it will change the contractions. The orientability ensure that also permuting the indices on a single vertex will change the contractions. We can now move away from the l-ped step by step, vertex by vertex, all the time fixing the indices by the requirement that the contractions should not be altered. Since the diagram is connected, we will in the end have fixed all indices.

In conclusion we have (by dividing out the common value of N^2 for all diagrams)

$$\dot{\mathsf{F}}_l(g) \equiv \sum_n \dot{\mathsf{F}}_{l,n} g^n = \langle \frac{1}{N} \mathrm{tr} M^l \rangle = \int_a^b \lambda^l v(\lambda) d\lambda \tag{3.37}$$

where $\dot{\mathsf{F}}_{l,n}$ is the number of triangulations consisting of n triangles and with a boundary of length l. We have used that

$$\frac{1}{N} \mathrm{tr} M^l = \frac{1}{N} \sum_{i=1}^{N} \lambda_i^l \sim \int_0^1 \lambda^l(x) dx \tag{3.38}$$

and

$$\langle \int_0^1 \lambda^l(x) dx \rangle = \langle \int_a^b \lambda^l \int_0^1 \delta(\lambda - \lambda(x)) dx d\lambda \rangle = \int_a^b \lambda^l v(\lambda) d\lambda \tag{3.39}$$

We now proceed to find the generating function for $\dot{\mathsf{F}}_l(g)$. If we introduce

$$\mathsf{R}_n(1/j) = 2j^n \int_a^b \mu^{n-1} \frac{v(\mu)}{(1-j\mu)^n} d\mu \tag{3.40}$$

we have

$$\mathbb{V}'_n(1/j) = 2j^{n+1}\int_a^b \mu^{n-1}\frac{-nv(\mu)}{(1-j\mu)^{n+1}}d\mu \tag{3.41}$$

and thereby

$$\begin{aligned}\frac{d}{dj}\left[\frac{(n-1)!}{j^n}\mathbb{V}_n(1/j)\right] &= (n-1)![\frac{-n}{j^{n+1}}\mathbb{V}_n(1/j) + \frac{1}{j^n}\mathbb{V}'_n(1/j)\frac{-1}{j^2}] \\ &= 2(n-1)!\int_a^b \mu^{n-1}v(\mu)(\frac{-n}{j(1-j\mu)^n} + \frac{-n}{-j(1-j\mu)^{n+1}}) \\ &= 2(n-1)!\int_a^b \mu^n\frac{nv(\mu)}{(1-j\mu)^{n+1}}d\mu = \frac{n!}{j^{n+1}}\mathbb{V}_{n+1}(1/j)\end{aligned} \tag{3.42}$$

Using $\mathbb{V} = \mathbb{V}_1$ we get

$$\frac{d^l}{dj^l}(\frac{1}{2j}\mathbb{V}(1/j))_{|_{j=0}} = l!(\int_a^b \mu^l v(\mu)d\mu) = l!\dot{\mathsf{F}}_l \tag{3.43}$$

so the generating function for $\dot{\mathsf{F}}_l(g)$ is

$$\begin{aligned}\dot{\mathsf{F}}(g,j) &= \sum_{l=0}^{\infty} j^l\dot{\mathsf{F}}_l(g) = \frac{1}{2j}\mathbb{V}(1/j) \\ &= \frac{1}{2j^2} - \frac{g}{2j^3} - \frac{1}{2j^2}(1 - \frac{c}{2} - \frac{g}{j})\sqrt{1 - c\frac{j}{g} + (\frac{3}{4}c^2 - c)(\frac{j}{g})^2} \\ &= 1 + \frac{1}{64g^3}(3c^4 - 8c^3 + 4c^2)j + O(j^2)\end{aligned} \tag{3.44}$$

where we have used Eq. (3.32) and Taylor expansion. From this we get

$$\dot{\mathsf{F}}_1(g) = \frac{1}{64g^3}(3c^4 - 8c^3 + 4c^2) = g + 4g^3 + 32g^5 + O(g^7) \tag{3.45}$$

The $1+4$ first diagram can be drawn as shown in Fig. (3.6).

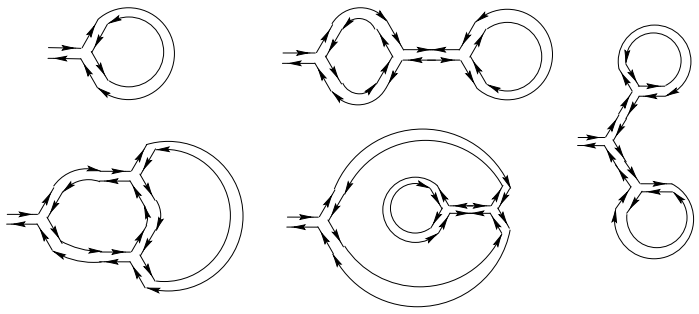

Figure 3.6: Diagrams for the first 5 rooted triangulations.

Note that all these diagrams (as expected) have a statistical weight of 1, since the two lines on the external leg is distinguishable (one is an upper index, the other a lower) or

in other words, the triangulation is oriented. Notice also that the diagrams all have two loops. The diagram with no loops are not contributing in the large N limit.

We could find a general formula for $\dot{\mathsf{F}}_l(g)$, we will, however, abstain from this, since it turns out to be somewhat complicated, and we will not need it anyway.

In the special case of $g = 0$ we find

$$\dot{\mathsf{F}}(0,j) = \frac{1}{2}j^{-2}(1-\sqrt{1-4j^2}) = 2\sum_{m=1}^{\infty} \frac{,\,(m+\frac{1}{2})}{,\,(m+1),\,(\frac{1}{2})(2m-1)}(2j)^{2m-2} = 1+j^2+2j^4+5j^6+O(j^8) \tag{3.46}$$

The "triangulations" corresponding to this limit contains no triangles, so what we count is branched rooted polymers (see Fig. (3.7)).

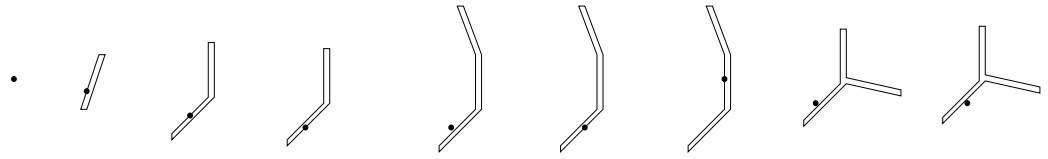

Figure 3.7: The first 9 rooted branched polymers.

As in the case of closed triangulations we can let $g = e^{-\mu}$ and if we also introduce the discrete cosmological constant for the boundary ξ and let $j = e^{-\xi}$ we get

$$\dot{\mathsf{F}}(\mu,\xi) = \sum_{n,l} e^{-\mu n} e^{-\xi l} \dot{\mathsf{F}}_{l,n} \tag{3.47}$$

which is the discrete form for the partition function for a universe with a boundary. We can note in passing that the branched polymer limit $g = 0$ correspond to an infinite cosmological constant $\mu \to \infty$.

Let us look at an important property for a one loop diagram. Either the marked link is a part of a triangle (the propagator end at a vertex), or a double link (the propagator end on the multi-ped). In the first case we can remove the triangle and get a triangulation with one more boundary link, in the second case we can remove the double link, and we obtain a splitting in two triangulations, one corresponding to the part of the diagram on each side of the propagator. These two procedures are illustrated in Fig. (3.8), where F indicate a loop diagram (possibly with more than one external leg). Note that in both cases the marks on the processed diagram are uniquely determined (using the orientation of the triangles) by the marking on the original triangulation.

We can reverse this process, and construct all possible one loop diagrams with a marked boundary of length l in the following way. Take all loop diagrams with a loop of length $l+1$ and connect a triangle to the marked leg and the neighboring leg (using the orientation to decide which neighbor to choose). Mark the last, free, leg, and we have obtained a triangulation with boundary l. Take also all pairs of loop diagrams which together has $l-2$ legs and glue these onto a prefabricated multiped with l legs of which two is already contracted by means of a propagator. Again we obtain a boundary of length l. From this we realize the following relation for the generating function must hold

$$\dot{\mathsf{F}}(g,j) = \frac{g}{j}\dot{\mathsf{F}}(g,j) + j^2\dot{\mathsf{F}}^2(g,j) \tag{3.48}$$

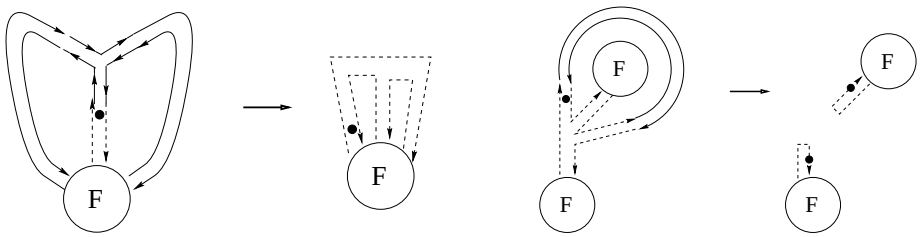

Figure 3.8: A diagrammatic representation of the loop equation.

Strictly speaking the decomposition/construction only work for large triangulations, for instance the empty triangulation corresponding to $\dot{\mathsf{F}}_{0,0}$ can not be decomposed (nor constructed) in this way. Correcting for this we obtain the *loop equation*

$$\dot{\mathsf{F}}(g,j) = \frac{g}{j}(\dot{\mathsf{F}}(g,j) - 1 - j\dot{\mathsf{F}}_1(g)) + j^2\dot{\mathsf{F}}^2(g,j) + 1 \tag{3.49}$$

where we in addition to adding the term +1 for the empty triangulation, have subtracted $\frac{g}{j}(1 + j\dot{\mathsf{F}}_1(g))$ since the first construction of inserting a triangle only works if the loop diagram we start with have more than 1 link. This equation is not only consistent with our solution Eq. (3.44), but can actually be used as a starting point for deriving it, see e.g.[51]. Since we already have obtained the solution we will not follow this path any further, and instead turn toward the introduction of more loops.

3.5 More loops

Having considered one loop on the surface, the most obvious generalisation would be to look at more loops in the same way. Let us consider $\langle N\mathrm{tr}M^{l_1}N\mathrm{tr}M^{l_2}\rangle$. This will count not only connected diagrams as in Fig. (3.9) (a), but also disconnected ones (b). Since

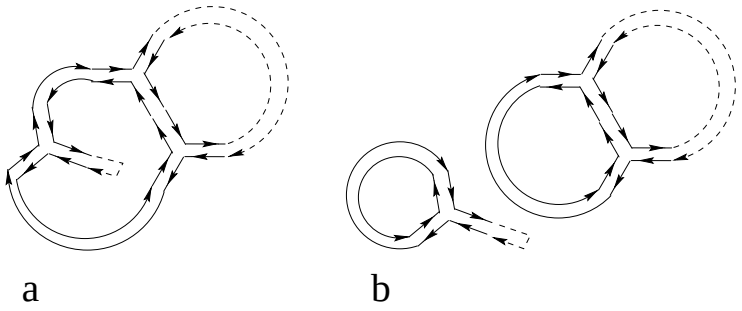

Figure 3.9: Connected and disconnected examples of two loop diagrams.

we are only interested in connected diagrams we can represent two loops by

$$\ddot{\mathsf{E}}_{l_1 l_2} = \langle \mathrm{tr}M^{l_1}\mathrm{tr}M^{l_2}\rangle - \langle\frac{1}{N}\mathrm{tr}M^{l_1}\rangle\langle\frac{1}{N}\mathrm{tr}M^{l_2}\rangle \tag{3.50}$$

We can also state the difference between the two diagrams in Fig. (3.9) in another way. If we remove the two boundary polygon and introduce one 3-gon instead, the second diagram can still be contracted to represent a boundary (of length 3) on the sphere, whereas the first will have only have one loop, and hence a value suppressed by $\frac{1}{N^2}$. It will therefore correspond to a boundary on the torus. A way to think of this is that we can take a sphere with two boundaries and glue them together to form a torus (with a boundary), whereas two spheres each with a boundary gives a sphere (with a boundary) when glued together along the boundaries. The new boundary can be viewed as a self-intersecting loop (See Fig. (3.10)).

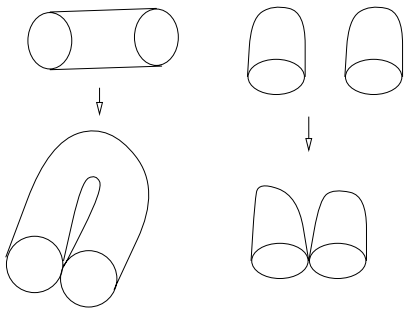

Figure 3.10: The formation of a torus with a boundary and a sphere with a boundary, from a connected and a disconnected two loop amplitude respectively.

We can also reverse this construction, by taking a triangulation with a loop of length $l = l_1 + l_2$ and replace the l-gon with a l_1 and a l_2-gon. In this way we obtain a two loop diagram, albeit a somewhat special one. On one hand we cannot be sure that the new diagram is connected. On the other hand we know from the origin as a one loop diagram, that no line from the diagram will separate the two multi-peds, they are in the same sector of the diagram. The interpretation is that the new diagram represents rather one self intersecting loop, than a genuine two loop triangulation. Since the multi-peds were just introduced to help in the counting, they should not be regarded as a part of the diagram. If we ignore them we arrive at the conclusion that a one loop diagram is equivalent to a diagram with a loop that intersect itself. The other way around is also valid, since a loop that intersects itself can be thought of as two loops touching each other. This means that the multi-peds must be placed at the same sector of the diagram, i.e. the should not have to cross any lines to meet. This is exactly the requirement for having a one loop triangulation of the sphere.

We are thus lead to the following general conclusion. We can connect any two triangles at the spikes without changing the diagram. If we connect sides, it is a complete different matter, and we will obtain a new diagram, i.e a different triangulation.

The above treatment of two loops can be generalized to any number of loops, but we will not pursue this further. Instead we will introduce the concept of distance between loops.

3.6 Loops with separation.

We will impose a further bound on the two loop amplitude in Eq. (3.50), namely that the two loops should be separated by a distance d, in the following sense. We say that a link, i.e. a propagator, is a distance d away from another link, if d is the minimal number of vertices passed through on any route from one to another.

$$d(\text{link}_1, \text{link}_2) = \min_{r \in \text{route from link}_1 \text{ to link}_2} \text{number of vertices in r} \tag{3.51}$$

We can generalize to the concept of distance between a link and a loop:

$$d(\text{loop}, \text{link}_2) = \min_{\text{link}_1 \in \text{loop}} d(\text{link}_1, \text{link}_2) \tag{3.52}$$

To convince ourself that these definitions makes sense we can consider the case of a flat triangulation (Fig. (3.11)).

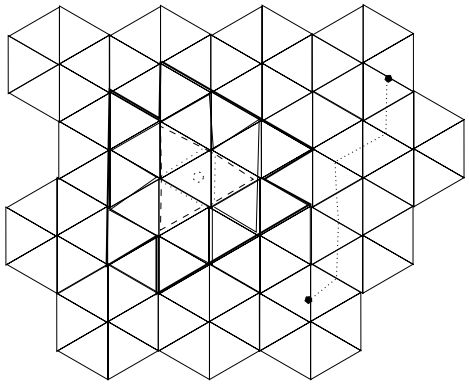

Figure 3.11: Distance on a flat triangulation. The number of links from a center grows as: $3, 6, 12, 15, 21, 24 \ldots$ i.e (approx.) linearly.

We see that the distance measure is not exactly geodesic distance. It does however have some pleasant features among which are:

- $d(\text{link}_1, \text{link}_2) \geq 0$
- $d(\text{link}_1, \text{link}_2) = 0 \Rightarrow \text{link}_1 = \text{link}_2$
- $d(\text{link}_1, \text{link}_2) + d(\text{link}_2, \text{link}_3) \geq d(\text{link}_1, \text{link}_3)$ (triangle inequality).
- For the flat plane the length of the loop of links which has distance d to some fixed point, grows linearly with the distance.

The first three properties show that d does indeed give our triangulation the structure of a metric space, and the last quality show that our distance measure gives a Hausdorff dimension of 2 for the flat plane, as expected. We will see later that when we sum over all triangulations we obtain a different dimension for the effective surface.

As d is a lattice distance is does posses some peculiarities

- In general there will be many routes which gives the (same) minimal distance.
- Two links which meet at a point can nevertheless be arbitrary far apart if enough triangles meet at the same point.

None of these features are very welcome if we expect d to describe distance on a flat surface. On a curved surface they are not as disturbing. Even the (true) geodesic distance could be obtained by following various routes, e.g. any great circle gives the minimal distance from the south to the north pole on a sphere. Our d gives a (unwanted) choice of route even in the flat case. This is an (unfortunate) effect of the discretization. To some extent also the last property is an artifact of the discretization, which forces any two links to have a distance of at least 1 between them. But it also reflects the fact that distances gets distorted in the neighborhood of large curvature.

The upshot of this whole discussion is that we should be somewhat precautios when using our distance measure. We will see shortly (Sec. (3.7)) how to take care of some of the discretization effects. We will also see (later, Sec. (4.6)) how the "problem" disappear when we take the continuum limit. This is an important demonstration, as it support the hope that our distance reduces to that of geodesic distance in the continuum limit.

We now consider a triangulation with two loops, and impose the condition that any link on the second loop should be separated by d from the first loop.

$$\forall \text{link}_2 \in \text{loop}_2 : d(\text{loop}_1, \text{link}_2) = d \tag{3.53}$$

Notice the slight asymmetry, that whereas any link on loop_2 will have a distance d from loop_1 there might be links on loop_1 which have a greater distance to loop_2. An example is shown in Fig. (3.12) where the thick loop has a distance $d = 1$ from the dotted loop.

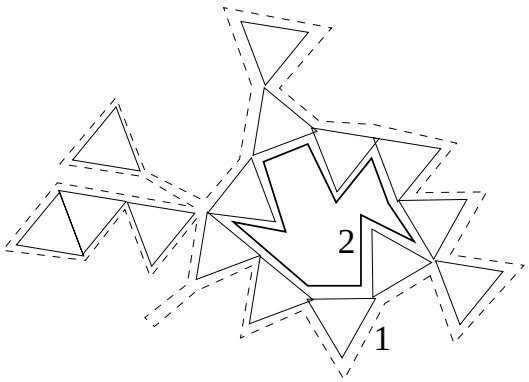

Figure 3.12: Two loops separated by a distance $d = 1$

If we start with a loop of length l_1 and want to consider how many triangulations gives a loop of length l_2 such that loop_2 has a distance $d = 1$ from loop_1 we can proceed in the following way.

Consider a diagram with a loop of length l_1. If we move one step away (one vertex down in Fig. (3.13)) from the l_1-ped and mark the propagators, we can interpret the marked propagators as parts of a set of new loops. In general the propagators will be

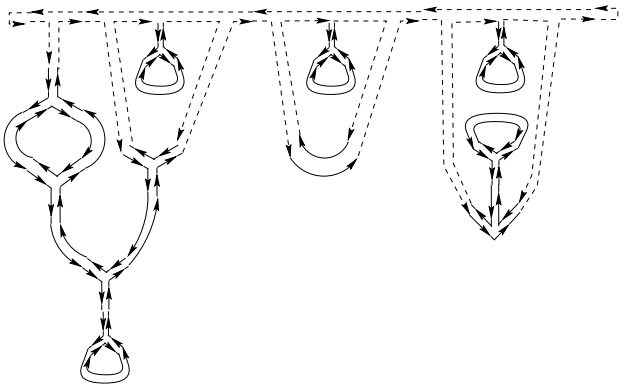

Figure 3.13: A general loop diagram.

in different sectors of the diagram, separated by a closed loop. From the triangulation point of view this means the links are part of different loops. Let us choose one of the sectors and cut away everything in that part of the diagram, leaving only the l_1-ped, the vertices we crossed, and the other sectors. The result is a diagram with the four distinct structures shown in Fig. (3.14).

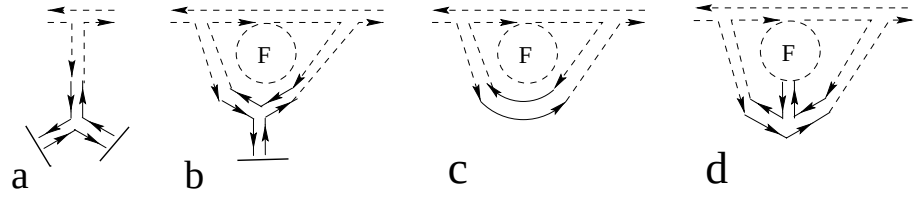

Figure 3.14: The structures arising when seeping down one step

The F's in the figure represents a loop diagram, and the solid lines are the places where we cut away the chosen sector. We can now glue on a multi-ped to the amputated legs, and this can be interpreted as a loop with distance $d = 1$.

We can also look at this procedure from the triangulation point of view[20]. Here the climbing down one step will correspond to a one step deformation of the loop, and the structures corresponding to Fig. (3.14) have the form shown in Fig. (3.15).

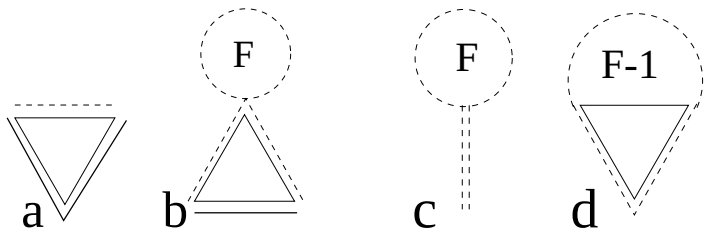

Figure 3.15: The structures from which two loops with distance $d = 1$ can be build

We notice that the F's represents parts of loop_1 which is farther away than $d = 1$ from loop_2.

We can now build up all triangulations with two loop separated by a distance $d = 1$ by combining the structures (a)-(d) shown in Fig. (3.15). To count the number of such diagrams we introduce the generating function:

$$\mathsf{N}(g, j_1, j_2) = \sum_{l_1, l_2=0}^{\infty} j_1^{l_1} j_2^{l_2} \mathsf{N}_{l_1 l_2}(g) = \sum_{l_1, l_2, n=0}^{\infty} j_1^{l_1} j_2^{l_2} \mathsf{N}_{l_1 l_2, n} g^n \tag{3.54}$$

where $\mathsf{N}_{l_1 l_2}(g)$ is the weight of triangulations with a loop of length l_1 and a exit loop of length l_2, and $\mathsf{N}_{l_1 l_2, n}$ is the number of such with n triangles.

Imagine now the construction of a diagram as putting beads on a string. For each bead we have the possibilities (a)-(d). Every time we put a bead of type (a) on the string, the following happens. We make loop_1 one link longer, loop_2 two links longer, and we add a triangle to the triangulation. The result is that we have a contribution of the form $g j_1 j_2^2$. The other contribution can be found in the same way, using that $\dot{\mathsf{F}}(g, j)$ is the generating functional for one loop diagrams.

If we stop after k beads, and glue the ends together we have exactly a triangulation with two loops separated by distance $d = 1$. An example (with $k = 12$) is shown in Fig. (3.12). We could have build the same string of beads starting at a different point. Taking this cyclic symmetry into account we arrive at the following expression for the generating function:

$$\begin{aligned} \mathsf{N}(g, j_1, j_2) &= \sum_{k=0}^{\infty} \frac{1}{k} [g j_1 j_2^2 + g j_1^2 j_2 \dot{\mathsf{F}}(g, j_1) + g j_1 (\dot{\mathsf{F}}(g, j_1) - 1) + j_1^2 \dot{\mathsf{F}}(g, j_1)]^k \\ &= -\log[1 - g j_1 j_2^2 - g j_1^2 j_2 \dot{\mathsf{F}}(g, j_1) - g j_1 (\dot{\mathsf{F}}(g, j_1) - 1) - j_1^2 \dot{\mathsf{F}}(g, j_1)] \end{aligned} \tag{3.55}$$

For convenience we mark the exit loop. The generating function for this is obtained as:

$$\dot{\mathsf{N}}_{l_1, l_2}(g) = l_2 \mathsf{N}_{l_1, l_2}(g) \qquad \dot{\mathsf{N}}(g, j_1, j_2) = j_2 \frac{\partial}{\partial j_2} \mathsf{N}(g, j_1, j_2) \tag{3.56}$$

since there is l_2 ways of placing the mark, and this factor exactly is obtained by differentiating with respect to j_2. We use the notation already introduced for $\dot{\mathsf{F}}$ that dotted partition functions refers to marked loops.

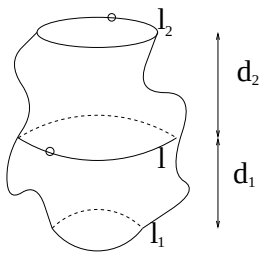

Figure 3.16: The decomposition in two cylinders

To get the generating functional for loops separated by a distance d we notice that for $d = 2$

$$\begin{aligned}\dot{\mathsf{N}}_2(g, j_1, j_2) &= \sum_{l,m,l_1,l_2=1}^{\infty} j_1^{l_1} \dot{\mathsf{N}}_{l_1 l} j_2^{l_2}(g) \dot{\mathsf{N}}_{m l_2}(g) \delta_{lm} \\ &= \frac{1}{2i\pi} \oint \dot{\mathsf{N}}(g, j_1, \frac{1}{z}) \dot{\mathsf{N}}(g, z, j_2) \frac{dz}{z} \end{aligned} \tag{3.57}$$

where we have used $\delta_{lm} = \frac{1}{2i\pi} \oint z^{m-l} \frac{dz}{z}$, valid for any curve which go once around the origin $z = 0$ in the complex plane. The above expression is easily generalized to the composition law

$$\dot{\mathsf{N}}_{d_1+d_2}(g, j_1, j_2) = \frac{1}{2i\pi} \oint \dot{\mathsf{N}}_{d_1}(g, j_1, \frac{1}{z}) \dot{\mathsf{N}}_{d_2}(g, z, j_2) \frac{dz}{z} \tag{3.58}$$

This equation has an obvious geometric interpretation as the split of a cylinder of height $d_1 + d_2$ into two cylinders of height d_1 and d_2 respectively, see Fig. (3.16).

To resume we have, following Ishibashi and Kawai[20], obtained the generating functional $\dot{\mathsf{N}}_d$ for two loops, where each link on the second (marked) loop has a distance d from the first.

3.7 Relaxed distance

We can note that the concept of selfintersecting loops as discussed in Sec. (3.5), give rise to the following seemingly paradoxical situation. If we consider the two part of the loop as distinct, we can find triangulations where the two loops are arbitrary far away from each other, although they are considered as sharing a point (at the intersection). This is a simple consequence of the above mentioned peculiarity that two links meeting at a point, might have nonzero distance. We can avoid this if we attach a double link to the triangulation at the point of intersection. On the dual graph this result in a propagator between the legs of the two peds. We have thus made the boundary loop two links longer, and we see that the number of diagrams with two loops of length l_1 and l_2 separated by a distance of zero (now in the sense of the minimum distance) is given by the number of diagrams with a marked loops of length $l_1 + l_2 - 2$. We write this as

$$\mathsf{G}_{l_1,l_2}(g) = \dot{\mathsf{F}}_{l_1+l_2-2}(g) \tag{3.59}$$

or in terms of the generating function

$$\mathsf{G}(g, j_1, j_2) = \sum_{l_1,l_2=1}^{\infty} j_1^{l_1} j_2^{l_2} \dot{\mathsf{F}}_{l_1+l_2-2}(g) \tag{3.60}$$

We can now glue a cylinder on one of the loops in order to count the number of possible triangulations with a minimal distance of d. This amount to the following calculation

$$\begin{aligned}\mathsf{G}_d(g, j_1, j_2) &= \sum_{l,m,l_1,l_2=1}^{\infty} j_1^{l_1} \dot{\mathsf{N}}_{d,l_1 l}(g) j_2^{l_2} \mathsf{G}_{m l_2}(g) \delta_{lm} \\ &= \frac{1}{2i\pi} \oint \dot{\mathsf{N}}_d(g, j_1, \frac{1}{z}) \mathsf{G}(g, z, j_2) \frac{dz}{z} \end{aligned} \tag{3.61}$$

Note that we have no marks on G. The reason is that the mark on the exit of the cylinder was used to count the different ways we could glue the two loops together.

It is perhaps instructive to express the former generating function in terms of $\dot{\mathsf{F}}$. Instead of gluing one cylinder onto one of the loops, we will glue a cylinder to each. Choose d_1 and d_2 such that $d = d_1 + d_2$ then

$$\begin{aligned}
\mathsf{G}_d(g, j_1, j_2) &= \sum_{k,l,m,n,l_1,l_2=1}^{\infty} j_1^{l_1} \dot{\mathsf{N}}_{d_1,l_1 k}(g) \mathsf{G}_{lm}(g) \dot{\mathsf{N}}_{d_2,l_2 n}(g) j_2^{l_2} \delta_{kl} \delta_{mn} \\
&= \sum_{k,l,m,l_1,l_2=1}^{\infty} j_1^{l_1} \dot{\mathsf{N}}_{d_1,l_1 k}(g) \dot{\mathsf{F}}_{l+m-2}(g) \dot{\mathsf{N}}_{d_2,l_2 m}(g) j_2^{l_2} \delta_{kl} \\
&= \oint \dot{\mathsf{N}}_{d_1}(g, j_1, \frac{1}{z}) z^2 \dot{\mathsf{F}}(g, z) \dot{\mathsf{N}}_{d_2}(g, j_2, \frac{1}{z}) \frac{dz}{z}
\end{aligned} \tag{3.62}$$

where we have inserted $\delta_{kl} = \oint z^{-k+(l+m-2)-m} z^2 \frac{dz}{z}$. A sketch of this situation is shown in Fig. (3.17).

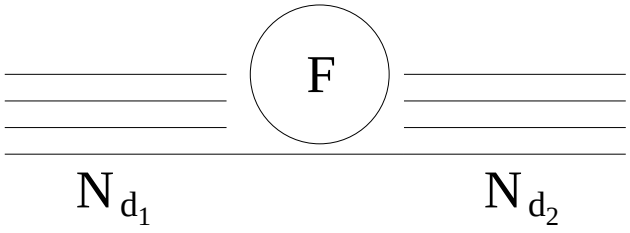

Figure 3.17: The diagram corresponding to two loops with a minimal distance of d can be composed from two cylinder diagrams glued together with a cap and a propagator.

As we saw above it is of some importance to keep track of the marking when we do the gluing. A general rule is that when gluing two loops together one of them should be marked, since this will ensure that we take into account the different ways of gluing. The markings also serve a slightly different purpose in the present case. The marks on the exit loops is used to identify which legs should be connected by the propagator. The mark on the cap is then used more conventionally to count the number of ways we can glue onto the composite of the two exit loops.

Furthermore, due to the asymmetry of $\dot{\mathsf{N}}$, it is important that it is the exit loops, where every point has distance d_1 respectively d_2 from the entrance loop, and not the entrance loops we glue together. Otherwise we could not be sure that the minimum distance was $d = d_1 + d_2$.

Let us end this chapter with a very short overview of what we have done. As promised in the beginning of the chapter we have introduced discrete versions of most of the concepts from the preceding discussion of the continuum approach. We have indeed found a generating function for triangulations with a single boundary and for those with two boundaries at a certain distance from each other. In the next chapter we will show how we can actually find continuum versions from these by a well defined limiting procedure.

Chapter 4

The continuum limit

Until now we have been investigating the behaviour of triangulations with a finite number of triangles. We now want to look at the limit where the various partition functions diverge as a power expansion in g and j. In this limit diagrams with a large number of triangles will dominate, and we can hope to make a sensible continuum limit by rescaling the loop length and the area as we approach the critical point $g \sim g_{crit}$, $j \sim j_{crit}$.

4.1 The continuum limit

If we look once again at the generating function for one marked loop,

$$\sum_{l,n=0}^{\infty} j^l g^n \dot{\mathsf{F}}_{l,n} = \frac{1}{2j^2}\left(1 - \frac{g}{j} - (1 - \frac{1}{2}c - \frac{g}{j})\sqrt{1 - c\frac{j}{g} - (c - \frac{3}{4}c^2)(\frac{j}{g})^2}\right) \tag{4.1}$$

we notice that the power series in j diverge when j becomes a root in the equation $g^2 - gcj - (c - \frac{3}{4}c^2)j^2$. Within the smallest root

$$j_{crit}(g) = 2g\frac{c - \sqrt{c(2-c)}}{3c^2 - 4c} \tag{4.2}$$

the function is analytic with regard to j. As we shall see soon this gives us the possibility to approach the critical point in a suitable way, so as to obtain a continuum limit. Before this, let us recall the analyticity properties with respect to g. The only way the power series in g will diverge is if the expansion of $c(g)$ in terms of g diverges. This will happen exactly when Eq. (3.28) acquires a double root, since at this point the solution to the cubic equation (3.28) is obtained by taking the square root in zero, where the square root has branch point, and the Taylor series diverge.

The discriminant for Eq. (3.28) is given by

$$D = 16g^4 - \frac{1}{3^3}$$

from which

$$g_{crit} = \frac{1}{2}3^{-3/4} \qquad c_{crit} = 1 - 3^{-1/2} \tag{4.3}$$

For comparison with the $g = 0$ case the distribution of eigenvalues at g_{crit} is depicted in Fig. (4.1). We note the important feature that the behavior in the positive end point

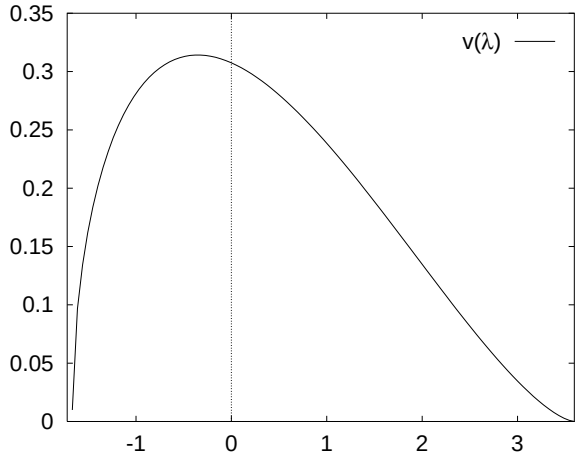

Figure 4.1: The critical distribution.

has changed from a squareroot to the more well behaved $\lambda^{3/2}$. This is a very important consequence of the fact that the g has a critical point.

The critical value of j at $g = g_{crit}$ is found to be

$$j_{crit} = \frac{1}{2}(3^{1/4} - 3^{-1/4}) \tag{4.4}$$

In order to see how we should approach the critical point let us estimate how the number of triangulations grow as we increase l and n. Since the sum is convergent for any $j < j_{crit}, g < g_{crit}$ it is clear that we must have an exponential bound on the number of triangulations:

$$\dot{\mathsf{F}}_{l,n} < e^{l\xi} e^{n\mu} \tag{4.5}$$

which is valid for any suitable constants

$$\xi > \xi_{crit} \equiv -\log j_{crit} \quad \text{and} \quad \mu > \mu_{crit} \equiv -\log g_{crit} \tag{4.6}$$

as long as l and n is large enough. From the divergence of the sum for $j > j_{crit}$ we can conclude that we also have an exponential lower bound

$$e^{l\xi} e^{n\mu} < \dot{\mathsf{F}}_{l,n} \tag{4.7}$$

valid for any

$$\xi < \xi_{crit} \quad \text{and} \quad \mu < \mu_{crit} \tag{4.8}$$

when l and n becomes large. In short we expect $\dot{\mathsf{F}}_{l,n} \sim e^{l\xi_{crit}} e^{n\mu_{crit}}$

If we want to see power correction to this generic exponential behaviour, we have look a bit closer at the expansion. Let us first consider the expansion in j at some fixed g i.e.

the coefficients $\dot{\mathsf{F}}_l(g)$. The part which diverge is the last term, which we can write (using $j_{crit}(g)$ is a root):

$$\sqrt{1 - c\frac{j}{g} - (c - \frac{3}{4}c^2)(\frac{j}{g})^2} = a(j)\sqrt{1 - \frac{j}{j_{crit}(g)}} \tag{4.9}$$

where $a(j)$ is some function of j which is analytic at $j = j_{crit}(g)$. From the Taylor expansion

$$\sqrt{1-x} = 1 - \sum_{m=1}^{\infty} \frac{, (m + \frac{1}{2})}{, (m+1), (\frac{1}{2})(2m-1)} x^m \tag{4.10}$$

and Stirling's approximation:

$$, (m+1) = \sqrt{2\pi m} m^m e^{-m}(1 + O(\frac{1}{m})) \tag{4.11}$$

we see that the coefficients to the m'th order term in the expansion of the square root goes as $\frac{1}{2\sqrt{\pi}} m^{-3/2}$ for large m. This give us the the following estimate (where $\sim$ indicate we have ignored terms analytic as $j \to j_{crit}(g)$ and dropped an overall constant):

$$j^l \dot{\mathsf{F}}_l(g) \sim (\frac{j}{j_{crit}(g)})^l (l^{-3/2} + O(l^{-5/2})) \tag{4.12}$$

only taking the most significant power correction we have:

$$\dot{\mathsf{F}}_l(g) \sim j_{crit}^{-l}(g) l^{-3/2} \tag{4.13}$$

From this we see that the asymptotic behavior of $\dot{\mathsf{F}}_l$ is independent of the value of g (as long as it is kept fixed), and that it corresponds to the asymptotic behavior of the branched polymer case $g = 0$.

By similar considerations for the power expansion of $c(g) = \sum c_n g^n$ we can obtain (again ignoring overall constants and only taking most significant correction)

$$c_n \sim g_{crit}^{-n} n^{-3/2} \tag{4.14}$$

which for any fixed l should give us the asymptotic behaviour of $\dot{\mathsf{F}}_{l,n}$, in specific we would expect

$$\dot{\mathsf{F}}_{1,n} \sim g_{crit}^{-n} n^{-3/2} \tag{4.15}$$

Here the above approach plays a trick on us. Remember that the generating function for $\dot{\mathsf{F}}_{1,n}$ is given by $\dot{\mathsf{F}}_1 = \frac{1}{64g^3}(3c^4 - 8c^3 + 4c^2)$. A more careful investigation will reveal that the most significant correction is actually cancelled among the the different terms in this expression. This means that we should use the second most significant term and the expression becomes

$$\dot{\mathsf{F}}_{1,n} \sim g_{crit}^{-n} n^{-5/2} \tag{4.16}$$

This cancellation is no coincidence, but more or less a direct consequence of the change of endpoint behavior for v mentioned above.

Now we want to approach j_{crit} and g_{crit} simultaneously. In order to avoid the surprises associated with cancellations, we will consider a more systematic method to extract the asymptotic behavior.

To do this let us introduce the physical characteristic length of the triangles ϵ. The physical area of a triangulation is now $V = \epsilon^2 n$ and the length of the boundary is $L = \epsilon l$. With these definitions, and introducing $\mu = -\log g$ and $\xi = -\log j$ we can write $\dot{\mathsf{F}}(g, j)$ as

$$\dot{\mathsf{F}}(\mu, \xi) = \sum_{n,l} e^{-\frac{\mu}{\epsilon^2}V} e^{-\frac{\xi}{\epsilon}L} \dot{\mathsf{F}}_{n,l} \tag{4.17}$$

From the above considerations we expect

$$\dot{\mathsf{F}}_{n,l} \sim l^\alpha n^\beta e^{l\xi_{crit}} e^{n\mu_{crit}} = (\frac{L}{\epsilon})^\alpha (\frac{V}{\epsilon^2})^\beta e^{l\xi_{crit}} e^{n\mu_{crit}} = \epsilon^{-\alpha-2\beta-3} \dot{F}(V, L) \epsilon^3 e^{L\frac{\xi_{crit}}{\epsilon}} e^{V\frac{\mu_{crit}}{\epsilon^2}} \tag{4.18}$$

for some critical exponents α and β and $\dot{F}(V, L) \equiv V^\beta L^\alpha$.

Inserting in Eq. (4.17) we get

$$\dot{\mathsf{F}}(\mu, \xi) \sim \sum_{n,l} e^{-\frac{\mu-\mu_{crit}}{\epsilon^2}V} e^{-\frac{\xi-\xi_{crit}}{\epsilon}L} \epsilon^{-\alpha-2\beta-3} \dot{F}(V, L) \epsilon^3 \tag{4.19}$$

So in order to keep the physical cosmological constant $\Lambda = \frac{\mu-\mu_{crit}}{\epsilon^2}$ and $X = \frac{\xi-\xi_{crit}}{\epsilon}$ finite as we let $\epsilon \to 0$ we should approach the critical point in the following way:

$$j = j_{crit} e^{-\epsilon X} \qquad g = g_{crit} e^{-\epsilon^2 \Lambda} \tag{4.20}$$

In this limit the sum becomes an integral with respect to $dV = \epsilon^2$ and $dL = \epsilon$. In conclusion we can obtain

$$\dot{F}(\Lambda, X) \equiv \int e^{-\Lambda V - XL} \dot{F}(V, L) dV dL \tag{4.21}$$

by extracting the nonanalytic part of $\lim_{\epsilon\to 0} \dot{\mathsf{F}}(\mu, \xi)$ and multiply this with $\epsilon^{\alpha+2\beta+3}$. Let us therefore proceed to take this limit.

Inserting Eq. (4.20) in Eq. (3.30) a straight forward calculation reveal

$$c(g) = c_{crit} - \frac{2}{3}\sqrt{\Lambda}\epsilon + \frac{2}{9\sqrt{3}}\Lambda\epsilon^2 - \frac{22}{81}\Lambda^{3/2}\epsilon^3 + O(\epsilon^4) \tag{4.22}$$

and from this we get by inserting in Eq. (4.1)

$$\dot{\mathsf{F}}(g_{crit}e^{-\epsilon^2\Lambda}, j_{crit}e^{-\epsilon X}) = \frac{1}{2}(1+\sqrt{3})(1-\sqrt{3}\epsilon X) + \frac{1}{4}(1+\sqrt{3})^{5/2}\dot{F}(\Lambda, X)\epsilon^{3/2} + O(\epsilon^2) \tag{4.23}$$

where

$$\dot{F}(\Lambda, X) = (2X - \sqrt{,})\sqrt{X + \sqrt{,}} \tag{4.24}$$

and

$$, = \frac{4(\sqrt{3}-1)^2}{3}\Lambda \tag{4.25}$$

We have introduced , purely for convenience, since it makes the formulas shorter. We will use , and Λ interchangeable as the cosmological constant in the following. This is certainly allowed since we have used only a characteristic length in our definition of the area/side-length, and hence have no strict set of units for macroscopic entities, such as V, L, Λ and , . This should not cause any confusion, as long as we use the same units when comparing derived results.

The first term of $\dot{\mathsf{F}}$ stems from the analytical part $\frac{1}{2j^2}(1-\frac{g}{j})$ and should be dropped as it corresponds to triangulations with one or zero triangles.

After a "wave-function" renormalisation, i.e. the multiplication with $\epsilon^{\alpha+2\beta+3} = \epsilon^{-3/2}$, we are left with the universal part $\dot{F}$, meaning the part which survives the removal of any finite set of triangulations, and hence (hopefully) is independent of our choice of discretization scheme.

It is now quite easy to remove the mark on the loop by noticing that the generating function for loops without mark F must satisfy

$$\frac{\partial}{\partial X}\mathsf{F}(g, j_{crit}e^{-\epsilon X}) = -\epsilon j\frac{\partial}{\partial j}\mathsf{F}(g, j_{crit}e^{-\epsilon X}) = -\epsilon\dot{\mathsf{F}}(g, j_{crit}e^{-\epsilon X}) \tag{4.26}$$

which imply

$$\mathsf{F}(g,j) = -\epsilon\int\dot{\mathsf{F}}(g,j)dX = k\epsilon + \frac{1}{4}(1+\sqrt{3})(\sqrt{3}\epsilon^2X^2 - 2\epsilon X) + \frac{1}{10}(1+\sqrt{3})^{5/2}F(\Lambda,X)\epsilon^{5/2} + O(\epsilon^3) \tag{4.27}$$

where k is some (non-universal) constant and

$$F(\Lambda, X) = (\sqrt{\ ,}\,X + 3,\ -2X^2)\sqrt{X + \sqrt{\ ,}} \tag{4.28}$$

is the universal part.

We can also use our method to find the continuum limit of $\dot{\mathsf{F}}_1(g)$. Inserting Eq. (4.22) in Eq. (3.45) reveal

$$\dot{\mathsf{F}}_1(g) = 3^{1/4}\left(\sqrt{3} - \frac{3}{2} + \frac{75-43\sqrt{3}}{10\sqrt{3}-18}\Lambda\epsilon^2 + \frac{8(45-26\sqrt{3})}{3(45\sqrt{3}-78)}\Lambda^{3/2}\epsilon^3\right) + O(\epsilon^4) \tag{4.29}$$

which explicitly shows that the $\sqrt{\Lambda}\epsilon$ term vanishes, in accord with the above mentioned cancellation of the most significant power correction (it was actually with this demonstration in mind that we took so many terms in the expansion of $c(g)$ in Eq. (4.22)). We see that the universal part is $F_1(\Lambda) = \Lambda^{3/2}$ where we have removed the dot since there is only one link anyway.

As the reader might already have guessed the universal parts $F, \dot{F}$ and F_1 are to play the role of the continuum partition functions. Before we proceed to this identification we will take a minor detour in order to clarify the status of the parts we are about to throw away.

4.2 Nonuniversal Parts

What is the significance of the Non-Universal Parts (NUP's) encountered in the above calculation? And is there a systematic way of avoiding alternatively removing these parts?

As noted above the NUP's in our calculation arise from the part of Eq. (4.1) analytic in g, i.e. the first two terms. These two terms (proportional to g^0 and g^1) only contribute to triangulations with zero or one triangle. In the continuum limit these triangulations should be thrown away, since they will have microscopic (zero) volume, and the whole idea about the continuum limit was to count surfaces with a macroscopic volume. It might look a little arbitrary to throw certain terms away, and keep others, after all the NUP's seems dominating as $\epsilon \to 0$. Although the above arguments about macroscopic entities are completely valid, one would like a more systematic approach. Let us consider such. Instead of subtracting the NUP's away, let us differentiate them away. Indeed consider Eq. (4.1) and perform two differentiation with respect two g. Each differentiation can be viewed as the removal of a triangle, and a multiplication with a factor n for the different ways of doing this. In short,

$$\frac{\partial}{\partial g}\dot{\mathsf{F}}(g,j) = \frac{\partial}{\partial g}\sum_{n,l=1}^{\infty} g^n j^l \dot{\mathsf{F}}_{l,n} = \sum_{n,l=1}^{\infty} n g^{n-1} j^l \dot{\mathsf{F}}_{l,n} = \sum_{n,l=1}^{\infty} g^n j^l \hat{\mathsf{F}}_{l,n} = \hat{\mathsf{F}}(g,j) \tag{4.30}$$

This will leave us (after another differentiation) with a partition function $\hat{\hat{\mathsf{F}}}(g,j)$, not for triangulations with one boundary of length l, but for triangulation with one boundary of length l and two boundaries of length 3. We say that we have introduced two punctures in the surfaces. In taking the continuum limit we only scale the first loop, and keep the two punctures microscopic. The result will be a superficially more well defined continuum limit, in the sense that we do not have to throw (dominant) terms away. The two terms which caused any troubles have been removed by the differentiation. More over, the universal term will now be divergent as $\epsilon \to 0$ (in contrast to our case where it actually vanishes) and the renormalization will therefore be of a more conventional type, a division by an infinite constant instead of a multiplication with a such. An easy way to see this is by observing that as we take the continuum limit we have

$$\frac{\partial}{\partial g}\dot{\mathsf{F}}(g,j) = \frac{-1}{\epsilon^2 g_{crit}}\frac{\partial}{\partial \Lambda}\dot{\mathsf{F}}(g_{crit}e^{-\epsilon^2\Lambda}, j_{crit}e^{-\epsilon X}) \tag{4.31}$$

so any introduction of a puncture on the surface will lower the power of ϵ by two in each term. This also shows that already after insertion of one puncture we have a divergent universal part. Actually a short glance on Eq. (4.23) in conjunction with Eq. (4.31) will make it evident that the introduction of just one puncture, will be sufficient to eliminate the leading NUP. But why do we not need two differentiations, as we needed on the discrete level. The reason is quite straightforward. In taking the continuum limit we put $g \sim g_{crit}(1-\epsilon^2\Lambda)$. Its is only the first term which contribute to the leading NUP since the second term is proportional to ϵ^2 and is therefore dominated by the universal term. The first term (which do contribute to the leading NUP) is a constant and will therefore be removed by a single differentiation.

The conclusion is that in order to identify the universal part of an expression we should perform a number of differentiations with respect to g (or Λ if we already have taken the continuum limit). It is important to realize that it is no offence to do too many differentiations, as the universal part is determined by the limit of a infinite number of triangles. Any finite number of differentiation will only remove a finite set of triangles.

In terms of the generating function, n differentiations will cut of the first n terms in the expansion, which is immaterial for the continuum limit. For an explicit example we can consider the generating function for one loop. Loosely speaking the square root part will survive any number of differentiations, although it will change appearance slightly for each such introduction of a puncture (which is not surprising since we count surfaces with an increasing number of punctures).

Having sketched a systematic way of treating the non universal parts we now turn to the macroscopic content of the universal part.

4.3 Physical interpretation

Let us recall the form of the continuum partition function for a universe with a boundary Eq. (2.11):

$$F[\Lambda, X] = \int e^{-\Lambda V - XL} \mathcal{D}M \tag{4.32}$$

where V is the area of the surface and L is the length of the boundary.

Notice that $\dot{F}(V, L)$ which we introduced earlier can be interpreted as the density of triangulations with area between V and $V+\epsilon^2$ and marked boundary between L and $L+\epsilon$, i.e. the partition function for fixed area and marked boundary length. Now to get the partition function $F(V, L)$ for an unmarked loop of length L and with fixed area V we should divide by the loop length. This means that $\mathcal{D}M = F(V, L)dLdV = \frac{1}{L}\dot{F}(V, L)dLdV$. By comparing Eq. (4.32) with Eq. (4.21) we see that with this identification we have established a connection between our model and the continuum formalism, F playing the role of the Hartle-Hawking wave-function.

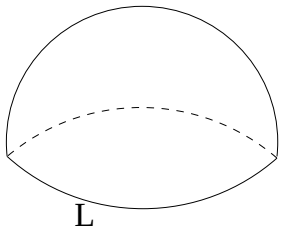

Figure 4.2: The loop of length L amplitude, or Hartle-Hawking wave-function

Since ϵ represents the characteristic length of the triangles we have immediately the following dimensions

$$\begin{aligned} [\epsilon] &= L \\ [\dot{F}] = L^{-3/2} \qquad & [F] = L^{-5/2} \\ [X] = L^{-1} \qquad & [,\,] = L^{-2} \end{aligned} \tag{4.33}$$

we note that the renormalization process have induced a nontrivial dimension to the partition function.

Before we proceed let us return to the question of non universal parts. This time from a continuum point of view. We saw earlier how we could remove NUP's by differentiating

with respect to Λ. We can now give this a new interpretation. Each differentiation brings down a factor of V in the integrand, as can be seen both from Eq. (4.32) and the fact that the insertion of a puncture give rise to a multiplication with the number of triangles in the triangulation (Cf. Eq. (4.30)). This will enhance the contribution from large universes, and hence suppress microscopic such. To further elucidate this point we can exploit some properties of the (inverse) Laplace transform. As explained in App. (D) the inverse Laplace transform of any polynomial has support in 0. In specific any term in $F(\Lambda, X)$ proportional to Λ^n for some integer $n \geq 0$ will stem from a part in $F(V, L)$ which has support in $V = 0$ (a delta function or derivatives thereof), and hence correspond to microscopic universes. Removing these (infinite) terms in $F(V, L)$ is identical to ignoring terms in the partition function which goes as Λ^n. This could for instance be obtained by differentiating $F(\Lambda, X)$ with respect to Λ, bringing us back to the systematic approach of last section. This would however mean that we would count surfaces with punctures, or in other word that we consider the Laplace transform of $V^n F(V, L)$. If we insist on counting surfaces without these we could remove the parts more directly by for instance expanding $F(\Lambda, X)$ in Λ and then subtract the part with Λ^n. We will see use of this method shortly.

All of these consideration goes for X and L as well. Differentiating $F(\Lambda, X)$ with respect to X removes NUP's in a systematic way (in this case microscopic loops), and changes the partition function to the Laplace transform of $LF(V, L)$. We have actually already used this in the opposite direction, namely when we integrated $\dot{F}$ with respect to X to get $F = \frac{1}{L}\dot{F}$. This introduced a NUP in the form of an integration constant k.

After this astray we return to the physical interpretation. Since F is the partition function for a universe with boundary, we have

$$\dot{F}(\Lambda, X) = -\frac{\partial F(\Lambda, X)}{\partial X} = \int L e^{-\Lambda V - XL} \mathcal{D}M \tag{4.34}$$

showing that $\dot{F}$ is the unnormalized expectation value for the length of a loop.

We can note that the reason we can obtain negative values for F and $\dot{F}$ for certain ranges of Λ, X is that for these values of X and Λ the partition function is dominated by triangulations with a finite number of triangles, but infinite loop length. In order to get sensible results for the expectation value we should remove these nonuniversal part by one the above mentioned methods. For instance differentiating twice with respect to Λ gives:

$$\frac{\frac{\partial^2}{\partial \Lambda}\dot{F}(\Lambda, X)}{\frac{\partial^2}{\partial \Lambda}F(\Lambda, X)} = \frac{1}{2\sqrt{,} + X} \tag{4.35}$$

We can also find the partition function for a closed universe $Z(\Lambda)$ by the following argument. Remember that F_1 as introduced earlier was the partition function for surfaces with a puncture (a microscopic boundary). This means that $F_1(\Lambda) \sim \int V Z(V) dV = \frac{\partial Z(\Lambda)}{\partial \Lambda}$. From Eq. (4.29) we have $F_1 \propto \Lambda^{3/2}$ and hence

$$Z(\Lambda) \propto \Lambda^{5/2} \tag{4.36}$$

From Eq. (4.16) we can also directly see $F_1(V) = V^{-5/2}$ and from $F_1(V) \sim V Z(V)$ we get

$$Z(V) \propto V^{-7/2} = V^{\gamma - 3} \tag{4.37}$$

where we have introduced the string susceptibility $\gamma = -1/2$ in order to compare with Liouville theory (Eq. (2.29)). We observe that the two theories agrees with respect to the critical exponent for the volume.

4.4 The operators $\mathcal{O}_k$

We now want to introduce a set of local operators. The idea is to consider a loop on the surface and then shrink it ad infinitum, the result being a puncture on the sphere. Introducing punctures in the surface can then be interpreted as insertion of operators, in a sense which will become more clear shortly.

We can obtain the effect of shrinkage in two ways. If we let the , $\to 0$ it will make the area $V \to \infty$, causing a relative shrinkage of the loop. More direct we can let $X \to \infty$ making the length $L \to 0$. Both cases correspond to an expansion of $\dot{F}$, the first in , the latter in X^{-1}. It turns out both expansions reveal the same result:

$$\dot{F}(, , X) = 2X^{3/2} - \frac{3}{4}, X^{-1/2} + \frac{1}{4}, {}^{3/2}X^{-3/2} + O(, {}^{5/2}) \tag{4.38}$$

which is not very surprising, since all terms must have the same dimension. What is surprising is perhaps that the term , ${}^{1/2}X^{1/2}$ have a coefficient equal to zero. This is again an effect of the cancellations mentioned in the discussion of the continuum limit of $\dot{F}_1$.

As argued in the preceding section, the first two terms of the expansion corresponds to universes with vanishing volume, and should hence be ignored. After having subtracted them, we can now write

$$\dot{F}(, , X) = \sum_{k=1}^{\infty} F_k(,)X^{-\frac{k+2}{2}} \tag{4.39}$$

We can obtain the thermodynamic limit[1] (Area $V \to \infty$) by taking , $\to 0$. And we see that only $F_1(,) = \frac{1}{4}, {}^{3/2}$ survives, since the other are suppressed by factors of $\Lambda \sim V^{-1}$. We write this as

$$F_1^{TD}(,) = F_1^{TD}, {}^{3/2} \tag{4.40}$$

where $F_1^{TD} = \frac{1}{4}$.

Finally we can interpret the coefficients of the expansion as (unnormalized) expectation values for operators $\mathcal{O}_k$. The coefficients F_k should not be confused with the continuum limit of $\dot{\mathsf{F}}_k$. The only exception is F_1 which can be thought of both as the limit of $\dot{\mathsf{F}}_1$ and the coefficient of $X^{-3/2}$. More on this in the following.

With the help of Eq. (4.33) and Eq. (4.36) we find the following dimensions

$$[F_k] = L^{-\frac{k+5}{2}} \qquad [\mathcal{O}_k] = [Z(\Lambda)^{-1}][F_k] = L^{\frac{5-k}{2}} \tag{4.41}$$

where we have divided by the partition function in order to get the dimension of the normalized operator.

[1] A term borrowed from statistical physics were the infinite volume limit is taken to ensure that fluctuations can be neglected, and hence that the thermodynamic quantities are well defined.

The physical interpretation of the operator $\mathcal{O}_1$ is that it counts the number of ways we can construct a surface with a simple puncture. This means that it should count in a surface a number of times proportional to its volume. After normalisation with the number of surfaces it should correspond to the volume operator

$$F_1 \propto \langle V \rangle \tag{4.42}$$

In perfect agreement with the dimension $[\mathcal{O}_1] = L^2$.

What are the other $\mathcal{O}_k$? From the matrix model point of view a first naive guess could be that they corresponded to $\langle \mathrm{tr} M^k \rangle$, since at least F_1 can be seen as the continuum limit of F_1. There is however a general argument why this cannot be the case. In the continuum limit all finite traces should give the same operator. This is exactly the point about the limit, that all differences on the microscopic level should be ignored. One link more or less on the loop should make no difference. We must therefore insist on all $\langle \mathrm{tr} M^k \rangle$ to correspond to the same operator ($\mathcal{O}_1$) in the continuum limit. This can also be seen from an explicit calculation of the continuum limit of F_k.

Although the most naive guess is clearly wrong it turns out that at least some of the operators do have a natural interpretation in the matrix model. One can show[33] that they can be identified with certain finite linear combinations of traces. To see why a sum of traces can give a different continuum limit in comparison with a single trace, we can recall how the cancellations in $\dot{\mathsf{F}}$ conspired to give a different result than c (Eq. (4.22)).

The geometric interpretation of these operators (apart from F_1) is unfortunately less clear. It would be nice to establish a relation to some set of geometrical invariants. This is not a trivial problem. For instance there are arguments[16] that even in the cases where $\mathcal{O}_k$ has the same dimension as $\int R^n \sqrt{g} d^2x$ for some n, they are not related.

4.5 The cylinder amplitude

Having found the continuum limit of F and introduced the operators $\mathcal{O}_k$, we now intend to find the continuum limit of the "two-loop with a separation d" generating functional. In order to do this we note that the composition law Eq. (3.58) indicate that we shall approach the critical value for the loops in a reciprocal way. Let us explain this in some more detail. From the considerations in Sec. (4.1) we expect the number of loops of length l to have an exponential increase $j^l = e^{\mu} l$. In the continuum limit we are not interested in this but only in power corrections. In the cap amplitude this was handled by a renormalization of the cosmological constant for the boundary $\xi = \xi_{crit} - X\epsilon$, where X was the physical cosmological constant. We intend to do something analogous for the cylinder amplitude, by introducing two physical cosmological constants X_1 and X_2, one for the entrance and one for the exit loop, and then keep them constant by a suitable renormalization of ξ_1 and ξ_2. In order for us to be to find a sensible limit of the composition law, we must choose a contour for the integration variable z such that the intermediate loop is macroscopic, in other word the modulus of z should approach the critical point for the entrance loop of $\dot{\mathsf{N}}$. Now from Eq. (3.58) we see that if j_{crit} is the critical point of the entrance loop, the only chance of taking a limit with $\frac{1}{z}$ approaching the critical value of the exit loop, is if this critical value is j_{crit}^{-1}. With this assumption, and taking for granted

that the entrance loop and the area cosmological constants should be renormalized as in the cap amplitude we must approach the critical point in the following way

$$j_1 = j_{crit}e^{-\epsilon X_1} \quad j_2 = j_{crit}^{-1}e^{-\epsilon X_2} \quad z = j_{crit}e^{-\epsilon X} \quad g = g_{crit}e^{-\epsilon^2\Lambda} \tag{4.43}$$

Inserting this into Eq. (3.55) yields

$$N(\Lambda, X_1, X_2) = -\log[\frac{4\sqrt{3}+13}{12}(X_1+X_2)\epsilon - \frac{3\sqrt{3}-4}{24}(1+\sqrt{3})^{5/2}\dot{F}(\Lambda, X_1)\epsilon^{3/2} + O(\epsilon^2)] \tag{4.44}$$

The continuum limit of the composition law, Eq. (3.58), becomes

$$\dot{N}_{d_1+d_2}(\Lambda, X_1, X_2) = \frac{\epsilon}{2i\pi}\int_{-i\infty}^{i\infty}\dot{N}_{d_1}(X_1, -X)\dot{N}_{d_2}(\Lambda, X, X_2)dX \tag{4.45}$$

where we have used $dz = -\epsilon z dX$.

Notice the absence of nonuniversal parts in Eq. (4.44), this is not the result of some subtraction procedure, but comes as automatic cancellations from the way we approach the critical point. This is a strong indication that the approach is indeed correct, and somewhat assuring considering that we had no a priori argument to ensure j_{crit}^{-1} was a critical point for the exit loop. In our previous calculation of F we had no qualms about the appearance of NUP's since we *knew* that there was a critical point and where it was.

We also have the "marking relation"

$$\dot{\mathsf{N}}(g, j_1, j_2) = -\epsilon^{-1}\frac{\partial}{\partial X_2}\mathsf{N}(g, j_1, j_2) \tag{4.46}$$

which used on Eq. (4.44) gives

$$\dot{N}(\Lambda, X_1, -X) = \frac{1}{(X_1 - X)}\epsilon^{-1} + \sqrt{2/(9\sqrt{3}-1)}\frac{\dot{F}(\Lambda, X_1)}{(X_1-X)^2}\epsilon^{-1/2} + O(1) \tag{4.47}$$

Using this in Eq. (4.45) with $d_1 = 1$ and $d_2 = d$ we obtain

$$\begin{aligned}\dot{N}_{d+1}(\Lambda, X_1, X_2) &= \frac{1}{2i\pi}\int_{-i\infty}^{i\infty}\left(\frac{1}{(X_1-X)} + \sqrt{2/(9\sqrt{3}-1)}\frac{\dot{F}(\Lambda, X_1)}{(X_1-X)^2}\epsilon^{1/2}\right)\dot{N}_d(\Lambda, X, X_2)dX \\ &= \dot{N}_d(\Lambda, X_1, X_2) - \sqrt{2/(9\sqrt{3}-1)}\dot{F}(\Lambda, X_1)\frac{\partial\dot{N}_d(\Lambda, X_1, X_2)}{\partial X_1}\epsilon^{1/2}\end{aligned} \tag{4.48}$$

By introducing the continuum "distance" $D = \sqrt{2/(9\sqrt{3}-1)}\sqrt{\epsilon}d$, we can write this as a differential equation

$$\frac{\partial\dot{N}}{\partial D} = -\dot{F}(\Lambda, X_1)\frac{\partial\dot{N}}{\partial X_1} \tag{4.49}$$

It is worth noticing the peculiar dimension of $[D] = L^{1/2}$. This is our first hint that the model has a fractal nature, a fact we will further expose in Chap. (5).

In order to find a unique solution for Eq. (4.49) we need to specify some boundary conditions. The natural choice is $\dot{N}(\Lambda, X_1, X_2, 0) = \frac{1}{X_2+X_1}$ since this corresponds to a

delta function $\delta(L_1 - L_2)$ in the loop length, as seen by performing the inverse Laplace transform:

$$\int_{c_2-i\infty}^{c_2+i\infty}\int_{c_1-i\infty}^{c_1+i\infty}\frac{e^{L_1X_1+L_2X_2}}{X_1+X_2}dX_1dX_2 = \int_{c_1-i\infty}^{c_1+i\infty}e^{(L_1-L2)X_1}dX_1 = \delta(L_1-L_2) \tag{4.50}$$

The solution can now be obtained[1] as

$$\dot{N}(\Lambda, X_1, X_2, D) = \frac{1}{X_2 + B(\Lambda, X_1, D)} \tag{4.51}$$

where

$$\begin{aligned} B(\Lambda, X, D) &= h(e^{aD}h^{-1}(X)) \qquad & a &= \sqrt{6\sqrt{,}} \\ h(y) &= a^2\left((\frac{1}{y-1}+\frac{1}{2})^2 - \frac{1}{6}\right) \qquad & h^{-1}(x) &= \frac{a}{\sqrt{x+\frac{a^2}{6}}-\frac{a}{2}}+1 \end{aligned} \tag{4.52}$$

with dimensions

$$[B] = [h] = L^{-1} \tag{4.53}$$

Notice that the asymmetry between the entrance loop and the exit loop, is reflected in the solution.

This continuum version of the cylinder amplitude has been obtained in various ways, strongly suggesting a universal character of the result (see e.g.[7]).

4.6 Loops with relaxed distance

Having obtained the solution to the cylinder generating functional, we want to calculate another "two-loop function". As in the continuum theory described in Chap. (2), we can consider two loops where the minimal distance is D. We saw in the last chapter that we could obtain this by gluing two cylinders together via a "cap amplitude" as shown in Fig. (4.3). The cap amplitude we used there were actually $j^2\dot{\mathsf{F}}(g,j)$ rather than $\dot{\mathsf{F}}(g,j)$

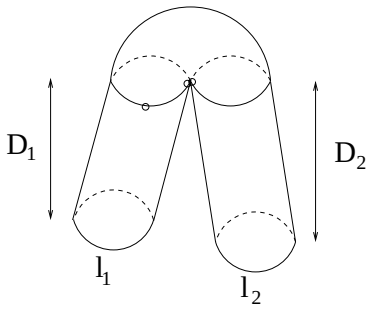

Figure 4.3: Gluing two cylinder together with the use of a cap.

but as an explicit calculation will show these have the same continuum limit (apart from a

nonuniversal constant). This is not surprising as the difference between a loop of length l and $l-2$ disappears in the limit of infinite loop. It is however an important demonstration that one of the effects of the discretization disappears in the continuum limit. It does not constitute a proof that D is indeed geodesic distance, but does indicate that it is universal.

When we glue in the continuum limit we should observe all the rules with respect to marking as in the discrete case, but we must also make sure that the exponential entropy factors of type $e^{l\xi_{crit}} \sim j_{crit}^{-l}$ cancels at the gluing. This is the same requirement as in the cylinder amplitude, when we found that the exit loop should renormalize reciprocal compared to the cap amplitude. The fact that we glue two exit loops onto the cap ensures this requirement is satisfied. Approaching the critical point in a way similar to the cylinder case we obtain (see App. (E) for details)

$$\begin{aligned} G(\Lambda, X_1, X_2, D) &= \frac{1}{2\pi i}\int_{-i\infty}^{i\infty} \dot{F}(\Lambda, X)\dot{N}(\Lambda, X_1, -X, D_1)\dot{N}(\Lambda, X_2, -X, D_2)dX \\ &= \frac{\dot{F}(\Lambda, B(\Lambda, X_1, D_1)) - \dot{F}(\Lambda, B(\Lambda, X_2, D_2))}{B(\Lambda, X_2, D_2) - B(\Lambda, X_1, D_1)} \\ &= 2a\left(\frac{1}{y_1y_2 - 1} - \frac{1}{y_1 - 1} - \frac{1}{y_2 - 1} - \frac{1}{2}\right) \end{aligned} \tag{4.54}$$

where $y_i = e^{aD_i}h^{-1}(X_i)$ and we choose D_1 and D_2 such that $D = D_1 + D_2$. We can also note that G in contrast to N is symmetric with respect to the two loops, as is evident both from the construction and the solution. Dimension wise we have $[G] = L^{-1/2}$.

As usual we can mark the entrance loops by differentiating with respect to X_1 and X_2

$$\begin{aligned} \ddot{G}(\Lambda, X_1, X_2, D) &= \frac{\partial}{\partial X_1}\frac{\partial}{\partial X_2}\frac{\dot{F}(B(\Lambda, X_1, D_1)) - \dot{F}(B(\Lambda, X_2, D_2))}{B(\Lambda, X_2, D_2) - B(\Lambda, X_1, D_1)} \\ &= 2a\frac{(1 + y_1y_2)}{(y_1y_2 - 1)^3}\frac{\partial}{\partial X_1}\frac{\partial}{\partial X_2}(y_1y_2) \end{aligned} \tag{4.55}$$

this changes the dimension to $[\ddot{G}] = L^{3/2}$. Since $y_1y_2 = e^{aD}h^{-1}(X_1)h^{-1}(X_2)$, we see explicitly that $\ddot{G}$, as expected, only depend on the sum $D = D_1 + D_2$.

As for the case of the cap amplitude we will now shrink the loops in order to obtain punctures. This could be done by expanding $\ddot{G}$ in , . This would give us at the same time an expansion in terms of $X_1^{-1/2}$ and $X_2^{-1/2}$ and D. Since this corresponds to letting $V \to \infty$ it will also shrink D which we want to keep fixed. We therefore expand in terms of $X_1^{-1/2}$ and $X_2^{-1/2}$ instead, corresponding to shrinking the loop without shrinking the distance D:

$$\ddot{G}(\Lambda, X_1, X_2, D) = \sum_{m,n=1}^{\infty} G_{mn}(\Lambda, D)X_1^{-\frac{m+2}{2}}X_2^{-\frac{n+2}{2}} \tag{4.56}$$

we can interpret the coefficients as (unnormalized) correlation functions for our set of operators

$$\langle \mathcal{O}_m\mathcal{O}_n(D)\rangle \sim G_{mn}(D) \tag{4.57}$$

with separation D. The coefficient are shown in App. (E). Dimension wise we have

$$[G_{mn}] = L^{-\frac{m+n+1}{2}} \qquad [\mathcal{O}_m\mathcal{O}_n(D)] = [Z(\Lambda)^{-1}][G_{mn}] = L^{\frac{9-m-n}{2}} \tag{4.58}$$

as expected since $[\mathcal{O}_m] = L^{\frac{5-m}{2}}$ and the fixing of D corresponds to a delta function with dimension $[\delta(D)] = [D^{-1}] = L^{-1/2}$.

We can now perform the $V \to \infty$ limit by expanding the coefficients $G_{mn}(D)$ in , . For the same dimensional reasons as in cap amplitude expansion, this will leave us with an expansion in D as well. We can also readily see which part survives the thermodynamic limit. As example consider

$$G_{11}(\Lambda, D) = a^3 e^{aD} \frac{e^{aD}+1}{2(e^{aD}-1)^3} = D^{-3} + \frac{Da^4}{240} + \frac{D^3 a^6}{3024} + O(a^8) \tag{4.59}$$

The first two terms has an even power of , (remember $a^4 = 36$,) and hence comes from small universes. For this reason they should be subtracted before we take the , $\to 0$ limit.

The only term surviving is thus $G_{11}^{TD} = \frac{D^3 a^6}{3024} = \frac{D^3 \Gamma^{3/2}}{14}$. In contrast to the cap amplitude case where only $F_1^{TD} \neq 0$, not only G_{11} survive the thermodynamic limit but also other G_{mn} will have $G_{mn}^{TD} \neq 0$. In this limit we write

$$G_{mn}^{TD}(\Lambda, D) = G_{mn}^{TD} D^{5-m-n}, \ ^{3/2} \tag{4.60}$$

where the coefficients for $m + n < 10$ are given in Tab. (4.1).

mn	11	12	13	22	14	23	15, 24, 33	16, 25, 34	17	26, 35, 44	18	27	36, 45
G_{mn}^{TD}	$\frac{1}{14}$	$\frac{3}{14}$	$\frac{3}{14}$	$\frac{3}{7}$	$\frac{1}{14}$	$\frac{3}{14}$	0	0	$\frac{1}{8}$	0	$\frac{3}{14}$	$\frac{3}{8}$	0

Table 4.1: Coefficients for $G_{mn}(D)$ in the thermodynamic limit

Finally we can give a physical interpretation to G_{11}. It simply counts a surface in as many times as we can puncture the surface twice, with a geodesic distance of D between the points. It it therefore proportional to the integrated volume $L(x, D)$ of the set of points at a distance D from x. That is

$$G_{11}(D) \propto \langle \int L(x, D) d^2 x \rangle \tag{4.61}$$

4.7 Three loops

It is now rather straight forward to generalize to three or even more loops. Let l_1, l_2 be two loops with separation D_{12}, and consider a third loop at a distance D_3 from the union of these two loops. Now there are three possibilities

- l_3 is equally close to l_1 and l_2.
- l_3 is closer to l_1 than to l_2.
- l_3 is closer to l_2 than to l_1.

The first case is a limiting case of the two others and should therefore not be considered in the continuum limit. The second case can be represented by a diagram like the one sketched in Fig. (4.4), and the third by the same diagram with l_1 and l_2 interchanged.

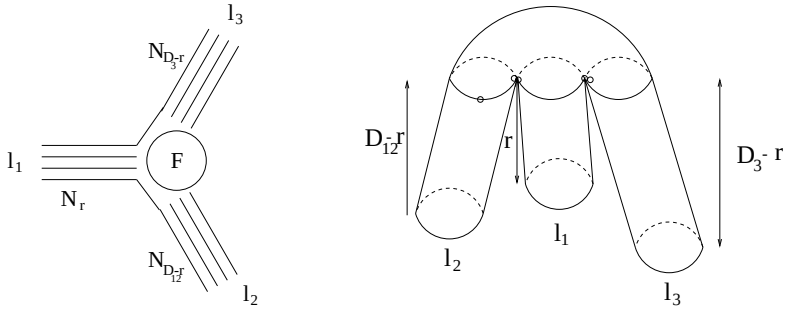

Figure 4.4: The diagram corresponding to three loops can be composed from three cylinder diagrams glued together with a cap and two propagators.

Let us see how we should glue this together. First we glue a cylinder of length r together with a cylinder of length $D_{12} - r$ with a single propagator. This can be done as many times as we can put mark on each exit loop. Next we glue a third cylinder of length $D_3 - r$ onto the first. In order to do this we must choose a leg on the exit loop of the first cylinder. This can be done by putting an extra mark on the loop. Having assembled this four holed structure we glue a (marked) cap on to close the hole from the three exit loops. Hence the partition function has the following appearance

$$H_r^1(\Lambda, X_1, X_2, X_3, D_{12}, D_3) =$$

$$\frac{1}{2\pi i}\int_{-i\infty}^{i\infty} \dot{F}(\Lambda, X)\ddot{N}(\Lambda, X_1, -X, r)\dot{N}(\Lambda, X_2, -X, D_{12}-r)\dot{N}(\Lambda, X_3, -X, D_3-r)dX \quad (4.62)$$

where we have used that $j^4\dot{\mathsf{F}}(j)$ have the same universal part as $\dot{\mathsf{F}}$.

Let us discuss the significance of r. If any diagram had a unique value of r associated with it, we just had to integrate over r to find all possible diagrams. Unfortunately this is not the case since it is somewhat arbitrary which part of the diagram we ascribe to the cylinders, and which to the cap. In other words we can obtain the same diagram using the above construction for different values of r. If we did the straightforward integration of H_r with respect to r we would have committed quite some over counting. We therefore have to be a little more ingenious.

Consider some random diagram with l_1 being the loop closest to l_3. In general it will be in H_r^1 for a lot of different values of r. Our aim is to choose some subset, such that all diagrams are present, yet none are counted twice. We can always choose an $r \leq \frac{1}{2}D_{12}$, an by doing so we avoid counting in diagrams where l_2 is closest to l_3. We can now split in two distinct cases

- For all r the l_2 and l_3 parts are connected if we remove the cylinder extending out from l_1. In this case let $r_0 = \frac{1}{2}D_{12}$.

- There exist an r such that with this choice of r, l_2 and l_3 will be disconnected if we remove the cylinder extending out from l_1. Let r_0 denote the smallest value for which this is the case. It will automatically be true for all $r > r_0$.

The two cases are shown in Fig. (4.5)

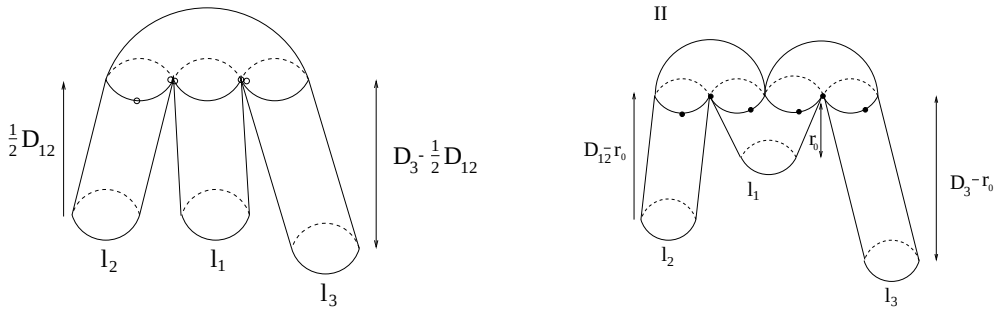

Figure 4.5: Possibilities with three loops.

If we now integrate over r_0 in the latter case and add the amplitude in the first case we will have counted all diagrams once. Actually the set of diagrams where $r_0 = \frac{1}{2}D_{12}$ is the smallest value where the cap will split after removal of the cylinder will be counted twice, but this is a limit case and hence have vanishing contribution. Finally we should add a contribution similar to (I) and (II), but with 1 and 2 interchanged, in order to count the diagrams where l_2 is the closer to l_3.

The contribution from the diagrams can be worked out as (see App. (E)):

$$\begin{aligned} H_I &= \frac{1}{B_2-B_1}\frac{1}{B_3-B_1}\ddot{F}(B_1) + \frac{1}{B_1-B_2}\frac{1}{B_3-B_2}\ddot{F}(B_2) + \\ &\quad \frac{1}{(B_1-B_2)(B_1-B_3)^2}\dot{F}(B_1) + \frac{1}{(B_2-B_1)(B_2-B_3)^2}\dot{F}(B_2) + \\ &\quad \frac{1}{(B_2-B_3)(B_1-B_3)^2}\dot{F}(B_3) + \frac{1}{(B_1-B_3)(B_2-B_3)^2}\dot{F}(B_3) \end{aligned} \tag{4.63}$$

where $B_1 = B(\Lambda, X_1, \frac{1}{2}D_{12})$,$B_2 = B(\Lambda, X_2, \frac{1}{2}D_{12})$,$B_3 = B(\Lambda, X_3, D_3 - \frac{1}{2}D_{12})$ and $\ddot{F} = -\frac{\partial}{\partial X}\dot{F}$.

For the case (II) we get the following[1]:

$$\begin{aligned} H_{II} &= \int_0^{D_{12}/2} dr[-\frac{1}{2}\ddot{F}(B_2)^2\frac{1}{B_1-B_2}\frac{1}{B_3-B_2} - \\ &\quad \dot{F}(B_2)\ddot{F}(B_2)\frac{1}{(B_1-B_2)^2}\frac{1}{B_3-B_2} + \dot{F}(B_1)\ddot{F}(B_2)\frac{1}{(B_1-B_2)^2}\frac{1}{B_3-B_2} + \\ &\quad \frac{1}{2}\dot{F}(B_2)^2\frac{1}{(B_1-B_2)^2}\frac{1}{(B_3-B_2)^2} - \dot{F}(B_1)\dot{F}(B_2)\frac{1}{(B_1-B_2)^2}\frac{1}{(B_3-B_2)^2} + \\ &\quad \frac{1}{2}\dot{F}(B_1)\dot{F}(B_3)\frac{1}{(B_1-B_2)^2}\frac{1}{(B_3-B_2)^2} + (1 \leftrightarrow 3) \end{aligned} \tag{4.64}$$

where $B_1 = B(\Lambda, X_1, D_{12} - r)$,$B_2 = B(\Lambda, X_2, r)$ and $B_3 = B(\Lambda, X_3, D_3 - r)$ and $((1 \leftrightarrow 3)$ indicate terms with 1 and 3 interchanged.

As for the case of two-loops we can expand in $X_i^{-1/2}$ in order to obtain correlation between local operators:

$$H(\Lambda, X_1, X_2, X_3, D_{12}, D_3) = \sum_{m,n,l=1}^{\infty} H_{mnl}(\Lambda, D_{12}, D_3) X_1^{-\frac{m+2}{2}} X_2^{-\frac{n+2}{2}} X_3^{-\frac{l+2}{2}} \tag{4.65}$$

where :

$$\langle (\mathcal{O}_m \mathcal{O}_n(D_{12})) \mathcal{O}_l(D_3) \rangle \sim H_{mnl}(\Lambda, D_{12}, D_3) \tag{4.66}$$

The dimensions are

$$[H_{mnl}] = L^{-\frac{m+n+l-3}{2}} \qquad [(\mathcal{O}_m \mathcal{O}_n(D_{12})) \mathcal{O}_l(D_3)] = L^{\frac{13-m-n-l}{2}} \tag{4.67}$$

Finally we can let , $\to 0$ in order to get the thermodynamic limit, giving us

$$H^{TD}_{mnl}(\Lambda, D_{12}, D_3) = \sum_k H^{TD}_{mnlk} D_{12}^{4-m-n+k} D_3^{5-l-k} \Lambda^{3/2} \tag{4.68}$$

for some coefficients H^{TD}_{mnlk}.

With the above formulation of the three point function with fixed geodesic distance we end this somewhat technical chapter. We have seen how it is possible to get from the discrete triangulations to a collection of continuum partition functions. In addition to this we have introduced a set of local operators with associated one, two and three point functions. In the next chapters we will use this framework to investigate the properties of our model.

Chapter 5

Two Dimensional Quantum Gravity

The former chapter culminated in the explicit formulation of a continuum limit for the discrete model considered earlier. In this chapter I will describe in general terms the conclusions about the nature of this model of 2D quantum gravity. Which things are certain and what questions remains unanswered. A lot of the conclusions will not be supported by any rigorous calculation, but will more have the character of an overview. This is not to say that the results are necessary very hard to derive, using our framework from the last chapter (although some are more conveniently discussed in slightly different notations, and others require longer calculations). The aim of this chapter is to give a notion of the kind of problems one can consider (and solve) in the model. In the next chapter we will then focus on one of these aspects in detail, the one this thesis owes its name to.

5.1 Universality

The first question one can ask when considering the continuum limit of a discrete theory is the question of universality. Is the behaviour of the continuum model independent of which discretization procedure is chosen? In the case of dynamical triangulation the answers seems to be in the affirmative.

A large number of different models have been considered, for instance models with quartic, quintic and even higher order vertices, corresponding to surfaces build from squares, pentagons and higher polygons [21, 14]. Also models with various classes of triangulations have been considered. Typically one restrict the triangulations so as not to allow for instance tadpoles or double links in the boundary [51]. All of these models have been shown to have the same continuum limit, a strong indication of universality.

We can understand the universality in the following way. Even if some structure, like a pentagon (a five legged vertex) or a double link, is not allowed on the fundamental level, it will arise on some other level (Fig.5.1). In approaching the continuum limit it will become unimportant if the structures are on the fundamental level, or on some level slightly above.

Given that the model is universal, the next question that arises is which continuum theory the model describes. In our case we expect (hope) the model corresponds to Liouville theory, but how can we check this? We are pretty much restricted to compare

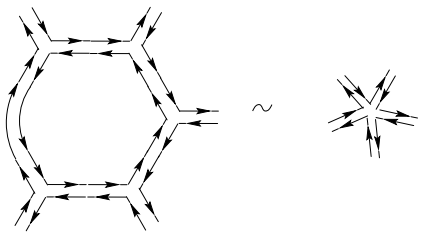

Figure 5.1: A five-vertex structure emerging from three-vertices.

result which are obtainable in both frameworks, e.g. the critical exponents. As mentioned in Sec. (2.7) Liouville theory predicts $\gamma = -1/2$ as also found in our model. We can extend this to models which includes matter with a given central charge. These turn out to agree as well, which give some support for the assumption that the models are identical. More important it has been shown that the 1,2,3 and 4 point function agree (that is the puncture limit of the loop function without any prescribed distance)[23]. This is good justification for the assumption that the two models indeed are identical. There is of course still a small chance that the theories are different in some aspect. For instance the concept of distance can not be treated in Liouville theory with the present techniques. One could therefore fantasize about possible discrepancies. But perhaps one should not worry to much about to what extent the two models agree. After all dynamical triangulation *do* give us a framework to sum up geometries, in a way which gives a welldefined and universal continuum limit. If this should turn out (however unlikely) to give results which are at odds with Liouville theory, it is not to say that any of the models are wrong, they are just different.

Having argued for the universality of the model and for the resemblance with Liouville theory, we now turn towards the description of the geometry of the effective surface.

5.2 Fractal nature

Let us make the notion of effective surface more precise. Consider some geometric quantity which can be defined on the set of manifolds. This could be volume, average distance between points, on any other of the geometrical invariants defined in Chap. (2).

We can now calculate the expectation value of such a quantity, by summing over all our triangulations, properly weighted. We now envision the effective surface as a surface with the property that the geometrical invariants exactly have the value of the expectations value. A priori we cannot be sure such a surface exist, especially not as we increase the number of requirements it should fulfill. It is no problem, given some Λ_0, to construct a surface with the proper volume $V_0 = \langle V(\Lambda_0) \rangle$. It might be harder to obtain the correct average distance, without changing the volume. We will in the following see that some of the requirements can only be satisfied if we allow a very broad definition of the term surface.

As mentioned in Chap. (2) we can define the effective Hausdorff dimension as

$$d_h = \lim_{D\to 0}(1 + \frac{D}{\langle V'(D)\rangle}\frac{\partial\langle V'(D)\rangle}{\partial D}) \tag{5.1}$$

where $\langle V'(D)\rangle$ is given by Eq. (2.18). In our present model we can achieve the $D \to 0$ limit by taking the area to infinity. Furthermore as noted in Sec. (4.6) $G_{11}(D)$ corresponds (apart from normalization) to the number of ways we can mark two points with a distance D, and F_1 give us the volume (again modulo normalisation). We can now get the value of $\langle V'(D)\rangle$ by dividing the two[1]. In the $V \to \infty$ limit we obtain:

$$\langle V'(D)\rangle = \frac{G_{11}^{TD}}{F_1^{TD}} = \frac{2}{7}D^3 \tag{5.2}$$

and thereby $d_h = 4$. This result is perhaps quite surprising at first glance. Each of the manifolds we sum over have Hausdorff dimension $d_h = 2$, since on a small enough scale we will be in the domain of a single triangle which is clearly two dimensional. How can we get a different result when we sum?

The answer is in the way we approach the $D \to 0$ limit. If we had taken this limit for each manifold independently we would have got two as the Hausdorff dimension of each of them. Instead what we do, is to take the $D \to 0$ limit for all manifolds at the same time. This has as a consequence that for any D however small it might be, it will be too large for some of the manifolds, to give something close to the correct Hausdorff dimension. In short

$$\lim_{V\to\infty}\sum_{\text{manifolds}} \neq \sum_{\text{manifolds}}\lim_{D\to 0} \tag{5.3}$$

From this point of view it is not that surprising that we get a different result than two. The surprising thing is perhaps that we get a result at all, i.e. that the limit exist, and why do we get $d_h = 4$? If we look at the dimension, the result makes a lot of sense. The volume within a certain distance will have dimension L^2, and since $[D] = L^{1/2}$ it is perhaps not that unexpected that $V \propto D^4$.

The previous result indicate a highly fractal nature of the effective surfaces. How can we visualize this behaviour? Let us first consider a 2-dimensional surface embedded in 3-dimensional space. If the surface is smooth, then on a small scale the set of point that is at a distance D from a selected point, reassemble a slightly distorted circle, as shown in Fig. (5.2)(a). If we introduce blobs on the surface the circle begin to have smaller circles inside, and starts looking more like the boundary of a slice of swiss cheese than a circle. This means in a sense that we have a too big D to measure the correct Hausdorff dimension.

If we consider the effective surface, the point is that we can never choose the D small enough to avoid that the sum will be dominated by surfaces which contain blobs inside the circle of radius D.

A surface with this property can be imagine as formed in a limit process, adding blobs on all scales. The result is a fractal, for which the circumference of a circle will have a two, three or even higher or fractional dimensional look, no matter how small the radius.

[1] this makes the normalisation cancel.

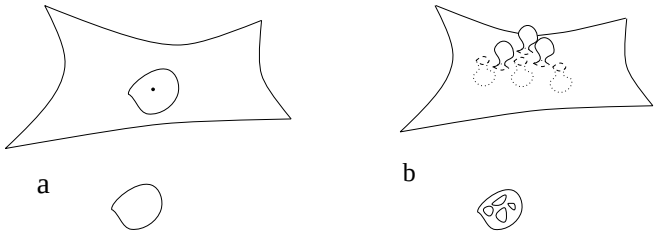

Figure 5.2: The difference between a smooth surface and a fractal.

In our model we have that the measure of the set of point at a distance D goes as D^3. If we were to embed this set in three dimensional space it would look something like a solid ball. This of course implies that we cannot embed the effective surface itself in 3-dimensional space, and it also shows we should be very careful when thinking of the effective surface as a surface.

Even if the notion of an effective surface can be deceptive, the notion of blobs will survive even if we look at the individual manifold. In the next section we will investigate their properties more closely.

5.3 Baby universes

The blobs are often called baby universes, and in this section we will review some of the things known about the density of such, in our model [36].

How can we define baby universes in our discrete model? The neck of the blob should be short compared with the volume of the interior. In matrix language it should be a part of the diagram connected to the rest through a few propagators, compared with the number of vertices in the sub-diagram. The minimal neck baby universe (or minbu[2] for short) will correspond to a sub-diagram which is connected to the rest by a single propagator. This means that we can explore the baby universe structure by splitting the diagram up in 1PI (one particle irreducible) diagrams, each representing a universe.

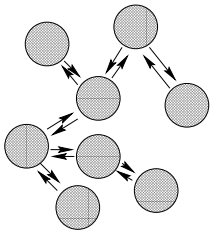

Figure 5.3: The structure of baby universes as 1PI diagrams.

This raises the following questions:

[2]The term minbu covers different neck length according to the set of triangulations used. See for instance[36].

- What is the average number of minbus in the continuum limit?
- What is the volume distribution of these?

In order to answer these questions let us investigate the discrete model first. The number of triangulations with one part with n_1 vertices and the other with n_2, separated by a marked propagator, is given by

$$\mathsf{B}_{n_1,n_2} = \mathsf{F}_{1,n_1}\mathsf{F}_{1,n_2} \tag{5.4}$$

where $\mathsf{F}_{1,n}$ is the number of diagrams of size n with one external leg. We notice that we count in a diagram as many times as it can be cut by a single vertex in two parts of size n_1 and n_2 respectively. This means that

$$\mathsf{B}_n = \sum_{m=1}^{n/2} \mathsf{B}_{n-m,m} \tag{5.5}$$

will count a diagram as many times as it has a single neck. The average number of $1PI$ parts in a diagram of size n is therefore given by

$$\Pi_n = \frac{\mathsf{B}_n}{\mathsf{z}_n} = \frac{1}{\mathsf{z}_n}\sum_{m=1}^{n/2} \mathsf{F}_{1,n-m}\mathsf{F}_{1,m} \tag{5.6}$$

or more convenient their density:

$$\rho_n = \frac{1}{n}\Pi_n \tag{5.7}$$

In the limit of large n we can now use $\mathsf{F}_{1,n} \sim g_{crit}^{-n} n^{-5/2}$ and $\mathsf{z}_n \sim g_{crit}^{-n} n^{-7/2}$ (Cf. Eq. (4.16)) and approximate the sum with an integral:

$$\rho_n \sim \frac{1}{n g_{crit}^{-n} n^{-7/2}} \int_1^{n/2} g_{crit}^{-(n-m)} (n-m)^{-5/2} g_{crit}^{-m} m^{-5/2} dm = \frac{2(16-24n+6n^2+n^3)}{3(n-1)^{3/2} n^{3/2}} \sim \frac{2}{3} \tag{5.8}$$

We see that the density of minimal necks is a constant independent of the size of the diagram, which is not surprising since the creation of blobs is in a sense a local phenomenon. The value of the constant is not really significant since it depends on multiplicative factors in the asymptotic behavior of $\mathsf{F}_{1,n}$ which have not been taken into account.

To investigate the volume distribution of the baby universes we consider the average number of places a diagram can be cut into pieces of size $n-m$ and m:

$$\frac{1}{\mathsf{z}_n}\mathsf{B}_{n-m,m} \sim n^{7/2}(n-m)^{-5/2} m^{-5/2} \tag{5.9}$$

where the $\sim$ indicate the behavior for large n and m. We note that if $m \ll n$ this reduces to $nm^{-5/2}$. Since $n \gg 1$ we have $n^{2/5} \ll n$ and using this value for m we see that the chance of being able to cut off a part goes down to order 1 for $m = n^{2/5}$, and hence is small for parts larger than this. One could argue that we should rather look for cut

off parts with sizes within some interval, say m to $2m$, but this would only change the exponent to $m = n^{2/3}$ as can be seen from

$$\int_m^{2m} nm^{-5/2}dm \sim nm^{-3/2} \tag{5.10}$$

where we have approximated the sum with an integral. There is still only a very small change of finding a cut off part of size of order $n \gg n^{2/3}$.

It is important to realize the following. Even if the diagram can be cut in two pieces of size n_1 and n_2 respectively, it by no means ensure there exist a 1PI diagram of size n_1 or n_2. The two parts will most certainly contain subdiagrams. Suppose now that the diagram can *not* be cut in two pieces of size $n_1 > n_2$. This means that we cannot cut a piece of the diagram of size n_2 off by cutting a single propagator. One could be tempted to infer from this that the diagram must consist of a large $n > n_1$ 1PI diagram with small diagrams of size $< n_2$ attached to it, since this would certainly make it impossible to cut off a part of size n_2. One can however construct diagrams with this property which have no large 1PI diagram. Consider the diagram in Fig. (5.4), and assume that all the blobs has the same size n. It is clear that no parts larger than $3n$ (and smaller than half the diagram) can be cut away, but nevertheless there is no blob larger than n.

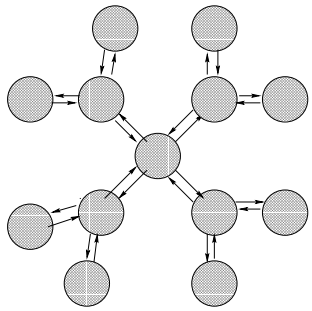

Figure 5.4: A diagram with no large 1PI parts

From this discussion we recognize that there are two distinct possibilities as we take the limit of large diagrams. Either all the 1PI parts becomes small (finite) compared to the size of the diagram, or at least one of them has size of order the diagram size. Which of these cases correspond to our model? In the first case we can neglect the differences between the size of the blobs, since they are all finite, and hence non universal. This means that the diagrams can actually be viewed as branched polymers, and we therefore expect the same behavior as in the $g = 0$ case. In other words we are in the case of $l \to \infty$ with g kept fixed. But this limit have a different behavior than our model where g is tuned to its critical value, along with $l \to \infty$, as the explicit calculations of the former chapter showed. The conclusion is that since we are not in the branched polymer case, we must have that the large diagram limit is dominated by diagrams with at least one large 1PI part.

Let us now consider in more detail this continuum limit. A natural question to pose when we take the limit of large diagrams is how many places we can cut the diagram

in two such that one contain a fraction between say a_1 and a_2 of the triangles. In other words the integral

$$\int_{a_1}^{a_2} \mathsf{B}_{n-an,an} da \tag{5.11}$$

In the large n limit we can use $\mathsf{F}_{1,m} \sim g_{crit}^{-m} m^{-5/2}$ with $m = an$ to obtain

$$\mathsf{B}_{n-an,an} \sim g_{crit}^{(a-1)n}((1-a)n)^{-5/2} g_{crit}^{-an}(an)^{-5/2} = (a-a^2)^{-5/2} g_{crit}^{-n} n^{-5} \tag{5.12}$$

putting $a_2 = \frac{1}{2}$ we obtain the weight for diagrams where we can cut such that more than a_1 of the diagram is in the cut off part.

$$\mathsf{B}_n(a_1) = g_{crit}^{-n} n^{-5} \int_{a_1}^{1/2} (a-a^2)^{-5/2} da = \frac{2\sqrt{a_1 - a_1^2}(1 + 6a_1 - 24a_1^2 + 16a_1^3)}{3(a_1-1)^2 a_1^2} g_{crit}^{-n} n^{-5} \tag{5.13}$$

Let us take the continuum limit of this expression. In order to do this we must cancel the factor g_{crit}^{-n}. This could be done by dividing the expression with $\mathsf{z}_n \sim g_{crit}^{-n}$ as in the discrete case, leading to the fixed volume partition function. This could then be Laplace transformed to give the full partition function. We will instead use the method introduced in the former chapter, and simply swallow the exponential decrease in a renormalization of the cosmological constant.

Consider the sum

$$\mathsf{B}(g) = \sum_{n=1}^{\infty} \mathsf{B}_n(a_1(n)) g^n = \sum_{n=1}^{\infty} n^{-5} g_{crit}^{-n} g^n \int_{a_1(n)}^{1/2} (a-a^2)^{-5/2} da \tag{5.14}$$

where a_1 is now a function of n since we intend to keep the volume W of the cut off part constant, independent of the volume of the full universe. We should now take $g = e^{-\mu}$ to its critical value, letting $\epsilon \to 0$ such that $\frac{\mu - \mu_{crit}}{\epsilon^2}$ is kept finite. Furthermore $W = a_1(n) n \epsilon^2$ should be kept finite. The first requirement is obtained in the usual way by letting $g = e^{-\Lambda \epsilon^2}$. The second can be fulfilled by letting $a_1(n) = \frac{W}{n\epsilon^2}$. With this inserted we arrive at

$$\begin{aligned}
\mathsf{B}_W(g) &= \sum_{n=1}^{\infty} n^{-5} \frac{g^n}{g_{crit}^n} \int_{\frac{W}{n\epsilon^2}}^{1/2} (a-a^2)^{-5/2} da \\
&= \epsilon^8 \sum_{n=1}^{\infty} e^{-\frac{\mu-\mu_{crit}}{\epsilon^2} n\epsilon^2} \frac{2\sqrt{(n\epsilon^2 - W)W}((n\epsilon^2)^3 + 6(n\epsilon^2)^2 W - 24(n\epsilon^2)W^2 + 16W^3)}{3(n\epsilon^2 - W)^2 W^2 (n\epsilon^2)^5} \epsilon^2 \\
&\sim \epsilon^8 \int_0^{\infty} e^{-\Lambda V} \frac{2\sqrt{(V-W)W}(V^3 + 6V^2 W - 24VW^2 + 16W^3)}{3(V-W)^2 W^2 V^5} dV \\
&= \epsilon^8 \int_0^{\infty} e^{-\Lambda V} B(V,W) dV
\end{aligned} \tag{5.15}$$

where

$$B(V,W) = \frac{2\sqrt{(V-W)W}(V^3 + 6V^2 W - 24VW^2 + 16W^3)}{3(V-W)^2 W^2 V^5} \tag{5.16}$$

is the number of places to cut of a part of size W in the ensemble of universes of size V. As mentioned before we could have obtained this result more or less straight from

Eq. (5.13), by substituting $n = V$ and $a_1 = W/V$. This would however have made the disappearance of the exponential factor less clear. One might worry that we use the large n limit for F_1, even if we sum from $n = 1$, but as discussed several times in the preceding chapter we can neglect any finite number of terms since they are non universal. We could therefore start the sum at some large n for which the approximation is good. Also along the lines of this discussion, we note that the ϵ^8 indicate a lot of nonuniversal terms which should be removed for instance by differentiations with respect to Λ.

In the limit $W \ll V$ we have $B(V,W) \sim V^{-7/2}W^{-3/2}$ or using $Z(V) = V^{-7/2}$

$$\frac{1}{Z(V)}B(V,W) \sim W^{-3/2} \tag{5.17}$$

which is more or less the continuum version of Eq. (5.10) where we have integrated all the way up to $n/2$ instead of $2m$.

5.4 The double scaling limit

So far we have completely neglected the summation over topology. The primary reason being simplicity. It is still an open question whether an actual physical model of quantum gravity should include summation over topology. It is however possible to address the matter to some extent within our present formalism.

Let us recall the form of the matrix model before the $N \to \infty$ limit. We found that the overall factor of N from a triangulation with Euler character χ was exactly $\chi = 2 - 2h$. We can therefore write the full partition function as

$$\mathsf{Z}[g] = \sum_h N^{2-2h}\mathsf{Z}_h[g] \tag{5.18}$$

where Z_h is the genus h partition function. It turns out that the critical value g_{crit} for Z_h is independent of genus[51]. This is perhaps not that surprising since we can construct a h-genus surface from a $2h$-loops diagram by gluing the loops together pairwise. As the partition function for $2h$-loop diagrams diverge at the point g_{crit} so will the partition function for genus h surface. On the other hand Z_h can not be divergent for $g < g_{crit}$ since this would imply that the $2h$ loop would also diverge (we can cut an h genus surface h times to obtain a $2h$ loop surface).

Remember now that before we renormalized the partition functions, we had a factor of $\epsilon^{3/2}$ associated with the universal part of the marked loop partition function, and a factor $\epsilon^{5/2}$ associated with the unmarked. We also had ϵ^3 in front of F_1 and from $V = \epsilon^2 n$ we get $\mathsf{Z}(g) \propto \epsilon^5 Z[\Lambda]$. From this we find that introducing one loop on the surface lowers the power of epsilon by $5/2$ and introducing a mark on the loop lowers the power by one more. The power of epsilon associated with a $2h$ loop diagram where h loops are marked is therefore given by

$$\dot{\mathsf{F}}_{2h} \propto \epsilon^5\epsilon^{-2h(5/2)}\epsilon^{-h} = \epsilon^{5(1-h)-h} \tag{5.19}$$

we should now glue h times, and as evident from the gluing in the cylinder case (Eq. (4.45)) this supply a factor of ϵ for each gluing[3]. We therefore expect that the universal part of

[3]In this calculation we completely ignore the exponential factors, which should be treated more carefully in a detailed calculation.

the partition function for genus h is given by

$$\mathsf{Z}_h(g) \sim \epsilon^{5(1-h)} Z_h(\Lambda) \tag{5.20}$$

We can note that for $h = 0$ we have that the power of epsilon is positive, which indicate that we have nonuniversal terms. This is not very surprising since they were already present in the cap amplitude. Also the $h = 1$ case requires some attention. Naively one would expect no divergences as $\epsilon \to 0$ but in reality one encounters logarithmic such. We will not dwell with these subtleties, just sketch a possible line of thought. For a more detailed exposition see e.g.[33].

It is now natural to write the all genus partition function as

$$\mathsf{Z}(g) = \sum_h (\epsilon^{\frac{5}{2}} N)^{2-2h} \frac{\mathsf{Z}_h(g)}{\epsilon^{5(1-h)}} \tag{5.21}$$

This shows that we can approach the $N \to \infty$, $\epsilon \to 0$ limit synchronously, keeping $\epsilon^{\frac{5}{2}} N$ and $v = \epsilon^2 n$ finite. This is known as *the double scaling limit*. Define G and κ by

$$G^{-1} = e^{\frac{1}{\kappa}} = \epsilon^{\frac{5}{2}} N \tag{5.22}$$

We can now use, that the power of epsilon in front of the universal part of the bare partition function must (for dimensional reasons) correspond to a power of $\sqrt{\Lambda}$ in the renormalized one, to obtain

$$\frac{\mathsf{Z}_h(g)}{\epsilon^{5(1-h)}} = Z_h(\Lambda) = \tau_h \Lambda^{\frac{5}{2}(1-h)} \tag{5.23}$$

where τ_h is some constant. The partition function takes the form

$$Z(\Lambda, G) = \sum_h e^{\frac{\chi}{\kappa}} Z_h(\Lambda) = \sum_h e^{\frac{\chi}{\kappa}} \tau_h \Lambda^{\frac{5}{2}(1-h)} = \sum_h \tau_h \left(\frac{G}{\Lambda^{\frac{5}{4}}} \right)^{-\chi} \tag{5.24}$$

which shows that κ can be interpreted as the renormalized gravitational coupling constant, and that the partition function only depends on $t = \Lambda G^{-\frac{4}{5}}$:

$$Z(t) = \sum_h \tau_h t^{-\frac{5}{2}(h-1)} \tag{5.25}$$

The only problem with the above treatment, apart from the subtleties with regard to $h = 0, 1$ discussed earlier, is that the sum is divergent for any set of g, κ. We can however find a function which has the same asymptotic expansion[4]. For convenience we introduce $u = \frac{\partial^2 Z}{\partial t^2}$ which must have an expansion like

$$u \sim \sum_h c_h t^{-\frac{5}{2}(h-1)-2} \tag{5.26}$$

[4] an *asymptotic expansion* of a function $f(x)$ as $x \to x_0$ is a formal sum $\sum a_n \phi_n(x)$ such that $f(x) = \sum_{n=1}^{N} a_n \phi_n(x) + o(\phi_N)$ as $x \to x_0$ for any N. The functions $\phi_n(x)$ are required to be an *asymptotic sequence*, i.e. $\phi_{n+1}(x) = o(\phi_n)$ as $x \to x_0$. In our case $x_0 = \infty$ and $\phi_n = x^{1-\frac{5}{2}n}$. For more on the subject see [61].

This expansion is also obtained for a solution to the differential equation

$$\frac{1}{3}u''(t) + u(t)^2 - t = 0 \tag{5.27}$$

known as the Painlevé equation. The question now is whether a solution to this equation can be considered as the non-perturbative sum over genus. Unfortunately the answer seems to be no. The solutions either contains unphysical singularities or attain imaginary values, which is equally unacceptable. The state of the matter seems to be that we do not have a nonpertubative formulation of the theory.

5.5 Including matter

Until now we have ignored matter completely in our discretized model. As in the continuum approach it is quite easy, on the formal level, to include matter fields in the description. We simply regard it as a ordinary lattice theory, albeit on a dynamic lattice. If for instance we have a bosonic field X given by

$$S_{matter}[g_{\mu\nu}, X] = \int (\partial_\mu X \partial^\mu X)\sqrt{g}d^2x \tag{5.28}$$

The discretized action becomes

$$\mathsf{S}_{matter} = \sum_{ij}(X_i - X_j)^2 \tag{5.29}$$

where the sum is over pair of vertices ij which share a propagator, i.e. neighbouring triangles.

A convenient way of solving models with matter is by means of multimatrix models. Let us modify our action Eq. (3.2), by introducing instead of one matrix, a pair of matrices, M_- and M_+, and change the Gaussian term in order to allow interaction between these :

$$S[M_+, M_-] = N\left(\frac{1}{2(1-e^{2\beta})}\mathrm{tr}(M_+^2 + M_-^2 - 2e^{-\beta}M_+M_-) + \frac{g}{3}(e^H \mathrm{tr}M_+^3 + e^{-H}\mathrm{tr}M_-^3)\right) \tag{5.30}$$

The physical interpretation of this model is that we have to distinct types of triangles $+$ and $-$, or rather one triangle with two states, which we could call spin up and spin down. The interaction is a nearest neighbour interaction with a factor $e^{-\beta}$ for gluing different spins. We can therefore identify this model with the Ising model at temperature $\frac{1}{\beta}$ and magnetic field H.

We can generalize this idea to an arbitrary number of matrices. In the limit of an infinite number of matrices (and a suitable coupling) we obtain the bosonic case described above. Both the Ising model and the single boson case can be solved[50]. In order to compare with continuum theory Sec. (2.7) one should note that the central charge for these models are $c = \frac{1}{2}$ and $c = 1$, giving $\gamma = -\frac{1}{3}$ and $\gamma = 0$ respectively. The agreement with Liouville theory is well established [14].

Having solved these two models it might seem easy to generalize to an arbitrary number of Ising spins, or bosonic degrees of freedom. In the case of a rigid lattice we can just solve

them independently, since they are noninteracting. On the dynamical lattice, however, we cannot avoid that they interact through the lattice, i.e. through gravity. This not only makes the solution much harder, there also seems to be some fundamental questions associated with $c > 1$ models. Although this is not quite clear in the discrete formulation, there certainly is a tremendous difference in the continuum formulation between theories with central charge smaller than one, and those with $25 > c > 1$, since for the latter Liouville theory predict a *complex* string susceptibility γ. The whole region of $1 < c < 25$ is very poorly understood, and the nature of the $c = 1$ barrier is still one of the most puzzling questions in two dimensional quantum gravity.

5.6 Multicritical models

We noted in Sec. (3.3) that the action we were using were unbounded. In order to cure this, one could try to add a quartic term, resulting in an action like:

$$S[M] = N(\frac{1}{2}\mathrm{tr}M^2 - \frac{g_3}{3}\mathrm{tr}M^3 - \frac{g_4}{4}\mathrm{tr}M^4) \tag{5.31}$$

This amounts to allowing squares in the build up (Cf. Sec. (5.1)). If we want to give these squares a positive weight, necessary for describing pure gravity, we must insist on the sign of g_4 be positive. With this choice of sign the action will still be unbounded from below, and the partition function $\int e^{-S}$ still rather ill defined. As mentioned above (Sec. (5.1)) this model gives the same results as ours in the scaling limit. It seems nothing is gained from the addition of the extra term, at least if we restrict ourselves to positive g_4.

If we allow negative weight to the squares we are no longer in the pure gravity regime, and we can expect to uncover a new universality class. To realize how this comes about, let us see how the new coupling changes the continuum limit. All of the calculations in Sec. (3.3) can be repeated with only minor changes, the only important thing will be the appearance of two coupling constants in the coefficients of Eq. (3.28), and that this equation will now be quartic, instead of cubic.

With these changes we have the possibility of approaching the critical point in a new way. Remember that the critical point for g was the point where Eq. (3.28) acquired a double root, the critical value of c. We now have two coupling constants, and by fine tuning the approach to the critical point, we can obtain that c_{crit} becomes a triple root. The resultant continuum model is also known as a multicritical model, and the point in coupling space is called a multicritical point.

It turns out that we can only obtain triple roots if we allow negative coupling. This in complete accord with the afore mentioned universality of pure gravity. We can generalize the above to quintic or higher power of interaction, and we expect to get different universal behavior for higher order multicritical point (quadruple roots etc.).

What is the physical interpretation (if any) of these multicritical models? Let us first consider the quartic model. This can be thought of as a *hard dimer problem*[51]. We simply view the the squares as two triangles with a colored gluing. The model now counts the number of triangulations where some gluings can be performed with colored glue, but only in such a way that each triangle has at most one side with colored glue.

The hard dimer problem on its side can be identified[32] with the Ising model in the limit of infinite temperature $\beta = 0$, and *imaginary* magnetic field $H = i\frac{\pi}{2}$. and we can go even further by noting that the critical behavior of the Ising model in an imaginary magnetic field is governed by the *Lee-Yang edge singularity*, and that it has been shown[51] that one can identify this model, at the critical point $H = i\frac{\pi}{2}$, with a socalled *minimal* $(2, 5)$ *conformal field theory*.

This discussion can be carried further, and it is possible to identify the higher order multicritical models with minimal $(2, 2m - 1)$ conformal field theory coupled to gravity, where m is the multiplicity of the root. The pure gravity case correspond to $m = 2$ and it turns out this is the only value of m for which the theory is unitary. All higher order models can be identified with non-unitary field theories.

With this interesting link to conformal field theory we end our overview of results achieved in the present model, and concentrate our attention on the possibility of extracting an Operator Product Expansion from the theory.

Chapter 6

Operator Product Expansion

In the last chapter we took a look on some of the geometrical properties of our model. We also considered the possibility of coupling matter fields to the model. In this chapter we will focus on the pure gravitational aspect of the model, in the sense that we will scrutinize the field theoretical properties of the model. To be more specific, we will investigate the possibility of formulating an operator expansion in the theory. Let us therefore first explain the term OPE.

6.1 OPE in ordinary field theory

The Operator Product Expansion were originally proposed as an alternative to the Lagrangian method[37], in the sense that it was thought off as a generalisation of equal time commutation relations. This will not be our perspective, however, as we will look at it from the point of view of ordinary quantum field theory described by some Lagrangian[52, 54].

Let us for definiteness consider a scalar theory in 4 (Euclidean) dimensions

$$\mathcal{L} = \partial^\mu \phi \partial_\mu \phi - \frac{m^2}{2}\phi^2 - \frac{g}{4!}\phi^4 \tag{6.1}$$

The two point function is to zeroth order in perturbation theory given by the propagator

$$\langle \phi(x)\phi(y)\rangle = \Delta(x-y) = \int \frac{e^{ip(x-y)}}{p^2+m^2}\frac{d^4p}{(2\pi)^4} \tag{6.2}$$

which is divergent for $x \to y$. Let us now look at the $2+n$ point function. This will be given by (again to zeroth order)

$$\langle \phi(x)\phi(y)\phi(z_1)\cdots\phi(z_n)\rangle = \langle \phi(x)\phi(y)\rangle(\langle \phi(z_1)\cdots\phi(z_n)\rangle) + \text{O.T} \tag{6.3}$$

where O.T indicate terms where $\phi(x)$ and $\phi(y)$ are contracted with the other $\phi(z_i)$. The point is that if we let $x \to y$ and keep the z_i's at a finite distance, the first term will be dominating. These means that in the $(x-y) \to 0$ limit the operators $\hat{\phi}(x)$, $\hat{\phi}(y)$ act as if one operator. We can write this as

$$\hat{\phi}(x)\hat{\phi}(y) \overset{x\to y}{\sim} \Delta(x-y)\hat{1} \tag{6.4}$$

where $\hat{1}$ is the identity operator. For higher orders in perturbation theory there will be diagrams where $\phi(x)$ and $\phi(y)$ are contracted, not with each other but via a vertex. These might also give divergent contribution in the coincidence limit. We can therefore extend the formula as

$$\hat{\phi}(x)\hat{\phi}(y) \overset{x\to y}{\sim} \Delta(x-y)\hat{1} + C(x-y)\hat{\phi}^2(x) \tag{6.5}$$

where $\hat{\phi}^2 =: \hat{\phi}\hat{\phi} :$ is a normalordered (and hence finite) operator, and $C(x-y)$ is some prefactor which is probably divergent in the $(x-y) \to 0$ limit with singularities of the type $(x-y)^{-p}$ with possible logarithmic corrections (a polynomial in $\log|x-y|$).

We can generalize this form to the product of two arbitrary operators $\mathcal{O}_A(x)$ and $\mathcal{O}_B(y)$

$$\mathcal{O}_A(x)\mathcal{O}_B(y) \overset{x\to y}{\sim} \sum_k C^k_{AB}(x-y)\mathcal{O}_k(x) \tag{6.6}$$

where we by $\sim$ mean that it is to hold between expectation values, and we have introduced a set of operators $\mathcal{O}_k(x)$. This last formula is called, for obvious reasons, an Operator Product Expansion or just OPE.

The expansion is similar to the multi-pole expansion of classical electrodynamics. The divergences is however a quantum effect often associated with the wild fluctuations induced by close observations of a quantum field[53].

6.2 Scaling of operators

Assume now that we have a complete set of operators which transform under a *scaling transformation* as

$$\mathcal{O}_k(x) \to s^{d_k}\mathcal{O}_k(sx) \tag{6.7}$$

where d_k is called the dimension of the operator. With the aid of such transformation we can put a rather strict constraint on the form of the coefficient C_k of the operator product expansion. To see how this come about apply the transformation (6.7) to Eq. (6.6):

$$s^{d_B}\mathcal{O}_B(sx)s^{d_A}\mathcal{O}_A(sy) \sim \sum_k C^k_{AB}(x-y)s^{d_k}\mathcal{O}_k(sx) \tag{6.8}$$

on the other hand from Eq. (6.6) applied in $x = sx, y = sy$ we have

$$\mathcal{O}_B(sx)\mathcal{O}_A(sy) \sim \sum_k C^k_{AB}(sx-sy)\mathcal{O}_k(sx) \tag{6.9}$$

assuming orthogonality of the set $\mathcal{O}_k$ (this can always be achieved by a Gramm-Smith like procedure) we deduce

$$C^k_{AB}(sx-sy) = s^{d_k-d_A-d_B}C^k_{AB}(x-y) \tag{6.10}$$

showing that only the pre factors for operators of dimension $d_k \leq d_a + d_B$ will be divergent, and more so the lower the dimension.

Let us again consider the example of a scalar theory in 4 dimensions and investigate what happens under a scaling $x \to s^{-1}x$. From the kinetic term of the Lagrangian we see

that ϕ has the dimension of inverse length, so we expect the field to scale as $\phi \to s\phi$. For infinitesimal $s = 1 + \delta s$ we now have

$$\delta\phi = s\phi(sx) - \phi(x) = \delta s(1 + x\frac{\partial}{\partial x})\phi(x) \tag{6.11}$$

or more general

$$\delta\phi^n = s^n\phi^n(sx) - \phi^n(x) = \delta s(n + x\frac{\partial}{\partial x})\phi^n(x) \tag{6.12}$$

We also have $\partial_\mu \to s\partial_\mu$, and hence

$$\delta\partial_\mu\phi = s\partial_\mu s\phi(sx) - \partial_\mu\phi(x) = \delta s(2 + x\frac{\partial}{\partial x})\partial_\mu\phi(x) \tag{6.13}$$

so the variation of the whole Lagrangian, Eq. (6.1), is

$$\begin{aligned}\delta\mathcal{L}(x) &= \delta s\left[x\frac{\partial\mathcal{L}}{\partial x} + 2\partial^\mu\phi(x)2\partial_\mu\phi(x) - 2\frac{m^2}{2}\phi^2(x) - 4\frac{g}{4!}\phi^4(x)\right] \\ &= \delta s\left[x\frac{\partial\mathcal{L}}{\partial x} + 4\mathcal{L} + 2\frac{m^2}{2}\phi^2(x)\right]\end{aligned} \tag{6.14}$$

Now the action $\int \mathcal{L}(tx)t^4d^4x$ is invariant under change of t, since this just corresponds to a change of coordinates[1]. Differentiation with respect to t at $t = 1$ gives

$$0 = \frac{\partial}{\partial t}\left[\int \mathcal{L}(tx)s^4d^4x\right]\Big|_{t=1} = \int(x\frac{\partial}{\partial x} + 4)\mathcal{L}d^4x \tag{6.15}$$

so the variation of the action under the infinitesimal scaling transformation is

$$\delta S = \int \delta\mathcal{L}(x)d^4x = \delta s\int(x\frac{\partial}{\partial x} + 4)\mathcal{L} + 2\frac{m^2}{2}\phi^2(x)d^4x = \delta s\int m^2\phi^2(x)d^4x \tag{6.16}$$

We conclude that a mass term $m > 0$ explicitly breaks scaling invariance of the action and hence of the theory. This is not surprising since it introduces a constant with a dimension, which does not scale qua being a constant. In comparison the interacting term has a dimensionless constant g and hence causes apparently no troubles.

Naively we would therefore expect a massless theory to be scaling invariant or conformal. This would give simple scaling relations like Eq. (6.7), where the dimension d_k could be determined by simple dimensional analysis.

There is however one aber dabei. In the case of an interacting theory one have to regularize and renormalize the theory in order to obtain finite results. During this process one must introduce some new quantity, for instance a cut-off, which also take part in the scaling, leading to so-called anomalous scaling of the physical objects. In short, the regularization and renormalization procedure ruins the simple scaling relation for the free field, making the exponent a function of s. There is one important exception. In the neighborhood of a fix point for the beta function we have a similar scaling relation, although the dimension will not necessary be a simple integer found by dimensional analysis.

[1] in contrast to the change of physical scale s

If we want the scaling invariance to survive we could have dropped the interacting part, and only considered the free theory. This is indeed a conformal theory. OPE plays an important role in such conformal field theories, exactly because such theories are invariant under scaling, and therefore have operators which obeys Eq. (6.7). We have already seen how the product $\hat{\phi}(x)\hat{\phi}(y)$ could be expressed in terms of the unit operator. One could extend this sort of analysis to other operators such as $\partial\phi$ and the like.

6.3 OPE in 2d quantum gravity

Since quantum gravity is a reparametrization invariant theory, it is natural to expect an OPE similar to the one in conformal field theory. There is one sophistication, namely that in our formulation of the operator product expansion we implicit assumed that the underlying space where x and y lives was a vector space. In quantum gravity this is not the case. We do have, however, a metric structure on the space, allowing us to generalize Eq. (6.6) to

$$\mathcal{O}_A(x)\mathcal{O}_B(y) \sim \sum_k C_{AB}^k(d(x,y))\mathcal{O}_k(x) \tag{6.17}$$

where $d(x,y)$ is the geodesic distance between x and y. Since we in our formalism have named no point explicitly, this becomes

$$\mathcal{O}_A\mathcal{O}_B(D) \sim \sum_k C_{AB}^k(D)\mathcal{O}_k \tag{6.18}$$

where D is the distance between observable A and B.

Let us assume that such a relation exist for the operators $\mathcal{O}_k$ we introduced in Sec. (4.4). From the dimension of $[\mathcal{O}_k] = L^{\frac{5-k}{2}} = [D]^{5-k}$ and $[\mathcal{O}_m\mathcal{O}_n(D)] = D^{9-m-n}$ we immediately see that we must require

$$C_{mn}^k(D) \propto D^{4-m-n+k} \tag{6.19}$$

so the hypothesis is that an expansion like

$$\mathcal{O}_n\mathcal{O}_m(D) \sim \sum_k C_{nm}^k D^{4-n-m+k}\mathcal{O}_k \tag{6.20}$$

is valid in the limit $D \to 0$ for some set of constants C_{mn}^k.

In order to obtain the $D \to 0$ limit we will look at the large area limit, since this will ensure a shrinkage of D as discussed in Sec. (4.6).

From (6.20) we can now immediately deduce the following statements about the expectation values:

$$G_{mn}^{TD}(D) =< \mathcal{O}_n\mathcal{O}_m(D) >=< \sum_k C_{nm}^k D^{4-n-m+k}\mathcal{O}_k >= \sum_k C_{nm}^k D^{4-n-m+k}F_k^{TD} \tag{6.21}$$

and

$$\begin{aligned} H_{mnl}^{TD}(D_{12},D_3) &= < (\mathcal{O}_n\mathcal{O}_m(D_{12}))\mathcal{O}_l(D_3) >=< \sum_k C_{nm}^k D_{12}^{4-n-m+k}\mathcal{O}_k\mathcal{O}_l(D_3) > \\ &= \sum_k C_{nm}^k D_{12}^{4-n-m+k}G_{kl}^{TD}(D_3) \end{aligned} \tag{6.22}$$

We can check these relation by using our previous derived result for the 1,2 and 3-point function. The comparison between for instance $F_1^{TD} = \frac{1}{4}$ and $G_{11}^{TD} = \frac{1}{14}$ gives us $C_{11}^1 = \frac{2}{7}$. The results for C_{mn}^1 are shown for $1 \leq m+n \leq 9$ in Table (6.1). Since we work in the

mn	11	12	13	22	14	23	$15, 24, 33$	$16, 25, 34$	17	$26, 35, 44$	18	27	$36, 45$
G_{mn}^{TD}	$\frac{1}{14}$	$\frac{3}{14}$	$\frac{3}{14}$	$\frac{3}{7}$	$\frac{1}{14}$	$\frac{3}{14}$	0	0	$\frac{1}{8}$	0	$\frac{3}{14}$	$\frac{3}{8}$	0
C_{mn}^1	$\frac{2}{7}$	$\frac{6}{7}$	$\frac{6}{7}$	$\frac{12}{7}$	$\frac{2}{7}$	$\frac{6}{7}$	0	0	$\frac{1}{2}$	0	$\frac{6}{7}$	$\frac{3}{2}$	0

Table 6.1: The coefficients C_{mn}^1 from the comparison of G_{mn}^{TD} with $F_1^{TD} = \frac{1}{4}$

thermodynamic limit we have that F_k is only nonzero for $k = 1$, so in order to obtain C_{nm}^k for $k > 1$ we have to compare $H_{mnl}^{TD}(D_{12}, D_3)$ and $G_{kl}^{TD}(D_3)$. Using the coefficients introduced in Chap. (4) we obtain

$$H_{mnl}^{TD}(D_{12}, D_3) = \sum_k H_{mnlk}^{TD} D_{12}^{4-m-n+k} D_3^{5-l-k} = \sum_k C_{nm}^k D_{12}^{4-n-m+k} G_{kl}^{TD}(D_3) \tag{6.23}$$

and hence

$$C_{nm}^k = \frac{H_{mnlk}^{TD}}{G_{kl}^{TD}} \tag{6.24}$$

Note that this gives us an independent calculation of C_{nm}^k for each value of l. They should all agree if the expansion proposed is valid. Furthermore the values for C_{mn}^1 obtained this way should agree with the ones found above by comparing G_{mn}^{TD} and F_1^{TD}.

The results obtained [1] for $(mn) = (11), (12), (13)$ and $l = 1 \ldots 10$, agrees up to $k = 6$. For $k = 7$ however, the results suddenly begins to disagree: different coefficients are obtained for various l.

6.4 A possible explanation

It is quite puzzling that the operator product expansion is consistent to such a degree, without being completely valid, or completely inconsistent. It has been proposed[1] that the inconsistencies should be interpreted as originating from baby universes. The picture is the following.

The third operator $\mathcal{O}_l$ is "observing" the two others from some distance D_3. The two are supposed to be so close together (at a distance D_{12}) that they effectively can be viewed as one. The way this is imagined to come about in conventional quantum field theory is by integrating out the local degrees of freedom. Now in quantum geometry the term local degrees of freedom is not really well defined. One can imagine situations where there is a baby universe in the neighborhood of the two operators, and this could be viewed as a fluctuation in the local geometry. If however the baby universe is quite extensive we could have the third operator be placed in it. This sort of configuration could give unexpected contributions to the expansion.

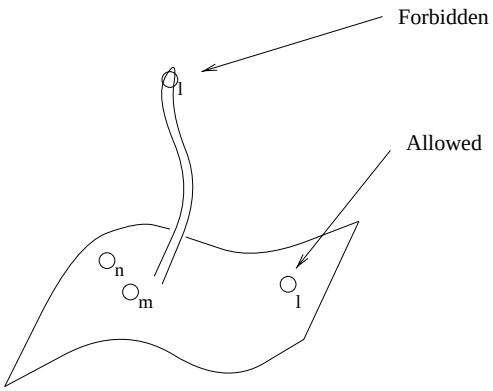

Figure 6.1: Two different cases for the position of the third operator

In [1] it is assumed that the babyuniverse part is proportional to Λ^0. From the dimension the of $G_{lj}(\Lambda, D)$, or equivalent the expansion in Λ we then obtain

$$G^{BA}_{lj}(\Lambda, D) = G^{BA}_{kl} D^{-1-l-j} \tag{6.25}$$

If we compare with the calculation Eq. (6.23) of C^k_{mn} we see that the baby universe configuration will only influence for $k > 6$ since only in that case exist $j > 0$ such that $-1 - l - j = 5 - l - k$.

If this explanation is correct, the solution to the inconsistencies seems to be that one should restrict the observer $\mathcal{O}_l$ to be in the mother universe. How this restriction could be imposed on the diagrams is not easy to see.

Even if the above consideration regarding the influence of babyuniverses is quite appealing from the physical point of view, and the analysis is somewhat more extensive in the referred paper[1], it still lack some mathematical rigor. If the term proportional to Λ^0 is important for babyuniverses, what about the term Λ^1 ? As we integrate over the position of the third operator, how come we get a contribution from the baby universes which have vanishing volume in the large V limit?

There is no doubt that something interesting happens around $k = 6$. This is also evident from pure dimensional reasons as $[\Lambda^{3/2}] = [D^6]$. The geometrical aspect of this could be interesting to investigate further.

Conclusion

We have seen in the former chapters how it is possible to formulate and solve a model for two dimensional quantum gravity. On the way we have obtained some insight into the geometrical as well as the field theoretical aspects of the theory. In specific we have seen that the concept of distance can be treated in a sensible way in the theory, and that it is possible to formulate an operator product expansion in a rather direct analogy to ordinary field theory. This is important insight, showing that one need not give up all hope that a sensible theory of quantum gravity exist, also in higher dimensions.

The jump to higher dimension is however far from trivial, since the integral over the curvature is no longer a topological invariant. The higher dimensional theories can not be solved in the same exact sense as the two dimensional case, but one can use the same techniques of discretization in computer simulations.

Even if the two dimensional model has been scrutinized for many years now, there still seem to be some open questions. What is the precise geometrical interpretation of the operators $\mathcal{O}_k$? Can we repair the inconsistencies in the OPE? And finally perhaps the most challenging: what happens for $c > 1$ models ?

It is the hope that the future may shed light on some of these issues, and perhaps through this provide further insight into the puzzling nature of quantum gravity.

Appendix A

Wick rotation

Let us consider an arbitrary manifold, with a metric $g_{\mu\nu}$, and introduce the Lagrangian density for some gauge theory coupled to a fermion field.

$$\mathcal{L} = \bar{\psi}_a(\gamma_\mu(D^\mu)^a_b + im\delta^a_b)\psi^b + \frac{1}{4}(F^{\mu\nu})^a_b(F_{\mu\nu})^b_a \tag{A.1}$$

where ψ is a spinor and $\bar{\psi}$ is an adjoint spinor, γ_μ are a representation of rotation group satisfying the Clifford algebra[1]

$$\{\gamma_\mu, \gamma_\nu\} = 2g_{\mu\nu} \tag{A.2}$$

and D^μ is the gauge covariant derivative

$$(D^\mu)^a_b = \delta^a_b\partial^\mu + i(A^\mu)^a_b \tag{A.3}$$

and finally

$$(F^{\mu\nu})^a_b = -i[(D^\mu)^a_c, (D^\nu)^c_b] \tag{A.4}$$

The Greek indices are spatial indices, the Latin indices are internal gauge indices and we have suppressed Dirac indices on the spinors and γ's. Lower indices corresponds to covariant vectors and upper to contravariant vectors. We have adopted the convention that we sum over indices occurring both as upper and lower.

Under a gauge transformation U all entities with upper Latin indices transform covariantly,

$$\psi^b \to \psi^a = U^a_b\psi^b \tag{A.5}$$

and those with lower transform contravariantly,

$$\bar{\psi}_a \to \bar{\psi}_b = (U^\dagger)^a_b\bar{\psi}_a \tag{A.6}$$

except the gauge field $(A^\mu)^a_b$ which transform like a Christoffel symbol:

$$(A^\mu)^a_b \to (A^\mu)^c_d = U^c_a(A^\mu)^a_b(U^\dagger)^b_d - (U^\dagger)^b_d\partial^\mu U^c_b \tag{A.7}$$

[1] strictly speaking since we are considering spinors we should allow *torsion* on the manifold, corresponding to the local choice of Dirac matrices, but since our main point is concerned with the signature, it will not influence our conclusions, and we will therefore omit this complication.

from this it is easily seen (using $U^a_c(U^\dagger)^c_b = \delta^a_b$), that the Lagrangian density is invariant under local gauge transformations. This is also manifest in the lack of internal indices on the Lagrangian density, as all indices are contracted leaving a scalar with respect to gauge transformation.

The exact same goes for the spatial indices. The whole Lagrangian density is invariant under local coordinate transformation provided the derivative ∂^μ is a covariant derivative with respect to spatial coordinate transformations (for simplicity we have left out the Christoffel symbols[2]).

Notice that we have put no restriction on the metric $g_{\mu\nu}$, except that it should be a tensor (or *two-form*), i.e. transform covariantly. Let us now consider two special cases.

1. The metric represents flat Minkowski space. This means that there exist a coordinate system in which the metric have the expression $g_{\mu\nu} = \eta_{\mu\nu}$ in every point.

2. The metric represents flat Euclidean space. This means that there exist a coordinate system in which the metric have the expression $g_{\mu\nu} = \delta_{\mu\nu}$ in every point.

In the first case we can use the usual Dirac matrices for the γ_μ's whereas in the second we should use a representation of the spinors in Euclidean space as is evident from Eq. (A.2).

If we introduce the following notation for the coordinates of $F^{\mu\nu}$ in our chosen coordinate system (suppressing gauge indices, and using that it is an antisymmetric tensor)

$$F^{\mu\nu} = \begin{bmatrix} 0 & -E_x & -E_y & -E_z \\ E_x & 0 & -B_z & B_y \\ E_y & B_z & 0 & -B_z \\ E_z & -B_y & B_x & 0 \end{bmatrix} \tag{A.8}$$

we see that in the case of Minkowski space

$$F_{\mu\nu} = g_{\mu\rho}g_{\sigma\nu}F^{\sigma\rho} = \eta_{\mu\rho}\eta_{\sigma\nu}F^{\sigma\rho} = \begin{bmatrix} 0 & E_x & E_y & E_z \\ -E_x & 0 & -B_z & B_y \\ -E_y & B_z & 0 & -B_z \\ -E_z & -B_y & B_x & 0 \end{bmatrix} \tag{A.9}$$

where as in the Euclidean case:

$$F_{\mu\nu} = g_{\mu\rho}g_{\sigma\nu}F^{\sigma\rho} = \delta_{\mu\rho}\delta_{\sigma\nu}F^{\sigma\rho} = \begin{bmatrix} 0 & -E_x & -E_y & -E_z \\ E_x & 0 & -B_z & B_y \\ E_y & B_z & 0 & -B_z \\ E_z & -B_y & B_x & 0 \end{bmatrix} \tag{A.10}$$

[2]or rather connection if we include torsion

Showing that the last part of $\mathcal{L}$ can be written as

$$\frac{1}{4}F^{\mu\nu}F_{\mu\nu} = -\frac{1}{2}(\vec{E}^2 - \vec{B}^2) \qquad \text{in Minkowski space} \tag{A.11}$$

$$\frac{1}{4}F^{\mu\nu}F_{\mu\nu} = \frac{1}{2}(\vec{E}^2 + \vec{B}^2) \qquad \text{in Euclidean space} \tag{A.12}$$

$$\tag{A.13}$$

In order to construct an action which is invariant under coordinate transformation we write

$$S = \int \mathcal{L}\sqrt{g}d^4x \tag{A.14}$$

in the Euclidean case this becomes

$$S_E = \int \bar{\psi}_a(\gamma_\mu(D^\mu)^a_b + im\delta^a_b)\psi^b + \frac{1}{2}(\vec{E}^2 + \vec{B}^2)d^4x \tag{A.15}$$

which can be recognized as the Euclidean QED action.

In Minkowski space we have

$$S_M = \int \mathcal{L}\sqrt{g}dtd^3x = i\int \mathcal{L}\sqrt{-g}dtd^3x = i\int \bar{\psi}_a(\gamma_\mu(D^\mu)^a_b + im\delta^a_b)\psi^b - \frac{1}{2}(\vec{E}^2 - \vec{B}^2)\sqrt{-g}dtd^3x \tag{A.16}$$

which is exactly iS_{QED} where S_{QED} is the ordinary (Minkowski) QED action. In both case (S_E and S_M) the quantum theory takes the form

$$Z = \int e^{-S[\bar{\psi},\psi,A]}\mathcal{D}[\bar{\psi},\psi,A] \tag{A.17}$$

where we have omitted all complications in terms of ghost fields, gauge fixing or the like.

Let us now show how to get from $S_{QED} = -iS_M$ to the Euclidean action S_E by means of the usual Wick rotation. First and foremost the time coordinate t should go into $-ix_0$ which means that

$$dt \to -idx_0 \tag{A.18}$$

We also need to impose the different transformation of the spinors and insist on using different Dirac matrices. Finally the time component of the gauge field A_t should go into $-iA_0$ resulting in

$$\vec{E} \to -i\vec{E} \tag{A.19}$$

With all these transformations carefully executed we obtain

$$iS_{QED} \to -\int \bar{\psi}_a(\gamma_\mu(D^\mu)^a_b + im\delta^a_b)\psi^b + \frac{1}{2}(\vec{E}^2 + \vec{B}^2)d^4x = -S_E \tag{A.20}$$

showing the equivalence of the Wick rotation prescribed Euclidean action, and the one obtained by simple substitution of $g_{\mu\nu} = \delta_{\mu\nu}$.

What are the differences between the two methods then? The first method focuses heavily on the geometry, and is truly covariant with no reference to a coordinate system. This allow the same form of the Lagrangian density to be used with any metric, or more general any two-tensor. The explicit form of the action depends of course on the

coordinate system it is described in, but only via the coordinates for the two-form $g_{\mu\nu}$. The value of the integral $\int \mathcal{L} d\mu$ is independent of the coordinates chosen.

The second method is the normal one in quantum field theory. It works with a specific set of coordinates (an inertial frame) and the rotation to Euclidean form is actually an analytic continuation to complex time. This is very convenient in quantum field theory since it allows calculation in the Euclidean formalism, and then the analytic continuation back to real time gives the physical results. From a geometric point of view this whole prescription is sort of ad hoc, and we need to introduce vielbeins[3] in order to make sense of it at all in curved space. But this does not solve problem in general, since we can no longer be sure that the action is analytic in time. On the contrary it will often be impossible to find a deformation of the path for the t integration which does not encounter singularities along the way. The singularities in flat space is situated on the real axis, which means that we can come arbitrary close to the Minkowski action, starting from the Euclidean. In the general case however the singularities can be anywhere in the complex t plane, making it impossible to get even close to the Minkowski or Euclidean starting from the other.

One final comment on the first method. Introducing the square root of the determinant g in our definition leave us with an ambiguity in the sign of the action. We have chosen a branch of the squareroot which agree with the usual convention used in flat space QFT. For arbitrary $g_{\mu\nu}$ some specification of the sign should be prescribed, especially if the intention is to integrate over geometries.

[3]Local inertial frames. Zweibeins, dreibeins, vierbeins etc. according to the dimension.

Appendix B

Feynman rules for the matrix model

Let us consider the action for a matrix model:

$$S[M] = N(\frac{1}{2}\mathrm{tr}M^2 - \frac{g}{3}\mathrm{tr}M^3) = \frac{1}{2}M^i_j M^k_l A^{jl}_{ik} - \frac{g}{3}M^p_q M^r_s M^t_u B^{qsu}_{prt} \tag{B.1}$$

where $A^{jl}_{ik} = N\delta^j_k\delta^l_i$ and $B^{qsu}_{prt} = N\delta^q_r\delta^s_t\delta^u_p$ and we sum over identical lower and upper indices. The upper index is a row index and the lower is a column index. We seek the perturbative expansion in g for the following integral:

$$Z[g] = \int e^{-S[M]}dM = \int e^{\frac{g}{3}M^p_q M^r_s M^t_u B^{qsu}_{prt}} e^{-\frac{1}{2}M^i_j M^k_l A^{jl}_{ik}} dM \tag{B.2}$$

We can rewrite this integral by introducing a source term $J^m_n M^n_m$ and rewrite the interaction term as a differential operator in J (Wicks theorem):

$$Z[g] = Z[g, J=0] = \left[e^{\frac{g}{3}B^{qsu}_{prt}\frac{\partial}{\partial J^q_p}\frac{\partial}{\partial J^s_r}\frac{\partial}{\partial J^u_t}} \int e^{-\frac{1}{2}M^i_j M^k_l A^{jl}_{ik} + J^m_n M^n_m} dM \right]\Bigg|_{J=0} \tag{B.3}$$

the latter integral can readily be solved by a completion of the square yielding

$$\left[e^{\frac{g}{3}B^{qsu}_{prt}\frac{\partial}{\partial J^q_p}\frac{\partial}{\partial J^s_r}\frac{\partial}{\partial J^u_t}} e^{\frac{1}{2}J^i_j J^k_l (A^{-1})^{jl}_{ik}} \right]\Bigg|_{J=0} \times \text{normalisation} \tag{B.4}$$

where $(A^{-1})^{jl}_{ik} = \frac{1}{N}\delta^j_k\delta^l_i$.

The perturbation series is now obtained by expanding the "interaction" exponential

$$e^{\frac{g}{3}B^{qsu}_{prt}\frac{\partial}{\partial J^q_p}\frac{\partial}{\partial J^s_r}\frac{\partial}{\partial J^u_t}} = 1 + \frac{g}{3}B^{qsu}_{prt}\frac{\partial}{\partial J^q_p}\frac{\partial}{\partial J^s_r}\frac{\partial}{\partial J^u_t} + \frac{1}{2!}(\frac{g}{3}B^{qsu}_{prt}\frac{\partial}{\partial J^q_p}\frac{\partial}{\partial J^s_r}\frac{\partial}{\partial J^u_t})^2 + ... \tag{B.5}$$

and let the differential operators work on the second factor. As an example consider the second order term:

$$Z^{(2)} = \frac{1}{2!}(\frac{g}{3}B^{bdf}_{ace}\frac{\partial}{\partial J^b_a}\frac{\partial}{\partial J^d_c}\frac{\partial}{\partial J^f_e})(\frac{g}{3}B^{qsu}_{prt}\frac{\partial}{\partial J^q_p}\frac{\partial}{\partial J^s_r}\frac{\partial}{\partial J^u_t})e^{\frac{1}{2}J^i_j J^k_l (A^{-1})^{jl}_{ik}} \tag{B.6}$$

We note that

$$\begin{aligned}\frac{\partial}{\partial J^u_t}(\frac{1}{2}J^i_j J^k_l (A^{-1})^{jl}_{ik}) &= \frac{\partial}{\partial J^u_t}\frac{1}{2N}[J^i_j J^k_l \delta^j_k \delta^l_i] \\ &= \frac{1}{2N}[\delta^i_u\delta^t_j J^k_l + J^i_j\delta^k_u\delta^t_l]\delta^j_k\delta^l_i = \frac{1}{N}J^t_u\end{aligned} \tag{B.7}$$

so the calculation of the second order term takes the form

$$\begin{aligned}
& \frac{g^2}{9} B^{bdf}_{ace} B^{qsu}_{prt} \frac{\partial}{\partial J^b_a}\frac{\partial}{\partial J^d_c}\frac{\partial}{\partial J^f_e}\frac{\partial}{\partial J^q_p}\frac{\partial}{\partial J^s_r}[\frac{1}{N} J^t_u e^{\frac{1}{2}J^i_j J^k_l (A^{-1})^{jl}_{ik}}] \\
= & \frac{g^2}{9} B^{bdf}_{ace} B^{qsu}_{prt} \frac{\partial}{\partial J^b_a}\frac{\partial}{\partial J^d_c}\frac{\partial}{\partial J^f_e}\frac{\partial}{\partial J^q_p}[(\frac{1}{N}\delta^t_s\delta^r_u + \frac{1}{N}J^t_u\frac{1}{N}J^r_s) e^{\frac{1}{2}J^i_j J^k_l (A^{-1})^{jl}_{ik}}] \\
= & \frac{g^2}{9} B^{bdf}_{ace} B^{qsu}_{prt} \frac{\partial}{\partial J^b_a}\frac{\partial}{\partial J^d_c}\frac{\partial}{\partial J^f_e}[(\frac{1}{N}\delta^t_s\delta^r_u\frac{1}{N}J^p_q + \frac{1}{N}\delta^t_q\delta^p_u\frac{1}{N}J^r_s + \frac{1}{N}J^t_u\frac{1}{N}\delta^r_q\delta^p_s + \frac{1}{N}J^t_u\frac{1}{N}J^r_s\frac{1}{N}J^p_q) e^{\frac{1}{2}J^i_j J^k_l (A^{-1})^{jl}_{ik}}] \\
= & \ ... \qquad \text{(B.8)}
\end{aligned}$$

In the end we should take $J = 0$ so only terms consisting purely of δ's will survive. Of these we will have terms representing all 15 possible ways of pairing up the $\frac{\partial}{\partial J^i_j}$. For instance a term like $\frac{1}{N}\delta^t_s\delta^r_u\frac{1}{N}\delta^p_f\delta^e_q\frac{1}{N}\delta^c_b\delta^a_d$ represents a pairing of $\frac{\partial}{\partial J^u_t}\frac{\partial}{\partial J^s_r}$, $\frac{\partial}{\partial J^q_p}\frac{\partial}{\partial J^f_e}$ and $\frac{\partial}{\partial J^d_c}\frac{\partial}{\partial J^b_a}$. These terms are then to be contracted with the B^{bdf}_{ace} and the B^{qsu}_{prt}. We could of course do the contraction with B^{qsu}_{prt} already after the first three differentiations, simplifying the above expression to:

$$\begin{aligned}
= & \frac{g^2}{9} B^{bdf}_{ace} \frac{\partial}{\partial J^b_a}\frac{\partial}{\partial J^d_c}\frac{\partial}{\partial J^f_e}[(3J^q_q + \frac{1}{N^2}J^t_q J^r_t J^q_r) e^{\frac{1}{2}J^i_j J^k_l (A^{-1})^{jl}_{ik}}] \\
= & \frac{g^2}{9} B^{bdf}_{ace} \frac{\partial}{\partial J^b_a}\frac{\partial}{\partial J^d_c}[(3\delta^q_f\delta^e_q + 3J^q_q\frac{1}{N}J^e_f + 3\frac{1}{N^2}J^e_q J^q_f + \ldots) e^{\frac{1}{2}J^i_j J^k_l (A^{-1})^{jl}_{ik}}] \\
= & \frac{g^2}{3} B^{bdf}_{ace} \frac{\partial}{\partial J^b_a}[(\delta^e_f\frac{1}{N}J^c_d + \delta^c_d\frac{1}{N}J^e_f + J^q_q\frac{1}{N}\delta^e_d\delta^c_f + \frac{1}{N^2}\delta^e_d J^c_f + \frac{1}{N^2}J^e_d\delta^c_f + \ldots) e^{\frac{1}{2}J^i_j J^k_l (A^{-1})^{jl}_{ik}}] \\
= & \frac{g^2}{3}(4N^2 + 1) + ... \qquad \text{(B.9)}
\end{aligned}$$

where the dots indicate terms with J which will be put to zero. This would however make the following identification with Feynman diagrams less lucid.

First draw a vertex for each factor B^{jln}_{ikm} as shown in Fig. (B.1). Note that incoming arrows signifies upper index while outgoing corresponds to lower.

Figure B.1: Matrix model vertex and propagator

Complete the diagram by drawing propagators, and calculate the value v_d of the diagram by assigning $\frac{1}{N}\delta^i_l\delta^j_k$ for each propagator from ij to kl (note again that arrows run from upper to lower indices), and a value of $\frac{g}{3}N\delta^j_k\delta^l_m\delta^n_i$ for each vertex. Next perform the sum over indices appearing both as upper and lower. This will give a factor of N for each closed loop in the diagram. Finally we should sum over all possible diagrams. In general the $n-$th order term is

$$Z^{(n)} = \frac{1}{n!}\sum_{d\in D_n} v_d \qquad \text{(B.10)}$$

where D_n is the set of diagrams with n vertices. The set D_n will consist of $(3n-1)!!$ elements for n even, and be empty for n odd, as can be seen in the following way. It clear that an odd number of legs can never be paired up. In the original differentiations scheme this is reflected in the fact that there will be at least one factor factor of J left in each term, making them give zero contribution when we take $J = 0$. Now for n even we choose a leg on one vertex. This will have $3n-1$ possible partners. The next leg will have $3n-3$ partners all the way down to the $n-1$ legs, which will have only one other leg. All in all $(3n-1)(3n-3)\cdots 3 \cdot 1 = (3n-1)!!$ different contractions.

With regard to the value of each diagram we make the following observation. As noted before, each time we have a loop in the diagram, i.e. a set of arrows closing on itself, we will have a contribution of the form $\delta^i_j \delta^j_k \ldots \delta^l_m \delta^m_i = \delta^i_i = N$. Since we are considering vacuum diagrams, this means that any diagram will contribute exactly N^{V-E+F}, where V is the number of vertices, E the number of propagators, and F the number of loops.

Not only will many of the diagrams give the same contribution, some of them will even be impossible to distinguish apart from the names of the indices. We can interchange the complete set of indices on the vertices[1], this can be done in $n!$ ways for a diagram with n vertices. We can therefore remove the factor of $\frac{1}{n!}$ in front of the sum in Eq. (B.10), if we identify diagrams with permuted vertices. We can also cyclic permute the names of the indices of any vertex without changing the diagram. This means that we can restrict the counting to diagrams distinguishable without indices on the vertex-legs, if we at the same time removes the factor of $\frac{1}{3}$ from each vertex. Note that since we have arrows on the lines, and hence an "orientation" of the vertex we will not have 3! ways of connecting three propagators to a vertex as in ordinary ϕ^3 theory, but only 3.

If the diagram have some symmetry two different labelling of the legs of the vertices will give the same contractions. In this case we should weight the diagram with a *statistical weight factor*

$$\omega_d = \frac{\text{number of different contractions}}{\text{number of labellings}} \tag{B.11}$$

which is strictly less than one.

To illustrate this let us consider the three possible diagrams with two vertices. See Fig. (B.2)

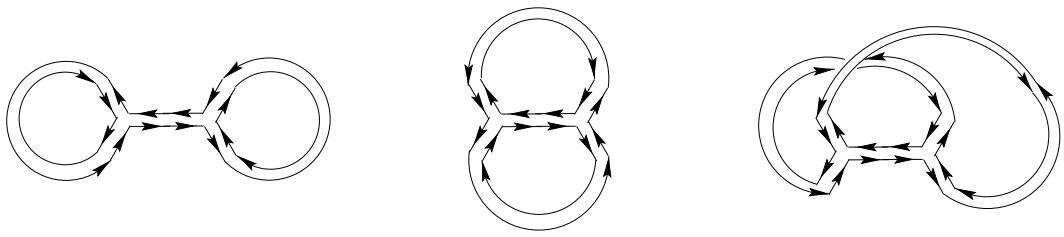

Figure B.2: The three possible diagrams with two vertices

In all three cases we have of course $2!3^2 = 18$ ways of labelling the legs of the vertices. In the first case only nine of these give different contractions, since interchanging the set

[1] the same as interchanging two vertices

of labels on the vertices give no new contractions. The factor of $\frac{1}{2!}$ will therefore not be cancelled, and the statistical weight is $\omega_1 = \frac{1}{2}$.

For the second diagram we have 3 different contractions. As before interchanging the vertices give no new contractions. Furthermore we obtain the same contraction of indices if we cyclic permute both set of indices at the same time, therefore only one of the factors of 3 will be cancelled. In conclusion the statistical weight is $\omega_2 = \frac{1}{6}$.

The third diagram has the same symmetries as the second, ergo $\omega_3 = \frac{1}{6}$

Since the first two diagrams have 2 vertices, 3 propagators and 3 loops, each have a value of $v_d = g^2N^2$. The third have only one loop, so the value for this becomes 1.

In conclusion we have

$$Z^{(2)} = (\frac{2}{3}N^2 + \frac{1}{6})g^2 \tag{B.12}$$

The same result as directly from Eq. (B.9) $Z^{(2)} = \frac{1}{2!}\frac{g^2}{3}(4N^2+1) = (\frac{2}{3}N^2 + \frac{1}{6})g^2$.

So far we have only considered vacuum blobs. We can now get the Greens functions by means of differentiation:

$$\langle M^i_j \dots M^k_l \rangle = \frac{1}{Z[g, J=0]} \left[\frac{\partial}{\partial J^j_i} \cdots \frac{\partial}{\partial J^l_k} Z[g, J] \right] \Big|_{J=0} \tag{B.13}$$

Or equivalent by constructing diagrams with external legs with indices $(ij)\dots(kl)$. The value of such a diagram will be (apart from statistical weight) $g^n N^{n-E+F}$ times some delta functions found by following the lines which start and end on external indices. A line that start at i and end at l will give δ^i_l.

To resume the Feynman rules: To calculate the $n-$th order contribution. Draw all diagrams distinguishable without any labels on the vertices (the set D), assigning a value of gN for each vertex, $\frac{1}{N}$ for each propagator, and N for each closed loop. Calculate the statistical weight factor ω_D as the ratio of the number of different contractions divided by the number of possible labellings $(n!3^n)$. Now

$$Z^n = \sum_{d \in D} \omega_D g^n N^{n-E+F} \tag{B.14}$$

If there are external legs we have

$$G^n(M^i_j \dots M^k_l) = \sum_{d \in D} \omega_d g^n N^{n-E+F} \delta^i_a \cdots \delta^k_b \tag{B.15}$$

where a and b are lower indices found by following the lines starting at i and k respectively.

Appendix C

Dictionary

This appendix should serve as a dictionary for translating between the matrix language, and that of triangulations.

Vertex 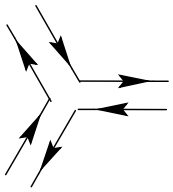

Triangle 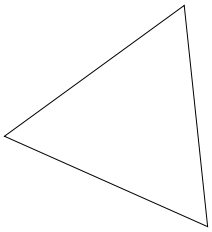

Propagator 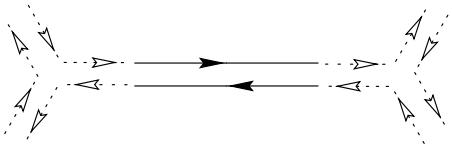

Gluing 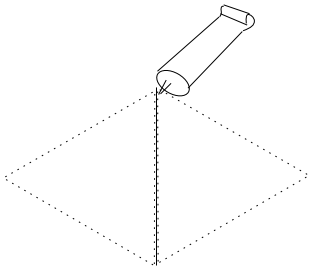

Tadpole 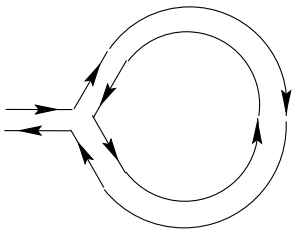

Cone 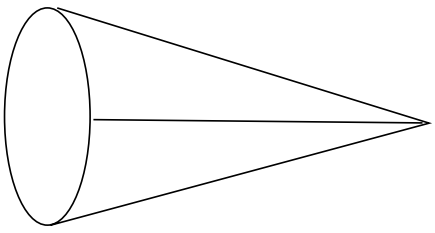

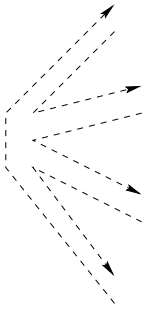

l-Ped

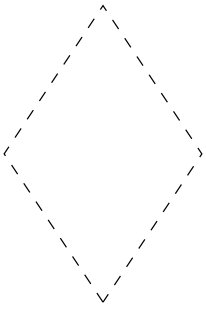

l-gon

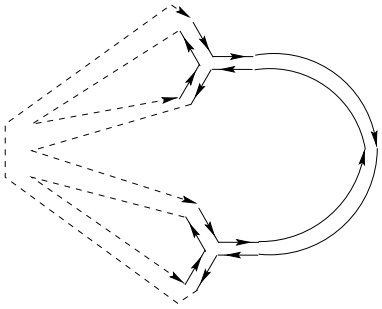

Loop diagram

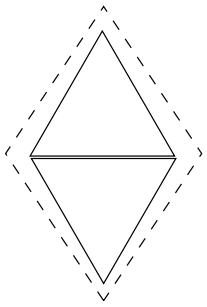

Boundary

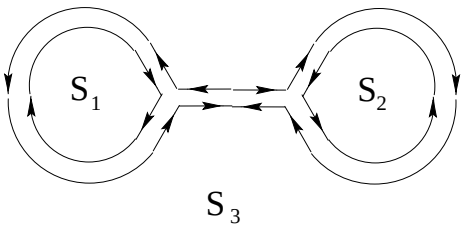

Sector

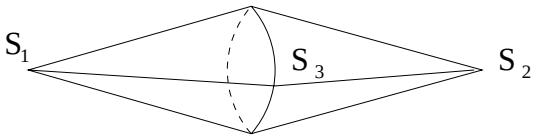

Dual vertices

Appendix D

Laplace transform

Let us first define two transformations which occur very frequently in physics.

Definition 1 *The Laplace transform of a function $f(s)$ is given by*

$$F(t) = \mathcal{L}\{f\}(t) = \int_0^\infty e^{-st} f(s) ds \tag{D.1}$$

Definition 2 *The Fourier transform of a function $g(s)$ is given by*

$$G(y) = \mathcal{F}\{g\}(y) = \int_{-\infty}^\infty e^{-ixy} g(x) dx \tag{D.2}$$

with the inverse transformation

$$g(x) = \mathcal{F}^{-1}\{G\}(x) = \frac{1}{2\pi} \int_{-\infty}^\infty e^{ixy} G(y) dy \tag{D.3}$$

satisfying $\mathcal{F}^{-1}\{\mathcal{F}\{g\}\}(x) = g(x)$.

Both transformations are defined on the space $\mathcal{S}$ of fast decreasing functions, but are easily extended by duality to the space $\mathcal{S}'$ of continuous functionals on $\mathcal{S}$, among which are not only all integrable functions, but also the Dirac distribution and other distributions with compact support, in addition to polynomials of any degree, but not for instance e^x [62].

A common problem is to find the *inverse Laplace transform* of some given function $F(t)$, i.e. a function $f(s)$ such that $\mathcal{L}\{f\}(t) = F(t)$. To this end we have the following

Theorem 1 *Assume $F(t) = \mathcal{L}\{f\}(t)$ is holomorphic and that there exist a constant $c > 0$ such that the integral*

$$\lim_{T\to\infty} \frac{1}{2\pi i} \int_{c-iT}^{c+iT} e^{ps} F(p) dp \tag{D.4}$$

is convergent for any $s > 0$ then $f(s) = \frac{1}{2\pi i} \int_{c-i\infty}^{c+i\infty} e^{ps} F(p) dp$.

To see why the above must hold consider $g(x) = e^{-cx}H(x)f(x)$ where H is the *Heaviside distribution*

$$H(t) = \begin{cases} 0 & \text{for} \quad t < 0 \\ 1 & \text{for} \quad t > 0 \end{cases} \tag{D.5}$$

and use $\mathcal{F}^{-1}\{\mathcal{F}\{g\}\}(x) = g(x)$ to reveal

$$\begin{aligned} H(s)f(s) &= \frac{e^{cs}}{2\pi}\int_{-\infty}^{\infty} e^{isy}\int_{-\infty}^{\infty} e^{-ixy}e^{-cx}H(x)f(x)dxdy \\ &= \frac{1}{2\pi}\int_{-\infty}^{\infty} e^{(c+iy)s}\int_{0}^{\infty} e^{-(c+iy)x}f(x)dxdy \\ &= \frac{1}{2\pi i}\int_{c-i\infty}^{c+i\infty} e^{ps}\int_{0}^{\infty} e^{-px}f(x)dxdp \\ &= \frac{1}{2\pi i}\int_{c-i\infty}^{c+i\infty} e^{ps}\mathcal{L}\{f\}(p)dp \end{aligned} \tag{D.6}$$

The integral in Eq. (D.4) is conveniently calculated by choosing a c such that all singularities of F are to the left of the line $\mathrm{Re}z = c$ and then complete the contour around these.

Quite often the integral in Eq. (D.4) will not be convergent for any c (as for instance for $F(t) = 1$) and we must use different methods. Here the following relationship between the two transformation comes in handy,

$$\mathcal{L}\{f\}(-it) = \mathcal{F}\{fH\}(-t) = 2\pi\mathcal{F}^{-1}\{fH\}(t) \tag{D.7}$$

Taking the Fourier transformed on both sides gives

$$\mathcal{F}\{\widehat{\mathcal{L}\{f\}}\}(s) = 2\pi f(s)H(s) = 2\pi\hat{f}(is)H(s) \tag{D.8}$$

where $\hat{f}(t) = f(-it)$. This gives us the possibility to find the inverse Laplace transform for functions which are not integrable. For instance assume $F(t) = t^n$ for some $n \in N$ then $\hat{F} = (-i)^n t^n$ and

$$2\pi f(s)H(s) = \mathcal{F}\{(-i)^n t^n\}(s) = (-i)^n\mathcal{F}\{t^n\}(s) = \partial^n\mathcal{F}\{1\}(s) = 2\pi\partial^n\delta(s) \tag{D.9}$$

where δ is the Dirac distribution, and we have used that Fourier transformation sends multiplication operators into differential operators. From the above we see that $f(s)$ has support in 0 for any n. Since $\mathcal{L}$ is linear we also deduce that the inverse Laplace transform of any polynomial has support in 0.

Appendix E

Two and three point functions

In order to calculate

$$G(\Lambda, X_1, X_2, D) = \frac{1}{2\pi i}\int_{-i\infty}^{i\infty} \dot{F}(\Lambda, X)\dot{N}(\Lambda, X_1, -X, D_1)\dot{N}(\Lambda, X_2, -X, D_2)dX \tag{E.1}$$

we will need

$$\dot{N}(X_1, X, D) = \frac{1}{X + B(X_1, D)} \tag{E.2}$$

and

$$\frac{1}{A-X}\frac{1}{B-X} = \frac{1}{B-A}\left[\frac{1}{A-X} - \frac{1}{B-X}\right] \tag{E.3}$$

inserting this we arrive at

$$G(\Lambda, X_1, X_2, D) = \frac{1}{2\pi i}\frac{1}{B(\Lambda, X_2, D_2) - B(\Lambda, X_1, D_1)}\int_{-i\infty}^{i\infty} \frac{\dot{F}(\Lambda, X)}{X + B(X_1, D)} - \frac{\dot{F}(\Lambda, X)}{X + B(X_2, D)}dX \tag{E.4}$$

We can now use

$$\frac{1}{2\pi i}\int_{-i\infty}^{i\infty} \dot{F}(X)\frac{1}{B-X}dX = \dot{F}(B) \tag{E.5}$$

to arrive at

$$G(\Lambda, X_1, X_2, D) = \frac{\dot{F}(\Lambda, B(\Lambda, X_1, D_1)) - \dot{F}(\Lambda, B(\Lambda, X_2, D_2))}{B(\Lambda, X_2, D_2) - B(\Lambda, X_1, D_1)} \tag{E.6}$$

with $y_i = e^{aD_i}h^{-1}(X_i)$ and using

$$\dot{F}(\Lambda, B(\Lambda, X, D)) = \dot{F}(\Lambda, h(y)) = 2a^3\frac{y(1+y)}{(y-1)^3} \tag{E.7}$$

and

$$B_i - B_j = h(y_i) - h(y_j) = a^2\left(\frac{y_i}{(y_i-1)^2} - \frac{y_j}{(y_j-1)^2}\right) \tag{E.8}$$

where B_i is shorthand for $B(\Lambda, X_i, D_i)$, this becomes

$$G(\Lambda, X_1, X_2, D) = 2a\left(\frac{1}{y_1y_2 - 1} - \frac{1}{y_1 - 1} - \frac{1}{y_2 - 1} - \frac{1}{2}\right) \tag{E.9}$$

as wanted. After differentiating with respect to X_1 and X_2 we obtain

$$\ddot{G} = 2a\frac{(1+y_1y_2)}{(y_1y_2-1)^3}\frac{\partial}{\partial X_1}\frac{\partial}{\partial X_2}(y_1y_2) \tag{E.10}$$

The power expansion of $\ddot{G} = \sum_{m,n=1}^{\infty} G_{mn}(\Lambda, D) X_1^{-\frac{m+2}{2}} X_2^{-\frac{n+2}{2}}$ leads to the following coefficients

$$G_{mn}(\Lambda, D) = -\frac{a^{l+k+1}}{2b_l b_k!}\frac{P_{lk}(e^{aD})}{(1-e^{aD})^{l+k+1}} \tag{E.11}$$

where $b_i = \{1, 1, 2, 6, \frac{96}{5}, 48, \frac{864}{7}, 864, \ldots\}$ and $P_{lk} = P_{kl}$ are the polynomials

$$\begin{aligned}
P_{11}(x) &= x(x+1)\\
P_{12}(x) &= x(1+4x+x^2)\\
P_{13}(x) &= x(1+x)(1+10x+x^2)\\
P_{22}(x) &= x(1+x)(1+10x+x^2)\\
P_{14}(x) &= x(1+26x+66x^2+26x^3+x^4)\\
P_{23}(x) &= x(1+26x+66x^2+26x^3+x^4)\\
P_{15}(x) &= x(x+1)(1+44x+198x^2+44x^3+x^4)\\
P_{24}(x) &= x(x+1)(1+56x+246x^2+56x^3+x^4)\\
P_{33}(x) &= x(x+1)(1+56x+246x^2+56x^3+x^4)\\
P_{16}(x) &= x(1+48x+471x^2+976x^3+471x^4+48x^5+x^6)\\
P_{25}(x) &= x(1+96x+951x^2+1936x^3+951x^4+96x^5+x^6)\\
P_{34}(x) &= x(1+120x+1191x^2+2416x^3+1191x^4+120x^5+x^6)\\
P_{17}(x) &= x(1+22x+x^2)^2(1+5x+5x^2+x^3)\\
P_{26}(x) &= x(x+1)(1+102x+1599x^2+4660x^3+1599x^4+102x^5+x^6)\\
P_{35}(x) &= x(x+1)(1+198x+3231x^2+9268x^3+3231x^4+198x^4+x^6)\\
P_{44}(x) &= x(x+1)(1+246x+4047x^2+11572x^3+4047x^4+246x^5+x^6)\\
P_{18}(x) &= x(1+10x+x^2)^2(1+50x+114x^2+50x^3+x^4)\\
P_{27}(x) &= x(1+22x+x^2)(1+84x+627x^2+1168x^3+627x^4+84x^5+x^6)\\
P_{36}(x) &= x(1+214x+5824x^2+35242x^3+62590x^4+35242x^5+5824x^6+214x^7+x^8)\\
P_{45}(x) &= x(1+406x+11680x^2+70570x^3+124990x^4+70570x^5+11680x^6+406x^7+x^8)
\end{aligned} \tag{E.12}$$

The expansion of $\ddot{G}_{mn}(\Lambda, D)$ in Λ and extraction of the part proportional to $\Lambda^{3/2}$ leads to the coefficients given table (4.1).

Three loop amplitude

The three loop amplitude can be calculated using similar methods. In addition to the above formulas we will need

$$\ddot{N}(\Lambda, X_1, X, D) = -\frac{\partial}{\partial X}\frac{1}{X + B(\Lambda, X_1, D)} = \frac{1}{(X + B(\Lambda, X_1, D))^2} \tag{E.13}$$

We can now get

$$\begin{aligned}
\ddot{N}(\Lambda, X_1, -X, \frac{1}{2}D_{12})\dot{N}(\Lambda, X_2, -X, \frac{1}{2}D_{12})\dot{N}(\Lambda, X_3, -X, D_3 - \frac{1}{2}D_{12}) &= \\
\frac{1}{(B(\Lambda, X_1, \frac{1}{2}D_{12}) - X)^2}\frac{1}{B(\Lambda, X_2, \frac{1}{2}D_{12}) - X}\frac{1}{B(\Lambda, X_3, D_3 - \frac{1}{2}D_{12}) - X} &= \\
\frac{1}{B_2 - B_1}\left[\frac{1}{B_1 - X} - \frac{1}{B_2 - X}\right]\frac{1}{B_3 - B_1}\left[\frac{1}{B_1 - X} - \frac{1}{B_3 - X}\right] &= \\
\frac{1}{B_2 - B_1}\frac{1}{B_3 - B_1}\left(\frac{1}{(B_1 - X)^2} - \frac{1}{B_3 - B_1}\left[\frac{1}{B_1 - X} - \frac{1}{B_3 - X}\right]\right. & \\
\left. - \frac{1}{B_1 - B_2}\left[\frac{1}{B_2 - X} - \frac{1}{B_1 - X}\right] + \frac{1}{B_3 - B_2}\left[\frac{1}{B_2 - X} - \frac{1}{B_3 - X}\right]\right) &= \\
\frac{1}{B_2 - B_1}\frac{1}{B_3 - B_1}\left(\frac{1}{(B_1 - X)^2} + \left[\frac{1}{B_1 - B_2} + \frac{1}{B_1 - B_3}\right]\frac{1}{B_1 - X}\right) &+ \\
\frac{1}{(B_3 - B_2)(B_1 - B_2)^2}\frac{1}{B_2 - X} + \frac{1}{(B_2 - B_3)(B_1 - B_3)^2}\frac{1}{B_3 - X} & \qquad \text{(E.14)}
\end{aligned}$$

We must add a similar contribution with 1 and 2 interchanged. This should then be multiplied with $\dot{F}(X)$ and integrated over X:

$$\begin{aligned}
H_I &= \frac{1}{2\pi i}\int \dot{F}(\Lambda, X)\ddot{N}(X_1, -X, \frac{1}{2}D_{12})\dot{N}(\Lambda, X_2, -X, \frac{1}{2}D_{12})\dot{N}(\Lambda, X_3, -X, D_3 - \frac{1}{2}D_{12}) + \\
&\quad (1 \leftrightarrow 2)\ dX \\
&= \frac{1}{B_2 - B_1}\frac{1}{B_3 - B_1}\ddot{F}(B_1) + \frac{1}{(B_1 - B_2)(B_1 - B_3)^2}\dot{F}(B_1) + \\
&\quad + \frac{1}{(B_2 - B_3)(B_1 - B_3)^2}\dot{F}(B_3) + (1 \leftrightarrow 2) \qquad \text{(E.15)}
\end{aligned}$$

where we have used

$$\frac{1}{2\pi i}\int \dot{F}(X)\frac{1}{(B - X)^2}dX = \ddot{F}(B) \qquad \text{(E.16)}$$

we can now use

$$\ddot{F}(B) = \ddot{F}(h(y)) = a\frac{1 + 4y + y^2}{1 - y^2} \qquad \text{(E.17)}$$

to arrive at

$$H_I = \frac{2}{a^3}\frac{(y_1 - 1)^2(y_2 - 1)^2}{(1 + y_1)(1 + y_2)(y_1y_2 - 1)}\frac{(y_3 - 1)^2}{(y_1y_3 - 1)(y_2y_3 - 1)}(y_1 + y_2 + (1 + y_1y_2y_3)\left[\frac{y_1 - 1}{y_1y_3 - 1} + \frac{y_2 - 1}{y_2y_3 - 1}\right]) \qquad \text{(E.18)}$$

Differentiating after X_1, X_2 and X_3 will introduce markings on the entrance loops. The differentiated expression should then be power expanded in X_1^{-1}, X_2^{-1} and X_3^{-1}, leading to e.g.

$$H_{I,111}(\Lambda, D_{12}, D_3) = P(e^{a\frac{1}{2}D_{12}}, e^{aD_3}) \qquad \text{(E.19)}$$

with

$$P(x, y) = \frac{y(x - 1)^3}{x^2(1 + x)^5(y - 1)^6}(14x^3 + 14x^4 + 6x^5 + x^6 - 52x^3y - 28x^2y$$

$$6x^4y + 12x^5y + 4x^6y + 18xy^2 + 51x^2y^2 - 51x^4y^2 - 18x^5y^2 + 52x^3y^3$$
$$-4y^3 - 12xy^3 + 6x^2y^3 + 28x^4y^4 - 14x^3y^4 - y^4 - 6xy^4 - 14x^2y^4) \quad \text{(E.20)}$$

Power expanding in a gives

$$H_{I,111} = \frac{D_{12}^3(5D_{12}^3 - 36D_{12}^2D_3 + 87D_{12}D_3^2 - 70D_3^3)}{256D_3^6} +$$
$$\frac{D_{12}^3(5D_{12}^7 - 60D_{12}^6D_3 + 243D_{12}^5D_3^2 - 350D_{12}^4D_3^3 + 232D_{12}D_3^6 + 560D_3^7)}{491520D_3^6}a^4 + \quad \text{(E.21)}$$
$$\frac{D_{12}^3(-5D_{12}^9 + 72D_{12}^8D_3 - 345D_{12}^7D_3^2 + 602D_{12}^6D_3^3 - 16D_{12}^3D_3^6 - 576D_{12)}^2D_3^7 - 2784D_{12}D_3^8 - 2240D_3^9)}{24772608D_3^6}a^6$$
$$+O(a^8)$$

from which we extract the part proportional to a^6 to obtain the thermodynamic limit. We can write this as (using $a = \sqrt{6\sqrt{,}}$):

$$H_{I,11l}^{TD}(\Lambda, D_{12}, D_3) = \sum_{k=1}^{10} H_{I,mnlk}^{TD} D_{12}^{2+k} D_3^{5-l-k}, \ ^{3/2} \quad \text{(E.22)}$$

with the coefficients given as

$H_{I,mnlk}^{TD}$		$k=1$	2	3	4	5	6	7	8	9	10
$l=1$	$\frac{1}{114688}$	−2240	−2784	−576	16	0	0	602	−345	72	−5
2	$\frac{3}{57344}$	1120	−928	−96	0	0	0	−301	230	−60	5
3	$\frac{3}{114688}$	2240	−928	0	0	0	0	1204	−1150	360	−35
4	$\frac{5}{28672}$	−112	0	0	0	0	0	−301	345	−126	14
5	$\frac{15}{16384}$	0	0	0	0	0	0	86	−115	48	−6
6	$\frac{3}{8192}$	0	0	0	0	0	0	−301	460	−216	30
7	$\frac{1}{8192}$	280	−348	144	−20	0	0	1204	−2070	1080	−165
8	$\frac{3}{14336}$	−560	928	−480	80	0	0	−903	1725	−990	165
9	$\frac{45}{114688}$	672	−1392	864	−168	0	0	602	−1265	792	−143
10	$\frac{5}{57344}$	−5600	13920	−10080	2240	0	0	−3311	7590	−5148	1001

Table E.1: Coefficients to $H_{I,11l}$ in the thermodynamic limit (the fraction in the first column is to be multiplied onto the other columns).

As should be evident the results get rather voluminous when consider three point function as compared with two points.

Bibliography

[1] H. Aoki, H. Kawai, J. Nishimura and A. Tsuchiya, *Operator Product Expansion in Two-Dimensional Quantum Gravity*, **hep-th/9511117 1 Dec 1995**.

[2] J. Ambjørn, J. Jurkiewicz and Y. Watabiki, *Dynamical Triangulations, a Gateway to Quantum Gravity ?* **J.Math.Phys. 36 (1995) 6299-6339, hep-th/9503108**.

[3] J. Ambjørn, J. Jurkiewicz and Y. Watabiki, *On the fractal structure of two-dimensional quantum gravity ?* **NBI-HE-95-22**.

[4] J. Ambjørn, B. Durhuus and J. Fröhlich *Diseases of triangulated random surfaces models, and possible cures.* **Nucl. Phys. B257 (1985) 433-449**.

[5] J. Ambjørn and Y. Watabiki, *Scaling in Quantum Gravity* **hep-th/9501049 13 Jan 1995**.

[6] Y. Watabiki, *Fractal structure of Space-time in 2D Quantum Gravity* **hep-th/9605185 25 May 1996**.

[7] Y. Watabiki, *Construction of Non-critical String Field Theory by Transfer Matrix Formalism in Dynamical Triangulation* **hep-th/9401096**.

[8] J. Jurkiewicz, *Universality in the critical behavior of the correlation functions in 2d simplical gravity* **hep-lat/9602023 24 Feb 1996**.

[9] M.J. Bowick, V. John and G. Thorleifsson, *The Hausdorff Dimension of Surfaces in Two-Dimensional Quantum Gravity Coupled to Unitary Minimal Matter* **hep-th/9608030 6 Aug 1996**.

[10] M.G. Harris, *The branching of graphs in 2-d Quantum Gravity* **hep-th/9607136 16 Jul 1996**.

[11] M.G. Harris and J. Ambjørn *Correlation functions in the multiple Ising model coupled to gravity* **hep-th/9602028 6 Feb 1996**.

[12] N. Sakai and Y. Tanii, *Operator Product Expansion and Topological States in $c = 1$ Matter Coupled to 2-D Gravity* **Prog. Theor. Phys. Suppl. 110 (1992) 117-134 hep-th/9111049 25 Nov 91**.

[13] H.W. Hamber and R.M. Williams, *Gauge Invariance in Simplical Gravity* **hep-th/9607153 18 Jul 1996**.

[14] J. Ambjørn, *Quantization of Geometry* **hep-th/9411179 22 Nov 1994**.

[15] G. Akemann, *Higher genus correlators for the hermitian matrix model with multiple cuts* **hep-th/9606004 3 Jun 1996**.

[16] J. Nishimura, S. Tamura and A. Tsuchiya, *Scaling Dimension of Manifestly General Covariant Operators in Two-Dimensional Gravity* **Int. J. Mod. Phys. A10 (1995) pp 859-874 hep-th/9402050 30 Aug 1994**.

[17] Y. Kazama and H. Nicolai, *On the Exact Operator Formalism of Two-Dimensional Liouville Quantum Gravity in Minkowski Spacetime* **Int. J. Mod. Phys. A9 (1994) pp 667-710 hep-th/9305023 7 May 1993**.

[18] M. Fukuma, H. Kawai and R. Nakayama, *Continuum Schwinger-Dyson equations and universal structures in two-dimensional quantum gravity* **Int. J. Mod. Phys. A6 (1991) pp 1385-1406**.

[19] R. Dijkgraaf, H. Verlinde and E. Verlinde *Loop equations and Virasoro constraints in non-pertubative two-dimensional quantum gravity* **Nucl. Phys. B 348 (1991) pp 435-456**.

[20] H. Kawai, N. Kawamoto, T. Mogami and Y. Watabiki, *Transfer Matrix Formulation for two-dimensional quantum gravity and fractal structure of space-time*, **Phys. Lett. B 306 (1993) pp 19-26**.

[21] S.S. Gubser and I. R. Klebanov, *Scaling Functions for Baby Universes in Two-Dimensional Quantum Gravity*, **hep-th/9310098 15 Oct 93**.

[22] N. Ishibashi and H. Kawai, *String field theory of noncritical strings*, **Phys. Lett. B 314 (1993) pp 190-196**.

[23] H. Kawai, *Quantum Gravity and Random Surfaces* **Nucl. Phys. B (Proc. Suppl.) 26 (1992) pp 93-110**.

[24] N. Ishibashi and H. Kawai, *String Field Theory of $c \leq 1$ Noncritical Strings*, **Phys. Lett. B322 (1994) pp 67 hep-th/9312047**.

[25] M. Fukuma, N. Ishibashi, H. Kawai and M. Ninomiya, *Two-Dimensional Quantum Gravity in Temporal Gauge*, **Nucl. Phys. B427 (1994) hep-th/9312175**.

[26] T. Aida, Y. Kitazawa, H. Kawai and M. Ninomiya, *Conformal Invariance and Renormalization Group in Quantum Gravity Near Two Dimensions*, **Nucl. Phys. B427 (1994) 158-180 hep-th/9404171**.

[27] V.G. Knizhnik, A.M. Polyakov and A.B. Zamolodchikov, *Fractal structure of 2d-Quantum Gravity* **Mod. Phys. Lett. A3 (1988) pp 819-826**.

[28] F. David, *Conformal field theories coupled to 2-D gravity in the conformal gauge* **Mod. Phys. Lett. A3 (1988) pp 1651-1656**.

[29] F. David, *Simplical Quantum Gravity and Random Lattice* **Les Houches 1992**.

[30] F. David, *Planar Diagrams, two-dimensional lattice gravity and surface models* **Nucl. Phys. B257 (1985) 45-58**.

[31] J. Distler and H. Kawai, *Conformal field theory and 2D quantum gravity* **Nucl. phys. B321 (1989) 509-527**.

[32] M. Staudacher, *The Yang-Lee edge singularity on a dynamical planar random surface* **Nucl. phys. B336 (1990) 349-362**.

[33] D.J. Gross and A. A. Migdal *A nonpertubative treatment of two-dimensional quantum gravity* **Nucl. phys. B340 (1990) 333-365**.

[34] T. Aida, Y. Kitazawa, J. Nishimura and A. Tsuchiya, *Two-loop Renormalization in Quantum Gravity near Two Dimensions* **Nucl. Phys. B444 (1995) 353-380 hep-th/9501056**.

[35] D. A. Johnston, *Gravity and Random Surfaces on the Lattice: A Review* **hep-lat/9607021**.

[36] S. Jain and S. D. Mathur, *World-sheet Geometry and Baby Universes in 2-D Quantum Gravity* **hep-th/9204017**.

[37] K. G. Wilson, *Non-Lagrangian Models of Current Algebra* **Phys. Rev. 179 (1969) pp 1499-1512**.

[38] W. Zimmermann, *Composite Operators in the Pertubation Theory of Renormalizable Interactions*, **Ann. of Phys. 77 (1973) pp 536-569**.

[39] W. Zimmermann, *Normal Products and the Short Distance Expansion in the Pertubation Theory of Renormalizable Interactions* **Ann. of Phys. 77 (1973) PP 570-601**.

[40] O. Andreev, *On 2D gravity coupled to $c \leq 1$ matter in Polyakov light-cone gauge* **hep-th/9601026**.

[41] Vl. S. Dotsenko, *Correlation Functions of Local Operators in 2D Gravity Coupled to Minimal Matter* **hep-th/9110030 12 Oct 1991**.

[42] E. T. Tomboulis *Exact Relation between Einstein and Quadratic Quantum Gravity* **hep-th/9601082 16 Jan 1996**.

[43] M. Goulian and M. Li, *Correlation Functions in Liouville Theory* **Phys. Rev. Lett. 66 (1991)**.

[44] Vl. S. Dotsenko and V. A. Fateev, *Operator Algebra of Two-Dimensional Conformal Theories with Central Charge $c \leq 1$* **Phys. Lett. 154B (1985)**.

[45] A. Carlini and J. Greensite, *Why is spacetime Lorentzian?* **gr-qc/9308012 August 1993**.

[46] M. Lehto, H.B. Nielsen and M. Ninomiya, *Pregeometric Quantum Lattice: a general discussion* **Nucl. Phys. B272 (1986) 213-227**.

[47] M. Lehto, H.B. Nielsen and M. Ninomiya, *Diffeomorphism symmetry in simplical quantum gravity* **Nucl. Phys. B272 (1986) 228-252**.

[48] E. Brézin, C. Itzykson, G. Parisi and J. B. Zuber, *Planar Diagrams* **Commun. math. Phys. 59 (1978) pp. 35-51**.

[49] E. Brézin and S. R. Wadia, *The large N Expansion in quantum field theory and statistical physics* **World Scientific Publishing Co. (1993)**.

[50] P. Ginsparg and G. Moore, *Lectures on 2D Gravity and 2D string Theory* **hep-th9304011** .

[51] J. Ambjørn, B. Durhuus and T. Johnsson, *Quantum Geometry - A statistical field theory approach* **in print ??**.

[52] J. Collins, *Renormalization* **Cambridge University Press (1984)**.

[53] J. L. Petersen, *Notes on Conformal Field Theory*, **NBI tryk (1994)**.

[54] C. Itzykson and J-B. Zuber. *Quantum Field Theory*, **McGraw-Hill (1980) pp 671-688** .

[55] L. H. Ryder, *Quantum Field Theory*, **Cambridge University Press (1996)**.

[56] P. Ramond *Field Theory: A Modern Primer*, **Addison-Wesley Publishing Company, Inc. (1989)**.

[57] P. G. Bergmann. *Introduction to the Theory of Relativity* **Dover Publications, inc. New York (1976)**.

[58] C. W. Misner, K. S. Thorne and J. A. Wheeler, *Gravitation* **W. H. Freeman and Company, New York (1973)**.

[59] B.A Dubrovin, A.T. Fomenko, S.P. Novikov, *Modern geometry- Methods and Applications , vol I-II* **Springer-Verlag, New York (1985)**.

[60] J. Irving and N. Mullineux, *Mathematics in Physics and Engineering* **Academic Press (1959)**.

[61] A. Erdély, *Asymptotic expansions* **Dover Publications (1956)**.

[62] G. Grubb, *Mat 3MA noter (III) Sobolev rum og Fourier Teori* **Matematisk institut, Københavns Universitet**.

[63] T. Regge, *General relativity without coordinates* **Nuovo Cimento 19 (1961) pp 558-571**

[64] S. W. Hawking, W. Israel et al. *General Relativity -an Einstein centenary survey* **Cambridge University Press (1979)**.